Stability Analysis of a Nonlinear System Stabilizing Controller for an Integrated Power System

by

Midshipman Daniel F. Chiafair, Class of 2002
United States Naval Academy
Annapolis, Maryland

_____

Certification of Advisor Approval

Assistant Professor Edwin L. Zivi
Weapons and Systems Engineering Department

_____

_____

Acceptance for the Trident Scholar Committee

Professor Joyce E. Shade
Deputy Director of Research & Scholarship

_____

_____

REPORT DOCUMENTATION PAGE

Form Approved OMB No. 0704-0188

1. REPORT DATE (DD-MM-YYYY)	2. REPORT TYPE	3. DATES COVERED (FROM - TO)
05-05-2002		xx-xx-2002 to xx-xx-2002

4. TITLE AND SUBTITLE
Stability Analysis of a Nonlinear System Stabilizing Controller for an Integrated Power System
Unclassified

5a. CONTRACT NUMBER

5b. GRANT NUMBER

5c. PROGRAM ELEMENT NUMBER

6. AUTHOR(S)
Chiafair, Daniel F. ;

5d. PROJECT NUMBER

5e. TASK NUMBER

5f. WORK UNIT NUMBER

7. PERFORMING ORGANIZATION NAME AND ADDRESS
US Naval Academy
Annapolis, MD21402

8. PERFORMING ORGANIZATION REPORT NUMBER

9. SPONSORING/MONITORING AGENCY NAME AND ADDRESS
,

10. SPONSOR/MONITOR'S ACRONYM(S)

11. SPONSOR/MONITOR'S REPORT NUMBER(S)

12. DISTRIBUTION/AVAILABILITY STATEMENT
APUBLIC RELEASE
,

13. SUPPLEMENTARY NOTES

14. ABSTRACT
See report.

15. SUBJECT TERMS

16. SECURITY CLASSIFICATION OF:			17. LIMITATION OF ABSTRACT	18. NUMBER OF PAGES	19. NAME OF RESPONSIBLE PERSON
			Public Release	92	email from USNA, (blank) lfenster@dtic.mil
a. REPORT Unclassified	b. ABSTRACT Unclassified	c. THIS PAGE Unclassified			19b. TELEPHONE NUMBER International Area Code Area Code Telephone Number 703767-9007 DSN 427-9007

Standard Form 298 (Rev. 8-98)
Prescribed by ANSI Std Z39.18

REPORT DOCUMENTATION PAGE

Public reporting burden for this collection of information is estimated to average 1 hour per response, including g the time for reviewing instructions, searching existing data sources, gathering and maintaining the data needed, and completing and reviewing the collection of information. Send comments regarding this burden estimate or any other aspect of the collection of information, including suggestions for reducing this burden to Washington Headquarters Services, Directorate for Information Operations and Reports, 1215 Jefferson Davis Highway, Suite 1204, Arlington, VA 22202-4302, and to the Office of Management and Budget, Paperwork Reduction Project (0704-0188), Washington, DC 20503.

1. AGENCY USE ONLY (Leave blank)	2. REPORT DATE 5 May 2002	3. REPORT TYPE AND DATE COVERED

4. TITLE AND SUBTITLE
Stability analysis of a nonlinear system stabilizing controller for an integrated power system

5. FUNDING NUMBERS

6. AUTHOR(S)
Chiafair, Daniel F.

7. PERFORMING ORGANIZATION NAME(S) AND ADDRESS(ES)

8. PERFORMING ORGANIZATION REPORT NUMBER

9. SPONSORING/MONITORING AGENCY NAME(S) AND ADDRESS(ES)
US Naval Academy
Annapolis, MD 21402

10. SPONSORING/MONITORING AGENCY REPORT NUMBER
Trident Scholar project report no. 289 (2002)

11. SUPPLEMENTARY NOTES

12a. DISTRIBUTION/AVAILABILITY STATEMENT
This document has been approved for public release; its distribution is UNLIMITED.

12b. DISTRIBUTION CODE

13. ABSTRACT:
Future electric warships will contain one integrated electrical power infrastructure for propulsion, ship's service, and weapons systems. This integrated power system (IPS) must provide continuous power to mission and life critical systems, including during major combat battle damage disruptions. This research investigated a novel nonlinear systems stabilizing control strategy and associated stability assessment tools recently proposed by Sudhoff. Using a MATLAB-based DC stability toolbox, nonlinear stability augmentation of a prototype DC IPS was investigated with respect to changes in system parameters and system structure. Today's warships are constructed with segregated mechanical propulsion and electric power systems. In current ships, the power dedicated to ship propulsion is about 90% of total ship power and power dedicated to electrical generation is about 10%. The existing ship service electrical system is not very robust: because the system is very tightly coupled, a single casualty can disrupt the entire system causing a total loss of electrical power. Even though the mechanical propulsion system may be in perfect working condition, it cannot provide any electrical power to the ship. An integrated power system will be deployed on future naval combatants to resolve this problem. The key advantage of an electronically controlled, integrated power system is the ability to actively control the flow of power throughout

14. SUBJECT TERMS
Integrated power system, stability, stabilizing control

15. NUMBER OF PAGES
91

16. PRICE CODE

17. SECURITY CLASSIFICATION OF REPORT	18. SECURITY CLASSIFICATION OF THIS PAGE	19. SECURITY CLASSIFICATION OF ABSTRACT	20. LIMITATION OF ABSTRACT

Abstract

**"Stability Analysis of a Nonlinear System Stabilizing
Controller for an Integrated Power System"**

Future electric warships will contain one integrated electrical power infrastructure for propulsion, ship's service, and weapons systems. This integrated power system (IPS) must provide continuous power to mission and life critical systems, including during major combat battle damage disruptions. This research investigated a novel nonlinear systems stabilizing control strategy and associated stability assessment tools recently proposed by Sudhoff. Using a MATLAB-based DC stability toolbox, nonlinear stability augmentation of a prototype DC IPS was investigated with respect to changes in system parameters and system structure.

Today's warships are constructed with segregated mechanical propulsion and electric power systems. In current ships, the power dedicated to ship propulsion is about 90% of total ship power and power dedicated to electrical generation is about 10%. The existing ship service electrical system is not very robust: because the system is very tightly coupled, a single casualty can disrupt the entire system causing a total loss of electrical power. Even though the mechanical propulsion system may be in perfect working condition, it cannot provide any electrical power to the ship. An integrated power system will be deployed on future naval combatants to resolve this problem. The key advantage of an electronically controlled, integrated power system is the ability to actively control the flow of power throughout distribution systems. The system requires sophisticated control algorithms and automation infrastructure to maintain power and, if necessary, re-route power to critical systems. The ultimate goal of integrating active, survivable control algorithms into an integrated, solid-state power distribution system will be to maintain power continuity during major, combat induced casualties.

This research analyzed a prototype DC Zonal Electrical Distribution System (DC-ZEDS) with respect to system parameter changes and casualty disruption. The DC-ZEDS testbed has been installed at the University of Missouri at Rolla as part of the Energy Systems Analysis Consortium and is funded by the U. S. Navy. This testbed is representative of future, integrated ship service power distribution systems. DC-ZEDS stability analysis was performed using Sudhoff's extensions of the Nyquist stability criteria and time-domain simulation. The results indicate that significant improvements in system stability can be achieved using innovative control strategies and algorithms.

Keywords

Integrated Power System, Stability, Stabilizing Control

Acknowledgements

Table of Contents

1 Introduction

Today's warships are constructed with segregated mechanical propulsion and electric power systems. In current ships, the power dedicated to ship propulsion is about 90% of total ship power and power dedicated to electrical generation is about 10%. The existing ship service electrical system is not very robust: because the system is very tightly coupled, a single casualty can disrupt the entire system causing a total loss of electrical power. Even though the mechanical propulsion system may be in perfect working condition, it cannot provide any electrical power to the ship. Incremental improvements have been implemented on DDG-51 Flight II. The next surface combatant will have a fundamentally new system.

To improve combat effectiveness and survivability, an Integrated Power System (IPS) will be deployed on future naval combatants. The key advantage of an electronically controlled, Integrated Power System is the ability to actively control the flow of power throughout distribution systems. In the event of a casualty to a generator, a ship with IPS can borrow power from another generator to keep critical systems online (Figure 1-1). IPS is the fundamental technology underlying the development of the Integrated Electric Warship, which envisions a unified power system for propulsion, ships service power and energy weapons.

Figure 1-1. Integrated Power System Advantage[1]
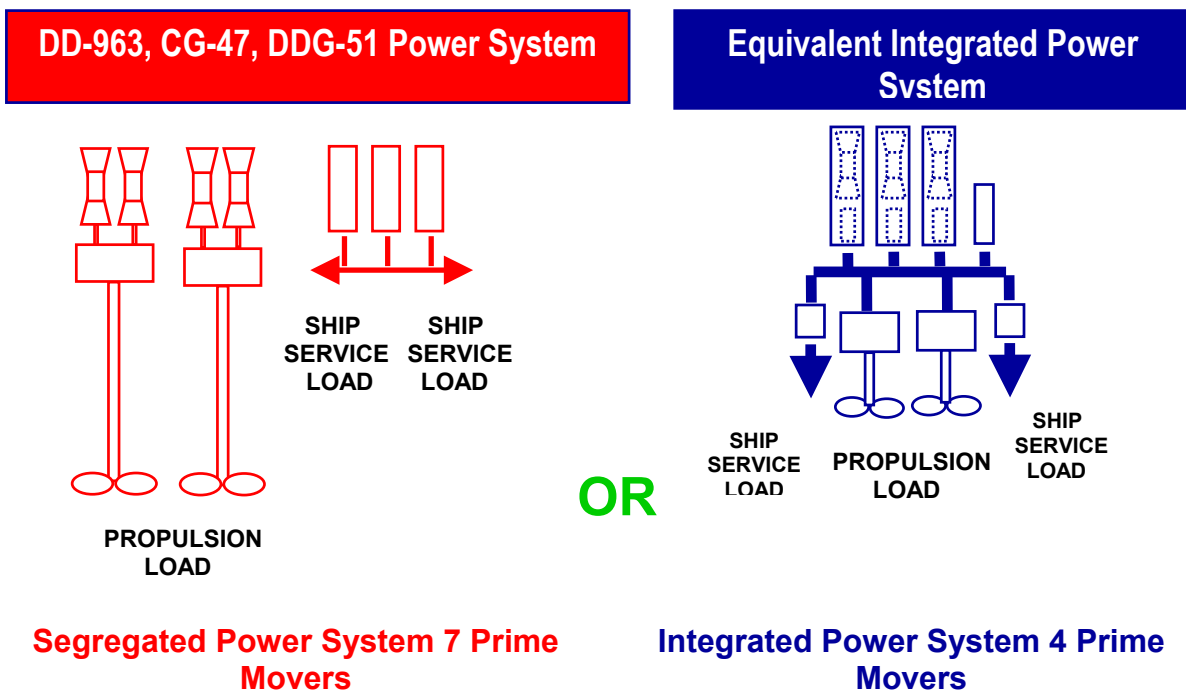
1.1 IPS Requirements

The Integrated Power System requires sophisticated control algorithms and automation infrastructure to maintain power and, if necessary, re-route power to critical systems. This control system is both hierarchical and distributed and must be highly survivable. During normal operation, the system is optimized by intelligent supervisory control. During casualties, effective autonomous control must be maintained for subsystems that are cut off from the central (supervisory) system. New control systems strategies and algorithms are being developed in order to maintain power continuity during major, combat induced casualties. A warship that has replaced manpower with automation will require continuous power distribution so that its systems can carry out damage control tasks. Furthermore, weapons systems need continuous power in a battlefield environment to protect the ship and complete the mission. Restoring power even after only a brief period of power outage is not sufficient. Linear and nonlinear control algorithms have been developed by Professor Sudhoff of Purdue University[2] and have been shown to maintain system stability during normal operation. It has not been determined what will happen to system transient performance and stability under casualty conditions. This research evaluates the performance of the control schemes proposed by Sudhoff under simulated combat-induced casualty conditions.

The Navy's call for a 70% crew size reduction requires that Integrated Power System casualty control be performed with minimal human intervention. In a casualty situation, the ship will probably suffer personnel casualties and control system damage. With the majority of the crew at designated watch stations, there will be relatively few crewmembers available for damage and engineering control. This requires that IPS be controlled by a minimum number of human operators. It is absolutely critical that the control system for IPS continues to function even when it receives considerable harm. The first task the control system must accomplish is to prevent the disruption from destabilizing the power system. A fault in one area of the ship must be contained in order to avoid catastrophic power failures. Major power failures in surface combatants could be fatal in a casualty situation because there are not enough people to fight the damage without automated systems. The control system will also be required to make decisions with regard to power distribution and prioritization, cutting power to less important systems in a power deficit, restoring service when sufficient power is present, and rerouting power as necessary. As shown in Figure 1-2, the system will need to provide accurate situational reports to human operator(s) and allow them to override computer decisions when necessary.

Land-based power systems have the distinct advantage of an essentially unlimited power supply from the national power grid. Traditional power analysis permits the assumption of an ideal source that can supply unlimited current to the system. Shipboard power systems have a markedly limited power source that is of the same order of magnitude as the loads they supply. The system can become unstable if the load demands more current from the source than it can supply.

Figure 1-2. Multi-Layer Control Capability[3]
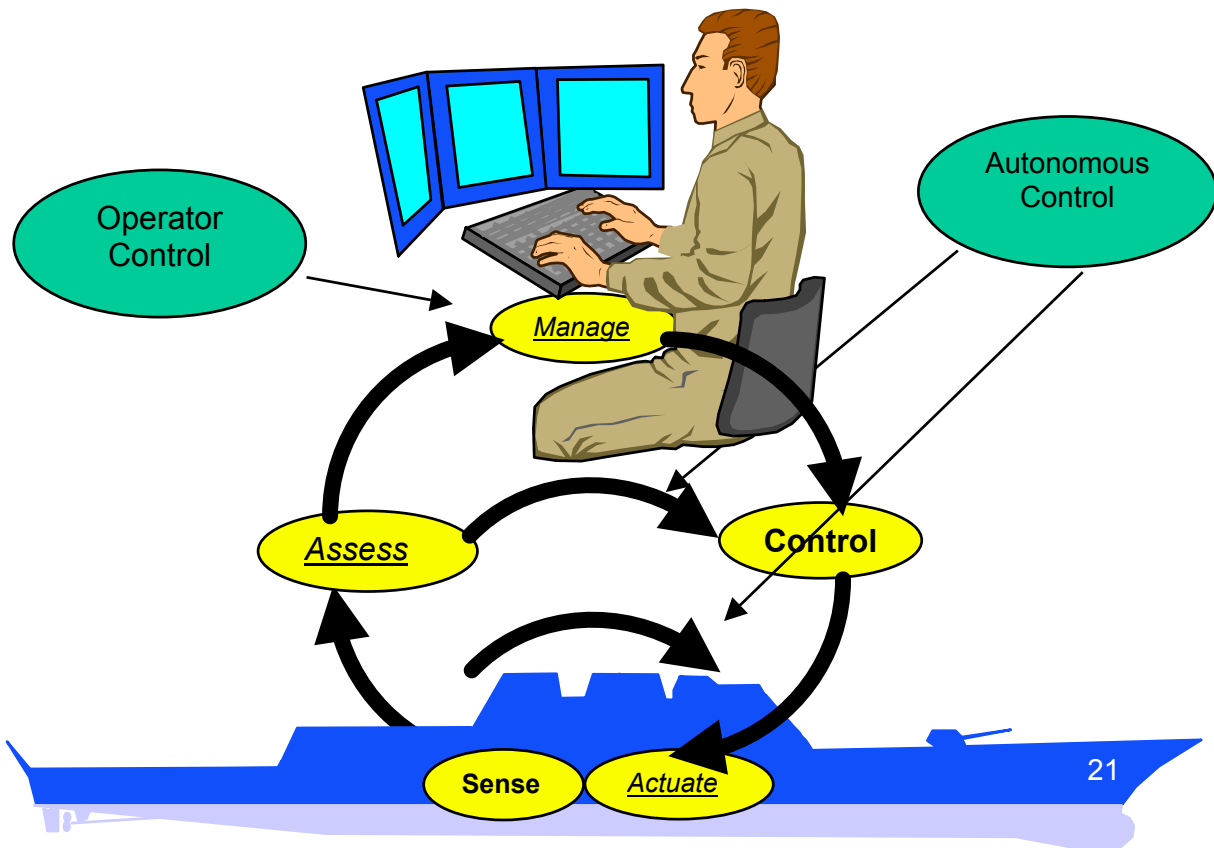
1.2 IPS as a Complex Interactive Network

The discussion in this section is based largely on Massoud Amin's paper, "National Infrastructures as Complex Interactive Networks."[4] A complex interactive network (CIN) is comprised of thousands of tightly interconnected components. Moreover, disruptions can be rapidly transmitted throughout the network and lead to widespread failures. Many interaction points further complicate the system. Several factors prevent conventional mathematical methodologies from successfully modeling and controlling a CIN. The coupled subsystems contain a heterogeneous mixture of dynamic, interactive, and nonlinear entities, unscheduled discontinuities, and numerous other significant effects. Numerous theoretical and practical challenges in modeling, prediction, simulation, cause and effect relationships, and analysis must be overcome to effectively control and manage CIN's. Nevertheless, a basic understanding of true system dynamics is necessary to manage disturbances and prevent cascading effects throughout the network. Average value models neglect higher order solid state switching transients and simplify the task without losing too much information. Average value models developed by ESAC will be used to reduce some of the structural variability into one "average" system.

It is not possible for a single entity to maintain effective control of these multi-scale, distributed, highly interactive networks. Cascading effects can lead to widespread failure almost instantaneously and require immediate attention by local controllers to contain the casualty. The ability to evaluate, monitor, and manage IPS in real time requires effective distributed control in order to keep networks operational and reconfigurable.

The complexity of the system and necessity of immediate action prevents human participants from detailed decision-making. Despite this fact, it turns out that in many complex networks, human participants are the most adaptable in the management of recovery. Therefore, some level of human interaction via supervisory control is highly desired; however, the correct amount of human involvement is difficult to determine.

Integrated power systems are numerically stiff with time constants ranging from microseconds to several seconds. This makes numerical integration a non-straightforward process. The possibility for numerical instability further complicates the problem since it may be difficult to determine if it was the system model or the numerical integration that caused the instability. In general, decreasing the step size an appropriate amount will stabilize a numerically unstable integration. If it is the system model that is unstable, varying the step size will not stabilize the simulation.

A primary goal for IPS is to avoid cascading failures within and across systems including electrical power, cooling, thermal management and fire fighting. As previously discussed, a single control element is not sufficient for complex interactive networks. Additionally, in a disruptive situation, the control elements themselves may suffer from simultaneous faults and failures. The solution is to incorporate distributed and hierarchical control methods. To combat the rapid spread of disruption through the system, lower reactive layers will have quick reaction times to curb harmful effects. They will operate on minimal information and will attempt to quickly stabilize local components. Higher cognitive layers will be slower to react to system changes but can coordinate lower layers to achieve longer-term goals and overall system stability.

1.3 The Control Architecture

Based on a review of research by Zivi and McCoy[5], the control architecture will contain zones of control distributed throughout the ship managed by a high level supervisory system (Figure 1-3). Each zone will consist of several component level hardware/software control kernels that will contain all damage sensors and casualty response systems. Control kernels will not rely on the supervisory system for any critical support or data and are therefore invariant to normal system changes and disruptions including damage, upgrades, faults, and failures. The kernels and zones will function autonomously when severed from the supervisory system because they do not rely on it for critical data or support. Autonomous elements must continue to carry out their function based on the last information received from the supervisory system as well as current information received from their own sensors. Control algorithms are in development to realize these concepts.

Figure 1-3. Integrated Power System Control Levels[6]
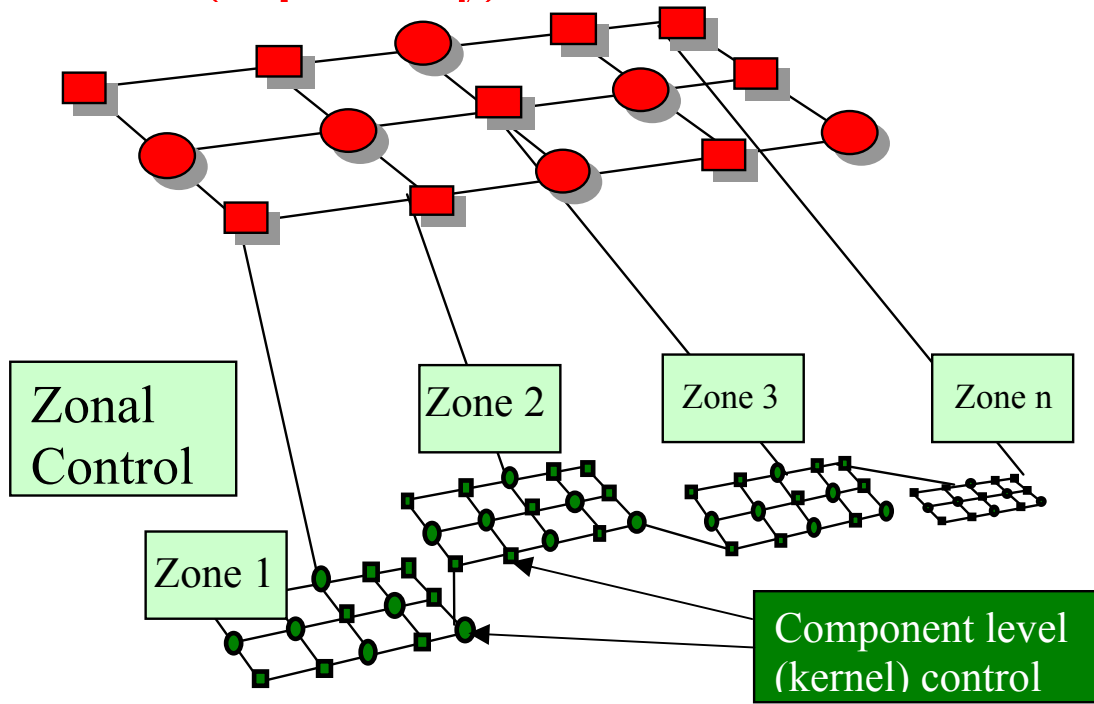
When global communication is present, primary control will reside with the high-level supervisory control system. This system will coordinate real-time information from and commands to the distributed zones. Individual zones will not communicate with each other but only report to the supervisory system. Supervisory control is ideal and enables coordination within the ship that would not otherwise be realized if each zone was completely autonomous. However, in the event the zones lose communications with the supervisory system, they will automatically take over and continue to function by themselves until communications can be recovered. The crew oversees supervisory control and delegates routine, repetitive tasks through it to automation systems. The control system makes the vast majority of the decisions so that the crew simply has to override control system decisions when necessary.

1.4 The Control Algorithms

Preliminary control algorithms exist to control the Integrated Power System. These still need to be thoroughly tested. More robust algorithms may be able to significantly improve the overall system survivability.

The control system will contain two or more levels of control; according to Lively et al., it should have three: supervisory, zonal, and local control.[7] The important thing to consider, however, is the interaction between a level of control and the level directly above it. As stated

above, disruptions to the supervisory system (higher system) do not adversely affect the local and zonal systems (lower systems). Each lower level has the ability to function on its own without support from the next highest level, so faults and disruptions above do not ripple down. However, the lower systems do affect the higher systems because they supply the higher systems with information, so information does ripple upward.   When the higher levels receive information from the lower, they must decide what to do with it. The key is finding the proper balance between a hierarchical, supervisory control system and an autonomous, highly distributed system.

The algorithms will include the management of power generation and the coordination of ship service and propulsion loads. Power management allocates power to system loads, starts additional power generators if available, and initiates load sheds according to priority in the event that there is not enough power for all systems. It also shuts down generators when doing so will not induce a load shed.

Most important, however, is the question of how the control system will function in a casualty. Casualty response algorithms are required to be very robust because they must continue to function properly when the control system itself suffers severe damage. Because the control system is distributed throughout the ship, it is guaranteed to suffer damage if the ship endures a casualty. Vital systems require continuous service even immediately after the initial hit to the ship. This will be achieved in part by minimizing the spread of a disruption throughout the ship. The potential short circuits and other faults created by a casualty can cause extreme stress in certain areas of the power system and can be transmitted throughout the ship if not contained. Ideally these faults would be contained at the next node. Without containment, it is very likely the ship will lose all power and go dark.

It is necessary to test new control theory for the IPS survivable control problem. Finding control algorithms that are capable of managing power amidst disruptions is essential to the incorporation of an integrated power system on future surface combatants.

1.5 State Space Representation

The Integrated Power System model is written as a system of differential and algebraic equations formulated in state-space. There are four categories of state equations ranging from general, difficult to solve formulations to simplified linear models. They are shown below, where **x** is the state variable vector, $\dot{\mathbf{x}}$ is the time derivative of the state variable vector, **u** is the input vector, and **y** is the output vector. The **C** and **D** matrices map the state and input vectors to the output vector.

- Implicit, Non-linear, Time-Varying:

$$\mathbf{f}(\dot{\mathbf{x}}(t),\mathbf{x}(t),\mathbf{u}(t),t) = 0 \qquad (1)$$

- Explicit, Non-linear, Time Varying:

$$\dot{\mathbf{x}}(t) = f(\mathbf{x}(t), \mathbf{u}(t), t) \qquad (2)$$

- Explicit, Linear, Time Varying:

$$\dot{\mathbf{x}}(t) = \mathbf{A}(t)\mathbf{x}(t) + \mathbf{B}(t)\mathbf{u}(t) \qquad (3)$$

- Explicit, Linear, Time Invariant:

$$\dot{\mathbf{x}}(t) = \mathbf{A}\mathbf{x}(t) + \mathbf{B}\mathbf{u}(t) \qquad (4)$$

In a lumped parameter system, the system can be described by a finite number of state variables using one of the equations given (1-4). The model of the system depends upon state space equations plus an output equation of the form:

$$\mathbf{y} = \mathbf{C}\mathbf{x} + \mathbf{D}\mathbf{u} \qquad (5)$$

IPS is a complex, nonlinear, variable structure system. Structure variations result from changes in alignment, power electronic switching, faults, and failures. There are two levels of variation. The first is on the local, detailed level and results from individual switches opening and closing. Complexity from these variations is simplified by using average value models. The second level is major structure changes resulting from power realignments, switching among power buses, faults, and failures. Major structural changes must be individually analyzed and controlled.[8]

1.6 Ensign Cerrito's 2000 Trident Project – Neural Nets

A major consideration in the derivation of the control system algorithms is that perfect information will almost never be present. This is certainly true in a casualty situation when it is most critical that the control system continues to work properly. Ensign Cerrito's 2000 Trident project[9] focused on estimation algorithms that are robust with respect to loss of sensors and data communications. He studied the fault tolerant estimation problem where sensors may malfunction or be destroyed. Cerrito explored a neural network's ability to correctly evaluate a situation in the presence of faulty or missing data. He showed that with proper "training," a network can be "taught" to distinguish between changes in the physical system and degradations in the sensor suite[10]. A trained human operator is able to look at a variety of data, determine which data is useful and accurate, and take appropriate action. The control algorithms replacing the human operator must be able to accomplish this function with the same level of success.

1.7 Ensign Vanecko's 2001 Trident Project – Network Fragment Healing

Another important consideration is communication path availability. In his 2001 Trident project "Survivable Shipboard Control Systems,"[11] Ensign Vanecko researched network fragment healing algorithms that maintain communication throughout the ship in the event that one or more communication paths are lost. The network that connects the local zones and control

kernels to the supervisory system should be robust as well. It is anticipated that the control systems of this project will employ a highly survivable network that can maximize communication continuity.

2 Prior Work

2.1 The Integrated Power System Model

At present, IPS does not exist on any ship, and therefore a computer model was used to simulate the system. Over the last fifteen years, the Energy Systems Analysis Consortium (ESAC) has spent considerable time and money developing this model under the direction of the United States Navy. A testbed that models this DC Zonal Electrical Distribution System (DC-ZEDS) has been installed at the University of Missouri at Rolla. This physical testbed and the associated Advanced Continuous Simulation Language (ACSL) and MATLAB simulation provide an essential baseline reference problem. The simplified baseline model is shown in Figure 2-1. Appendix A provides a list of the system parameters.

Figure 2-1. DC Zonal Electrical Distribution System[12]
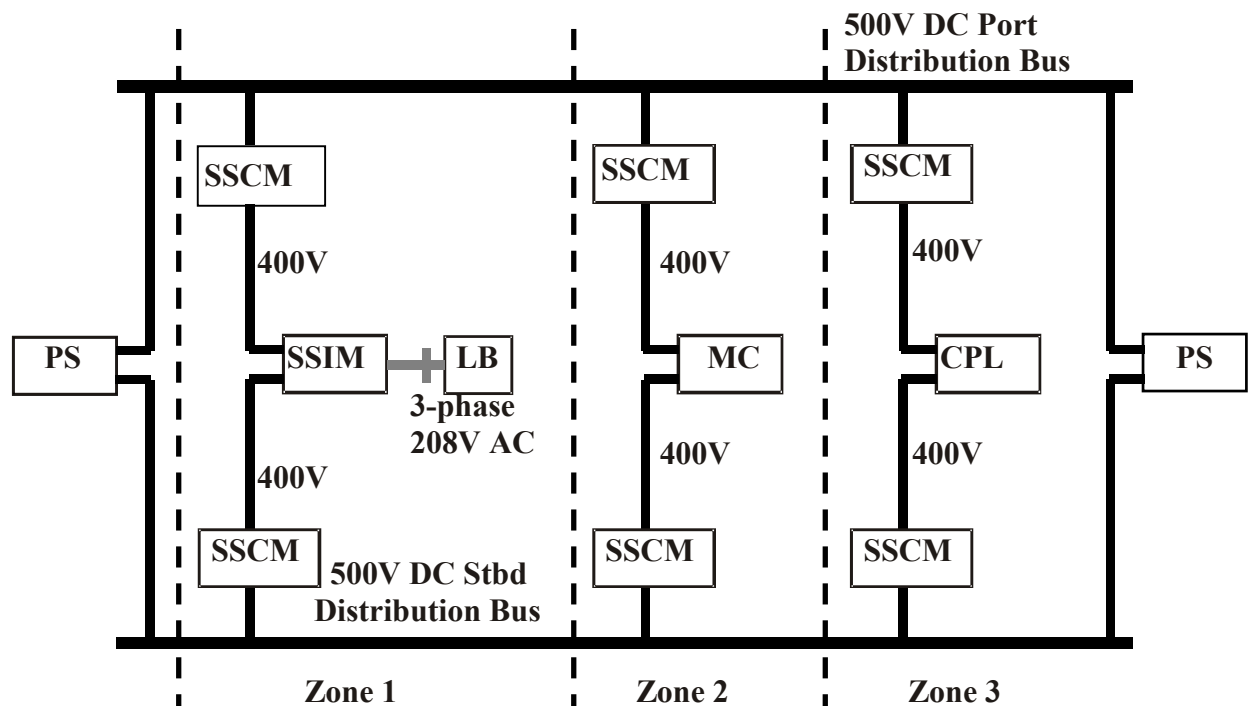
PS – Power Supply
SSCM – Ship Service Converter Module (DC/DC)
SSIM – Ship Service Inverter Module (DC/AC)
MC – Motor Control
CPL – Constant Power Load

2.2 "Negative Impedance" Stability

Traditional, passive loads and power systems are inherently stable. If the supply voltage drops, the resistive load draws less current and the system stabilizes by dissipating less power. Across the load, Voltage (V) vs. Current (I) is positively sloped. Therefore, if V goes down, I decreases and power, V*I, decreases. IPS contains power electronics that attempt to maintain a constant power supply to the loads, regardless of the state of the bus supply. Voltage vs. Current for these loads is negatively sloped implying that if the supply voltage decreases, the load draws more current to compensate for the voltage drop and maintain a constant power level to the load (Figure 2-2). Assuming the power bus can supply the current, this is a desirable characteristic. Unfortunately, these constant power loads may demand more current than the power bus can supply. This can result in a destabilizing effect known as "voltage collapse," in which the power bus, unable to supply the current demanded by the load, enters a limit cycle or shuts down altogether. The limit cycle is shown in Figure 2-3, which portrays the current demanded from an induction motor, i_{as}^*, the actual current to the motor, i_{as}, and the voltage of the supply DC bus, v_{dci}. The current supplied is nearly the same as the current demanded, however, this constant power load has caused the bus voltage to enter a limit cycle and destabilize. The high-frequency variation in voltage of the DC bus will greatly disrupt any other loads attached to the bus. The control system of IPS must intervene before this situation occurs. The approach used in this project is to alter the impedance characteristic of the ship service converter module, thereby limiting the maximum current it demands.
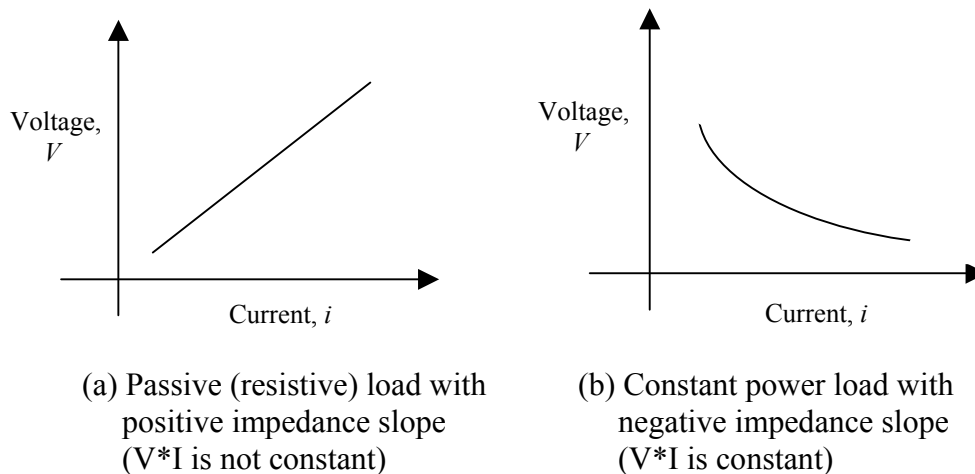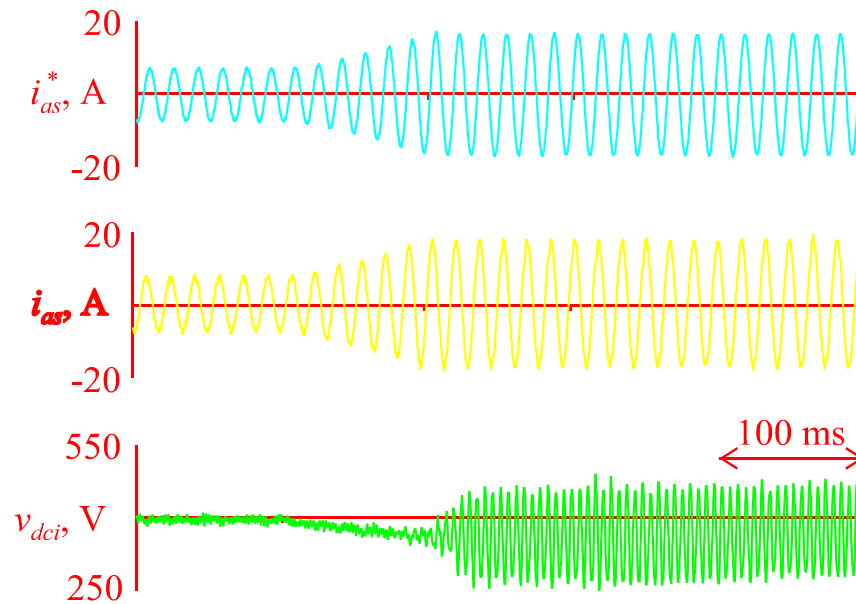
Figure 2-2. Impedance Slopes

(a) Passive (resistive) load with
positive impedance slope
(V*I is not constant)

(b) Constant power load with
negative impedance slope
(V*I is constant)

Figure 2-3. Instability Due To Constant Power Load[13]
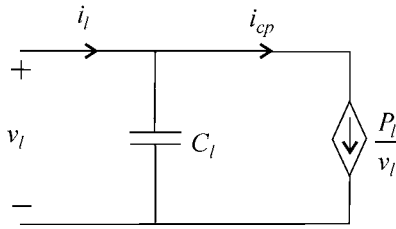

2.3 System Stabilizing Control

Today's shipboard power components are physically connected via heavy copper cables resulting in a tightly coupled, dynamically interdependent system. Existing electromechanical switches are too slow to contain a disruption to a single portion of the power system. Therefore, a disruption to one part of the ship immediately spreads throughout the rest of the power system, often causing complete system failure. Future integrated power systems will have power electronics based conversion modules, which enable the flow of power to be actively controlled. Unlike the tightly coupled copper cabling, a power electronics based system can minimize the propagation of disruptions. This disturbance propagation minimization algorithm was the first to be tested. It was observed that this control scheme is very stressful on the component faulted and forced it to bear the entire brunt of the disruption. In this case, large energy storage capacitances are required to ensure system stability. Losing one component is better than losing the entire system, but still undesirable. This component may be an entire distribution bus (port or starboard) or may be critical to the mission. The ideal solution would allow the system to absorb enough of the disruption that no components are lost while at the same time maintaining overall system stability. This end may be achieved if the disruption propagation is constrained in a manner which takes advantage of the overall system's ability to absorb the disruption without compromising system stability. In this scenario, the power electronics can be thought of as electric "rubber bands". Each "rubber band" will stretch just enough to absorb the shock to the system, but not so much that any rubber band will break. The goal is to distribute the energy shock to each component in the power system according to how much it can absorb without disrupting the component or system. This method greatly reduces the capacitive energy storage requirements, thereby decreasing size, weight, and fault protection requirements

2.4 Control Algorithm

Consider a generic constant power load depicted in Figure 2-4. It is modeled as a capacitance, C_l, in parallel with an ideal constant power load where $P_l = i_{cp} v_l = \dfrac{P_l}{v_l} v_l$. P_l is the power into the active portion of the converter.

Figure 2-4. Constant Power Load[14]

One Nonlinear Stabilizing Control (NSC) approach is to modulate the power requirement of the constant power load. In this case, if the load is going to demand enough power from the bus to destabilize the system, then the algorithm decreases the amount of power for which the load asks according to Figure 2-5. Essentially, the idea is to make the load a better customer for the system.

Figure 2-5. Nonlinear Stabilizing Control (NSC)[15]
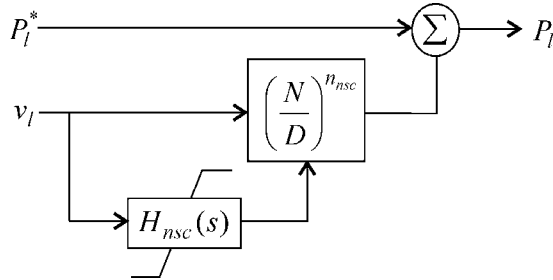
In this configuration, P_l^* is the power desired by the load and P_l is the actual power commanded by the load after it has been modified by the NSC. H_{nsc} is a low pass filter and n_{nsc} determines how much influence the NSC has on the load. By selecting n_{nsc} to be greater than 1, the negative impedance effect of the constant power load can be eliminated, thereby potentially reducing the energy storage requirements to operate the system. However, this approach isolates the load and does not take advantage of other energy storage components in the rest of the system. Moreover, this approach prevents the load from obtaining its full power requirement. In many applications, this constraint may not be acceptable.

Overall energy storage may be reduced if we allow some of the disturbance to propagate throughout the system. Instead of regulating the power delivered to the constant power load,

control is now directed at the converter modules located throughout the power distribution system. If a disturbance occurs on the zonal DC bus, then the converter module will allow some of that disturbance to affect its output in order to distribute the effects of the disruption. Note that this is the middle ground between allowing the disturbance to propagate completely through the system (such as would be achieved by simply connecting components with copper wiring) and not allowing the disturbance to propagate at all (as in the case just discussed). Now consider the one-source two-bus system shown in Figure 2-6.

Figure 2-6. One-Source Two-Bus System[16]
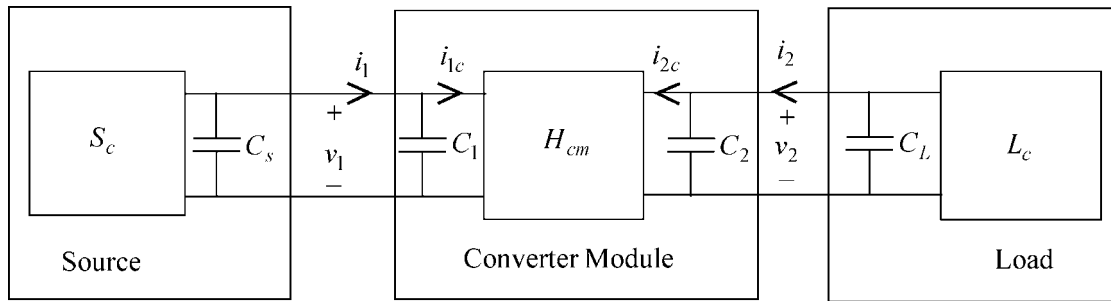
S_c is the linearized impedance of the core source converter, H_{cm} is the linearized model of the core converter module, and L_c is the linearized load admittance of the core load converter module. Control of the converter module is shown in Figure 2-7.

Figure 2-7. Generic Converter Module Control with Stabilizing Feedback[17]
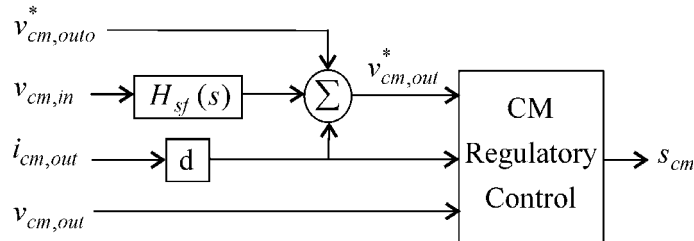
Therein $v^*_{cm,out0}$ is the nominal desired output voltage (in this case bus 2 voltage v_2), $v^*_{cm,out}$ is the instantaneous desired output voltage, $v_{cm,in}$ is the converter module input voltage (in this case bus 1 voltage v_1), $i_{cm,out}$ is current into the output port of the converter module, and s_{cm} is a vector which describes the switching states of each of the power electronic devices. The transfer function $H_{sf}(s)$ determines how much the input voltage is allowed to disturb the output voltage. $H_{sf}(s)$ is selected to be a bandpass filter with a passband gain K_{sf}. As K_{sf} increases, the power converter begins to approximate a wire and allows disturbances to propagate extensively. As K_{sf} decreases, disruptions are isolated to the load side of the converter and have minimal effect on

the overall system. The *d* term is used to implement voltage droop. The function of the regulatory control is to manipulate the switching of the power semiconductors such that the actual converter output voltage is as close as possible to the desired output voltage, $v^*_{cm,out}$.

2.5 Stability Analysis Using Admittance Space Constraints and Nyquist Theory

This section follows from Professor Sudhoff's research on stability analysis of DC distribution systems.[18] Stability analysis of an IPS is not a straightforward task because of the large number of loads within the system and its dynamic nonlinearities. These are coupled with a wide range of operating points and a high degree of reconfigurability. Nyquist theory and an admittance/impedance based design approach that explicitly incorporates uncertainties is used to determine stability. Appendix B gives a brief introduction to Nyquist theory.

Figure 2-8. Thevenin Equivalent Source and Load Converter Model[19]
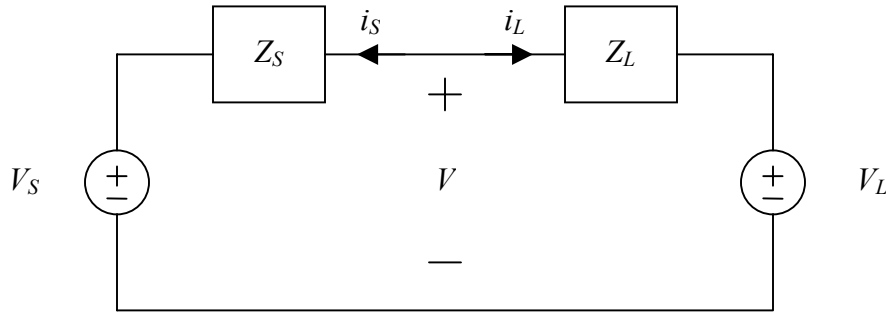
Impedance based stability of a single bus DC power system can be explained in terms of Figure 2-8. Herein, V_S and Z_S represent the Thevenin equivalent voltage and impedance of the linearized source converter model, V_L and Z_L represent the Thevenin equivalent voltage and impedance of the linearized load converter model, and i_S and i_L represent the currents flowing into the two converters, respectively. From Figure 2-4, it is clear that:

$$V = \frac{Z_L}{Z_S + Z_L} V_S + \frac{Z_S}{Z_S + Z_L} V_L \qquad (6)$$

It is convenient to define

$$Z_S(s) = \frac{N_S(s)}{D_S(s)} \qquad \text{and} \qquad Z_L(s) = \frac{N_L(s)}{D_L(s)} \qquad (7)$$

$Z_S(s)$ and $Z_L(s)$ are ratios of two polynomials in *s*. Therefore, $N_S(s)$ and $D_S(s)$ are polynomials in *s* with no common factors. $N_L(s)$ and $D_L(s)$ are also polynomials in *s* with no common factors. Clearly, the roots of $D_S(s)$ and $D_L(s)$ are equal to the poles of $Z_S(s)$ and $Z_L(s)$, respectively. Substitution of (7) into (6), manipulating, and suppressing the "*(s)*" portions of each term yields

$$V = \frac{N_L D_S V_S + N_S D_L V_L}{N_L D_S + N_S D_L} \qquad (8)$$

Assuming that the load operates in a stable fashion if supplied from an infinite source, N_L will not have any roots in the right half plane. Likewise, assuming that the source can operate in a stable fashion if supplying a constant current load, then D_S will not have any roots in the right half plane. Factoring these terms from the denominator of (8) yields

$$V = \frac{N_L D_S V_S + N_S D_L V_L}{N_L D_S (1 + Z_S Y_L)} \qquad (9)$$

where Y_L is the load admittance ($1/Z_L$). Since neither N_L or D_S have any roots in the right half plane, then the system is stable as long as $1 + Z_S Y_L$ does not have any zeros in the right half plane. Therefore, the number of unstable poles of the closed loop system is equal to the number of clockwise encirclements of -1 made by the Nyquist contour of $Z_S Y_L$.

2.6 Stability Criteria

There are several methods for ensuring that the Nyquist contour of $Z_S Y_L$ does not encircle the -1 point, thereby guaranteeing system stability. They are shown in Figure 2-9 and include Middlebrook, Opposing Argument, Gain Margin/Phase Margin, and ESAC. They range from most to least conservative, respectively, in terms of stability, but all guarantee stability. Each criterion states that as long as the Nyquist contour of the system does not enter the forbidden region, then the contour does not encircle the -1 point and the system is stable. For the Middlebrook criterion, the forbidden region is anywhere outside of a circle with radius $1/GM$, where GM is the gain margin. This constraint provides for a design criterion in that for a given Z_S the range of allowable Y_L is established according to

$$|Y_L| < \frac{1}{|Z_S| GM} \qquad (10)$$

This is highly overconservative, although it does lead to a bound on the load admittance magnitude via (10) which can then be used as a design specification. The Opposing Argument Criterion has a forbidden region to the left of the line at $s = -1/GM$. The GMPM and ESAC criteria are increasingly less conservative. The ESAC criterion has a further advantage in that components do not have to be appropriately grouped in order to determine stability, but can be grouped within the components in which they physically reside.

Figure 2-9. Stability Criteria[20]
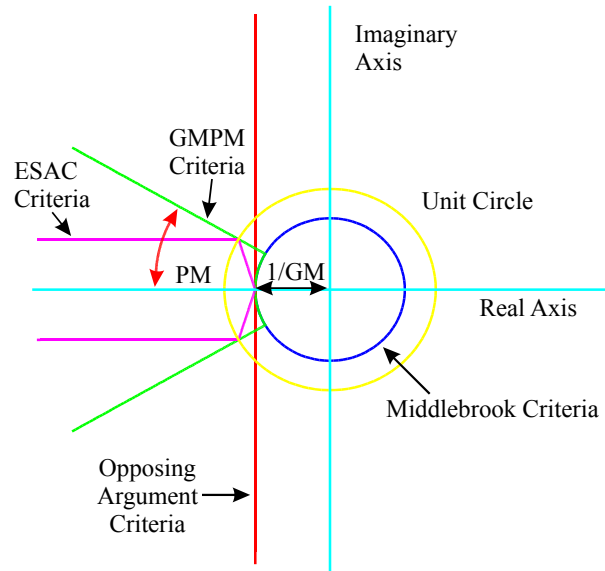
2.7 Formulation of a Load Admittance Constraint and Load Admittance Plot

In order to use the ESAC criterion for design, a straightforward method for deriving the design constraint must be used. Sudhoff sets forth a methodology[21] for accomplishing this task and has also created a DC Stability Toolbox for MATLAB to automate much of the stability analysis. The first step is to develop a stability constraint in terms of three dimensional admittance space, in which the three axes are frequency (x), phase (y), and magnitude (z). Figure 2-10 shows the ESAC criterion stability constraint along with the Nyquist contour of an arbitrary source impedance.

Figure 2-10. Construction of Admittance Constraint at a Particular Frequency[22]
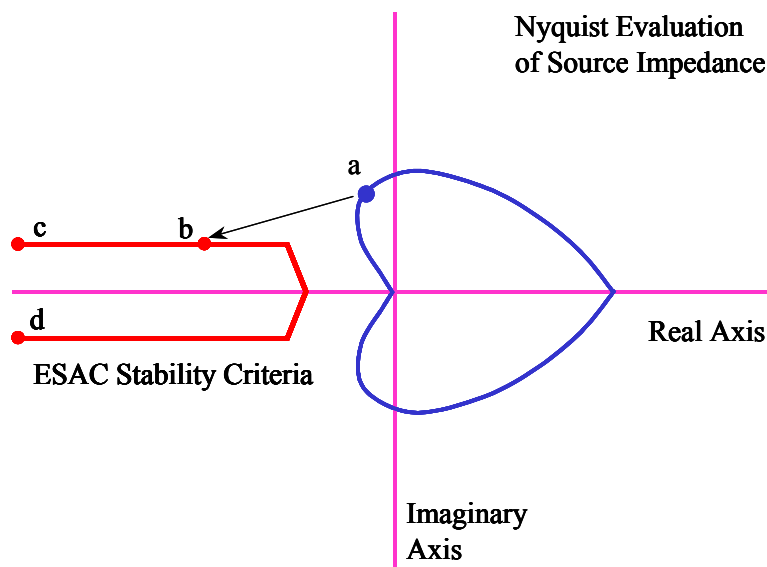
Point *a* corresponds to the value of source impedance at a certain frequency, f_a. Point *b* represents a point on the stability criterion. The load admittance that will cause the Nyquist contour of $Z_S Y_l$ to touch the stability criterion curve at point *b* at a frequency f_a is given by

$$Y_{l,ab} = \frac{b}{Z_{s,a}}$$

(11)

By sweeping point *b* over the entire stability constraint curve a constraint is placed on the load admittance at frequency f_a as depicted in Figure 2-11.

Figure 2-11. Admittance Constraint at a Particular Frequency[23]
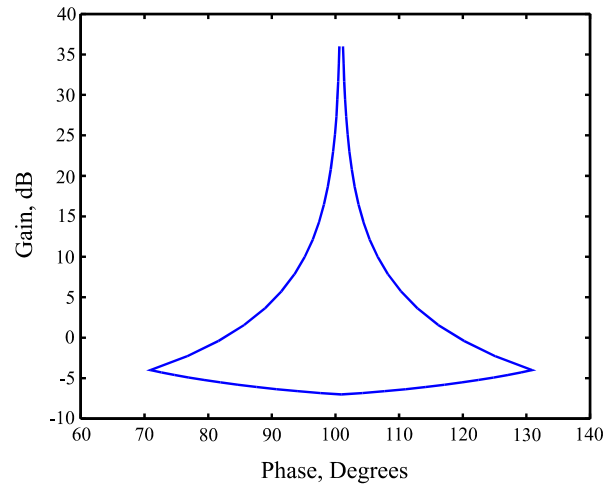
Repeating this process over all frequencies of interest results in the three-dimensional load admittance constraint curve depicted in Figure 2-12.

Figure 2-12. Admittance Constraint in Admittance Space[24]
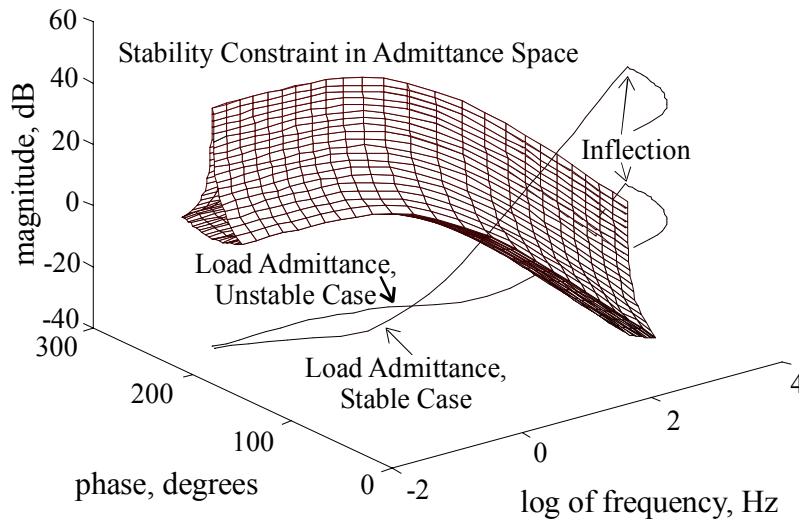
The constraint curve is now complete. The final step is to plot the three-dimensional load admittance curve. In order to meet the constraint and thus be stable at all frequencies, the load admittance curve must fall outside of the enclosed volume. Two cases are shown in Figure 2-12. The unstable case passes through the forbidden region and is unacceptable as a design. The stable case does not pass through the forbidden region and therefore meets the requirements for stability.

This technique can be generalized to nonlinear and uncertain systems. This is achieved by representing the source impedance and load admittance as generalized sets, which encompass the full range of possible operating conditions. The source/load is characterized over all combinations of operating conditions and possible parameter values (accounting for system uncertainty) and then the result is bounded. The region enclosed by this boundary is the generalized impedance/admittance. To illustrate with an example, the generalized impedance of a generator rectifier was constructed using the following procedure[25]. Nominal angular velocities were defined in 5 increments for the range of 228-279 rad/s, as were output voltages in 5 increments for 380-420 V, and output powers in 5 increments for 0-4.07 kW. The plant was then linearized about every combination of speed, voltage, and output power, yielding a set of 125 operating conditions for the generator rectifier. This resulted in a set of 125 source impedances, which was then bounded, giving the generalized source impedance of the rectifier. The final construction is depicted in Figure 2-13.

Figure 2-13 Generalized Source Impedance of a Generator Rectifier[26]
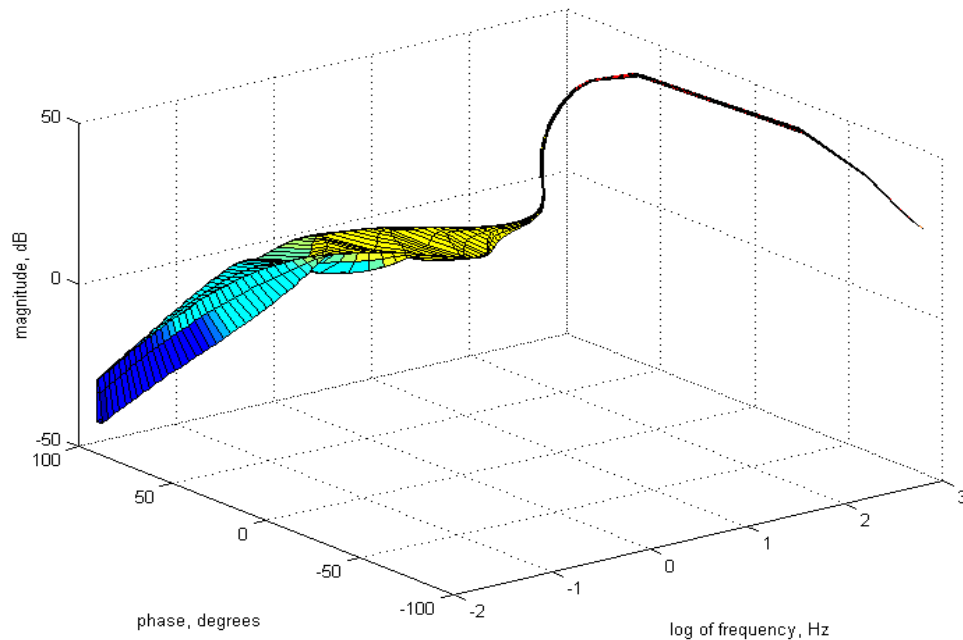
Now the two procedures can be put together. An impedance/admittance constraint is constructed in an appropriate manner as illustrated above. Then the generalized impedance/admittance of the source or load is constructed on the same plot. Analysis is rather simple. If the two volumes intersect, the system is potentially unstable. If they do not intersect, the system is guaranteed to be stable. Note that satisfying the stability criterion is a sufficient but not necessary condition for stability. It is possible for the system to be stable even though the impedance/admittance volume intersects with its corresponding constraint. For further clarification, consider the example system in Figure 2-14.

Figure 2-14. Example System[27]
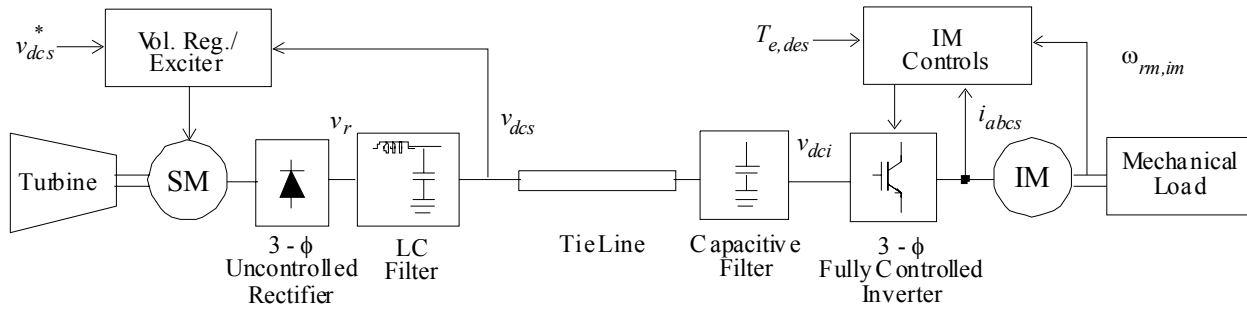
In this system, analysis of the stability between the tie line and the induction motor drive (abbreviated "IM" in Figure 2-14) is briefly set forth. The generalized load admittance was obtained from linearizing every combination from the set of angular velocities (ranging from 0-200 rad/s in 6 steps), torque commands (0-20.9 Nm in 6 steps), and input voltage (380-420 V in 6 steps) for a total of 216 different plants.[28] Figure 2-15 depicts the load admittance constraint and generalized load admittance using the ESAC criterion with a 3 dB gain margin and 20° phase margin. From this diagram, it is apparent that instability could result because of the intersection of the load admittance with the constraint.

Figure 2-15. Load Admittance Constraint with Generalized Load Admittance for Tie Line and Induction Motor Drive[29]
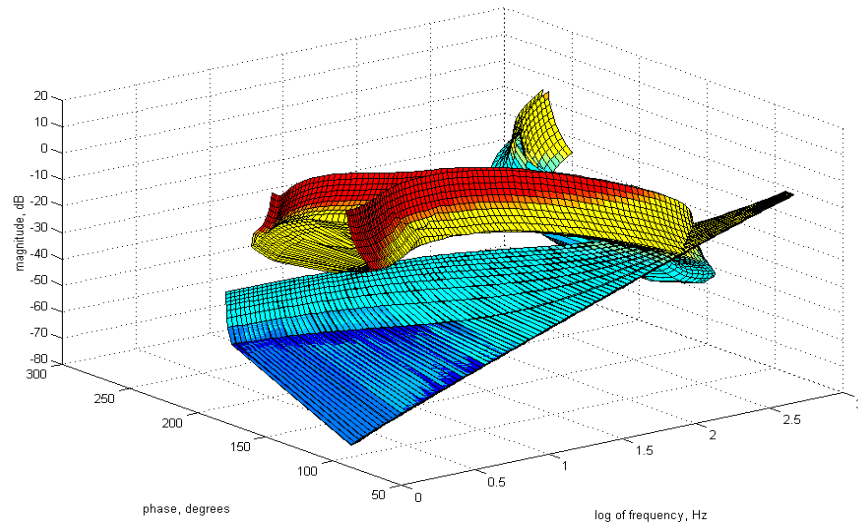

Figure 2-3 depicts the measured system performance during a ramp increase in torque command. Actual current matches almost perfectly commanded current, however, the DC bus voltage is driven to instability. In order to correct the stability problem, stabilizing control is incorporated to alter the generalized load admittance volume and keep it clear of the constraint.[30] Figure 2-16 shows the new generalized load admittance and unchanged constraint volume, which do not intersect (the appearance of an intersection is a line of sight effect). As seen in Figure 2-17, the DC bus voltage now remains stable throughout operation.

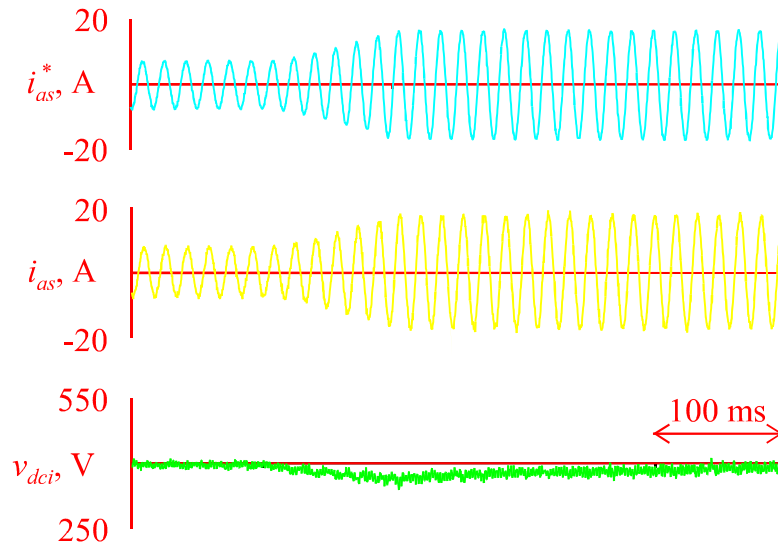Figure 2-16. Load Admittance Constraint and Generalized Admittance when utilizing Stabilizing Control[31]
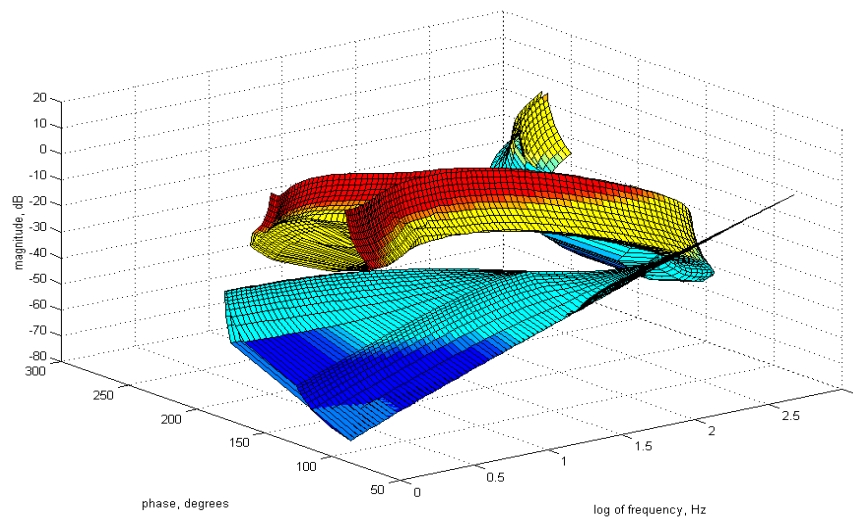
Figure 2-17. Simulated System Performance During a Ramped Torque Command with Stabilizing Control[32]


2.8 Analyzing Systems – Reduction to a Single Source and Load

Thus far stability analysis has been focused on a single source and load only. An approach must be set forth to analyze a power system with multiple, interconnected components. This is accomplished via several steps by reducing the system into an equivalent, single source/single load model. Reduction is achieved by the combination of one component with another and running stability sub-tests to determine if the combination is stable. If the sub-tests pass, then the combination is stable and further reductions to the system can be made. If any sub-test fails, the combination (and therefore the system) is potentially unstable. Each component of the power system can be classified as some type of "converter." The definitions and combinations are set forth by Professor Sudhoff in his Stability Toolbox[33]. The converter definitions are as follows:

S-converters: These devices physically often represent sources and are stable if connected to a constant current source.
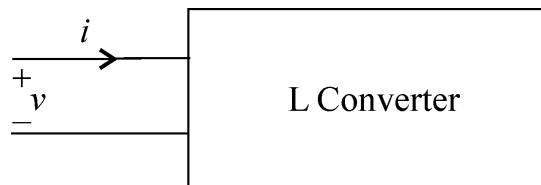
Figure 2-18. S-converter
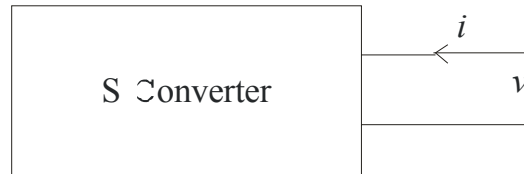
$$\frac{v}{i} = S = \frac{N_S}{D_S}$$

Roots of D_S in LHP

L-converters: These devices often physically represent loads and are stable if connected to a constant current source.
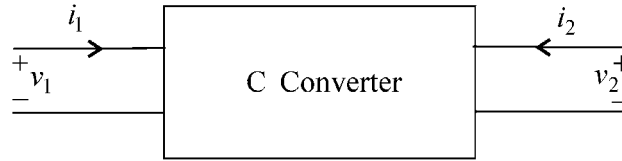
Figure 2-19. L-converter

$$\frac{i}{v} = L = \frac{N_L}{D_L}$$

Roots of D_L in LHP

C-converters: Are cables between converters.
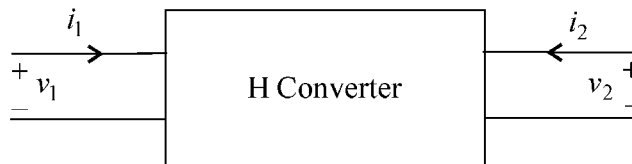
Figure 2-20. C-converter

$$i_1 = -i_2 = C(v_1 - v_2) = \frac{N_C}{D_C}\left(v_1 - v_2\right)$$

Roots of D_c in LHP

H-converters: Usually interface between two converters and are stable if Port 1 is fed by a voltage source and Port 2 is fed by a current source.

Figure 2-21. H-converter

$$\begin{bmatrix} v_2 \\ i_1 \end{bmatrix} = \begin{bmatrix} H_{11} & H_{12} \\ H_{21} & H_{22} \end{bmatrix} \begin{bmatrix} v_1 \\ i_2 \end{bmatrix}$$

$$\begin{bmatrix} v_2 \\ i_1 \end{bmatrix} = \begin{bmatrix} \dfrac{N_{h11}}{D_h} & \dfrac{N_{h12}}{D_h} \\ \dfrac{N_{h12}}{D_h} & \dfrac{N_{h22}}{D_h} \end{bmatrix} \begin{bmatrix} v_1 \\ i_2 \end{bmatrix}$$

Roots of D_h in LHP

H'-converters: Are special cases of H converters in which Port 2 outputs can be paralleled. H'-converters are H converters in which the roots of N_{22} are in the left half plane.

Y-converters: Physically represent a load fed from two buses and are stable if both ports are fed from ideal voltage sources.
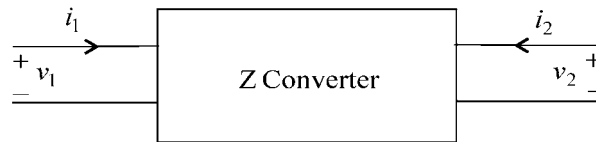
Figure 2-22. Y-converter
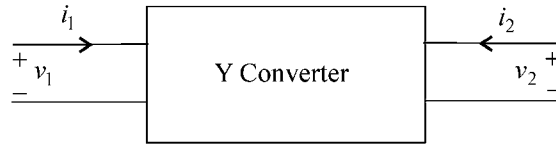
$$\begin{bmatrix} i_1 \\ i_2 \end{bmatrix} = \begin{bmatrix} Y_{11} & Y_{12} \\ Y_{21} & Y_{22} \end{bmatrix} \begin{bmatrix} v_1 \\ v_2 \end{bmatrix}$$

$$\begin{bmatrix} i_1 \\ i_2 \end{bmatrix} = \begin{bmatrix} \dfrac{N_{y11}}{D_y} & \dfrac{N_{y12}}{D_y} \\ \dfrac{N_{y21}}{D_y} & \dfrac{N_{y22}}{D_y} \end{bmatrix} \begin{bmatrix} v_1 \\ v_2 \end{bmatrix}$$

Roots of D_y in LHP

Z-converters: Physically represent a dual output source and is stable if both ports are connected to a constant current source.

Figure 2-23. Z-converter

$$\begin{bmatrix} v_1 \\ v_2 \end{bmatrix} = \begin{bmatrix} Z_{11} & Z_{12} \\ Z_{21} & Z_{22} \end{bmatrix} \begin{bmatrix} i_1 \\ i_2 \end{bmatrix}$$

$$\begin{bmatrix} v_1 \\ v_2 \end{bmatrix} = \begin{bmatrix} \dfrac{N_{z11}}{D_z} & \dfrac{N_{z12}}{D_z} \\ \dfrac{N_{z21}}{D_z} & \dfrac{N_{z22}}{D_z} \end{bmatrix} \begin{bmatrix} i_1 \\ i_2 \end{bmatrix}$$

Roots of D_z in LHP

2.9 Converter Combinations

The definitions in Section 2.8 can be used to describe the different components of the DC ZED System. Accordingly, they can be combined using the process of *mapping* to reduce the system to fewer, but equivalent, components. For each reduction, a stability test is often required to see if the components can be grouped together. By repeatedly applying mappings, the system can be

reduced to an equivalent system with a single source and single load. The DC Stability Toolbox provides functions that perform the mappings and stability tests automatically. An error message is generated if two components cannot be grouped together due to a potential instability. Appendix G explains the mapping functions provided by the toolbox. They are listed here:

Source—Cable…..……..Source
Load—Cable…………..Load
H—Load……………...Load
Source—H…………....Source
Parallel Loads………...Load
Parallel Y's…………...Y
H—Load—H'………....Y
Y—Source………..…...Load
Y……………………...Load
Source—Source……….Source

2.10 Reduction and Analysis of the DC-ZED System

This section reduces and analyzes the full configuration of the DC-ZED System. Parameter values are those listed in Appendix A. Refer to Appendix C for the MATLAB source code. Each zone is reduced to an equivalent converter and stability tests are performed. The result is three converters in parallel. These are combined to one equivalent converter, which is then combined with the right power supply to form an equivalent load. This leaves a single power source (the left power supply) with a single, equivalent load. The final stability test is then performed and evaluated. Details of the reduction follow.

Figure 2-24. DC-ZED System
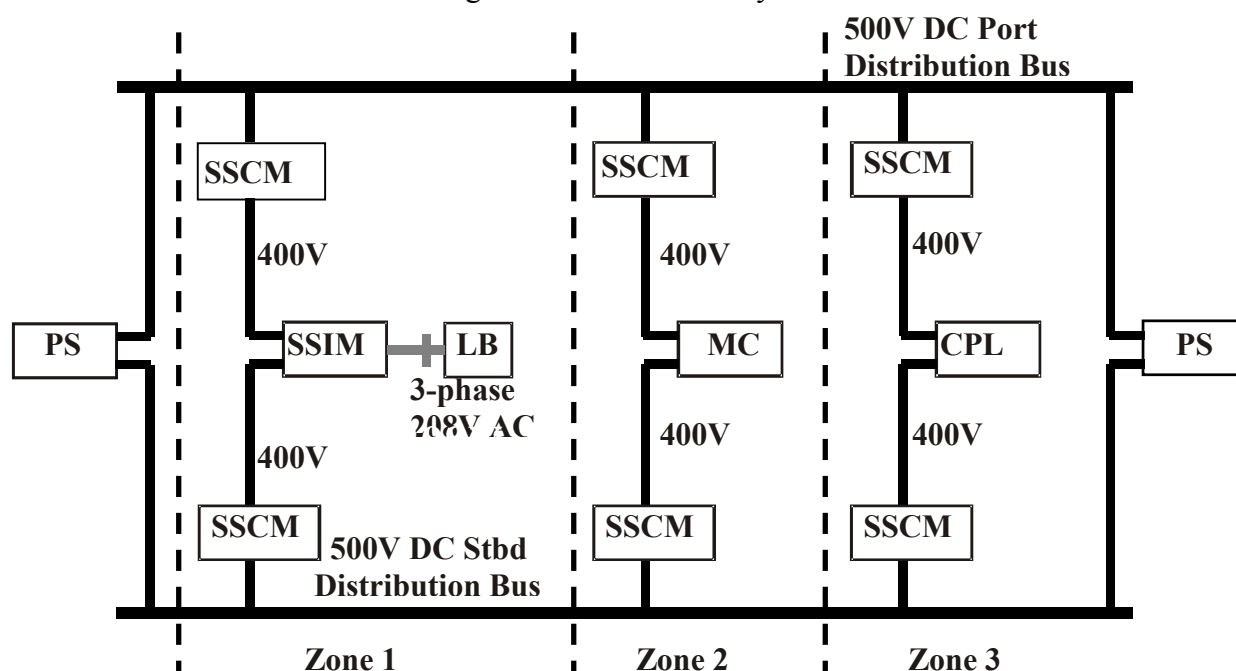
All three zones (zones one through three) are in the configuration of an H converter (SSCM, or PCM1) and an H' converter (other SSCM) feeding into a load (the component between the two SSCMs, i.e. SSIM, MC, or CPL). Using Professor Sudhoff's Stability Toolbox command **HLHp_to_Y**, all three zones are reduced to equivalent Y converters. Two stability subtests are required for each zone. The tests for Zone 1 are: 1) PCM1_H12 as the source and PCM1_H12inv as the load, 2) parallel combination of PCM1_H12 with the other PCM1_H12 as the source and the SSIM, or PCM2_L, as the load. The two graphs of the stability curves and their constraints are shown in Figures 2-25 and 2-26.

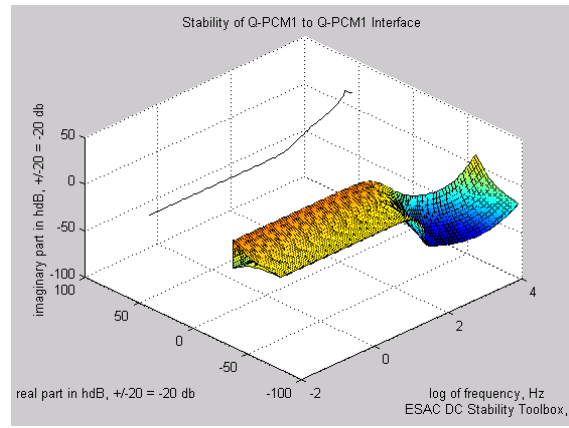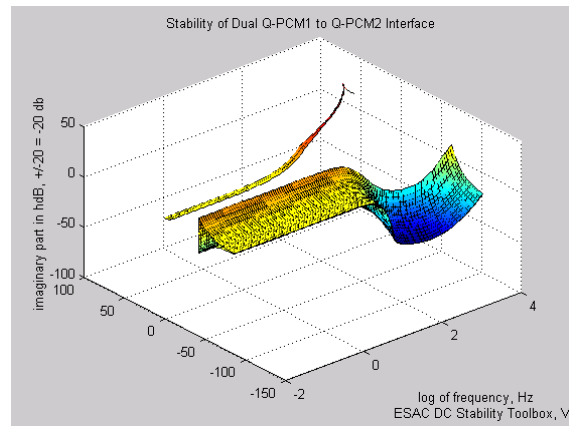Figure 2-25. Zone 1 – Stability of Q-PCM1 to Q-PCM1 Interface

Figure 2-26. Zone 1 – Stability of Dual Q-PCM1 to Q-PCM2 Interface

For Zone 2, the stability subtests are: 1) PCM1_H12 as the source and PCM1_H12inv as the load, 2) parallel combination of PCM1_H12 with the other PCM1_H12 as the source and the MC, or MC_L, as the load. Results are shown in Figures 2-27 and 2-28.

Figure 2-27. Zone 2 – Stability Q-PCM1 to Q-PCM1 Interface
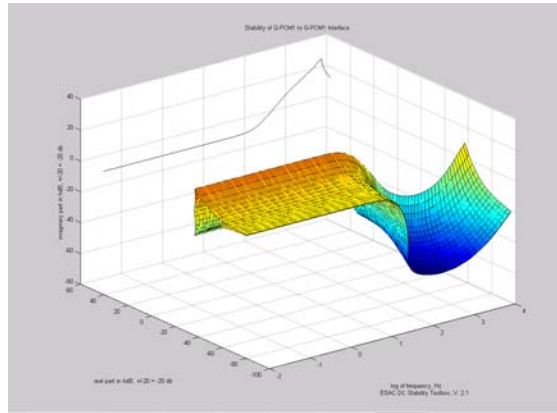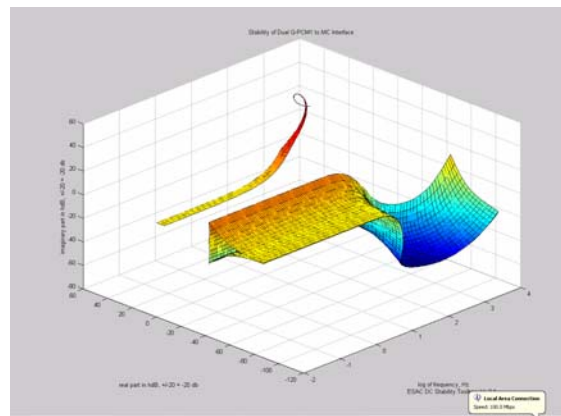

Figure 2-28. Zone 2 – Stability of Dual Q-PCM1 to MC Interface

For Zone 3, the stability subtests are: 1) PCM1_H12 as the source and PCM1_H12inv as the load, 2) parallel combination of PCM1_H12 with the other PCM1_H12 as the source and the CPL, or CPL_L, as the load. Results are shown in Figures 2-29 and 2-30.

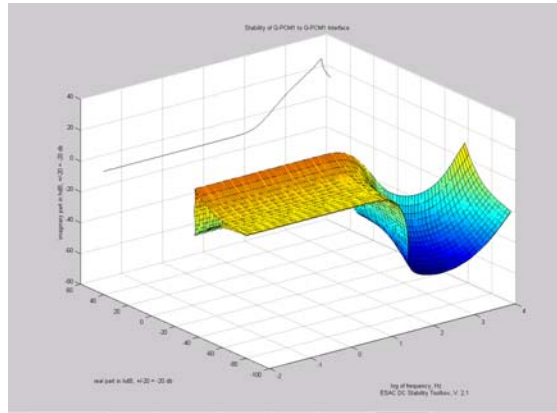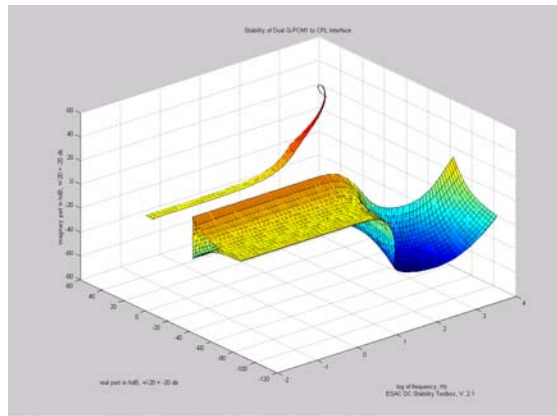Figure 2-29. Zone 3 – Stability of Q-PCM1 to Q-PCM1 Interface

Figure 2-30. Zone 3 – Stability of Dual Q-PCM1 to CPL Interface

As can be seen from Figures 2-25 to 2-30, there are no intersections in any of the graphs. Therefore, all subtests pass and the combinations are permissible (i.e. are stable). The reduced system is shown in Figure 2-31 and consists of three Y converters in parallel being fed from either side by two power supplies.

Figure 2-31. Reduction One - Equivalent DC-ZED System
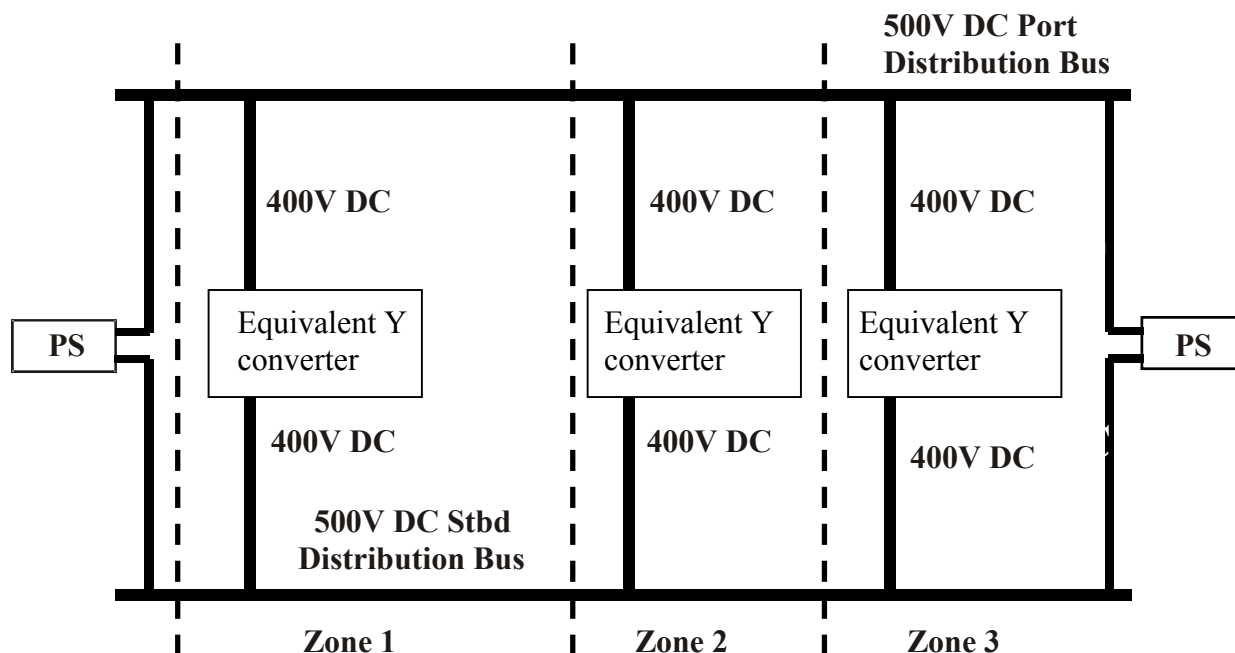
The three Y converters are in parallel, and so they may be combined using **parY_to_Y** into an equivalent Y converter without the need of a stability test. The result is shown in Figure 2-32 and is a system with two power supplies feeding either side of the Y converter.

Figure 2-32. Reduction Two - Equivalent DC-ZED System
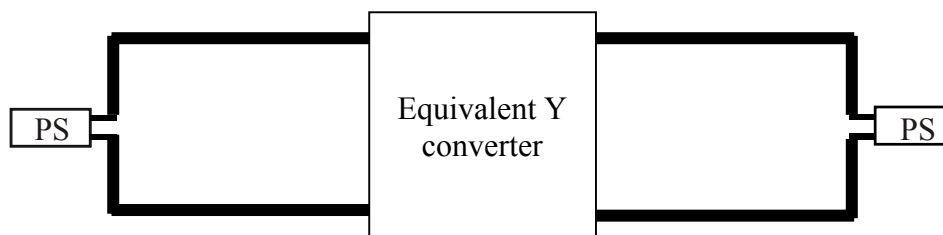
The Y converter and the power supply on the right may be combined into an equivalent L converter (load) using **YS_to_L**. A stability subtest is required – the power supply (PCM4_S) as the source and Y_{22} (AgZ_Y22) as the load. The result of the stability test is shown in Figure 2-33.

Figure 2-33. Stability of Three Zonal Load and Starboard Power Supply Interface
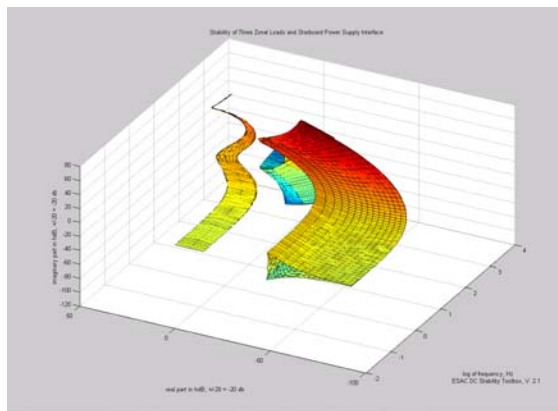

The final reduction is shown in Figure 2-34 and is a single source feeding a single load that is equivalent to the entire original system.   For emphasis, Figure 2-24 and Figure 2-34 are mathematically equivalent for analysis purposes.

Figure 2-34. Final Reduction - Equivalent DC-ZED System
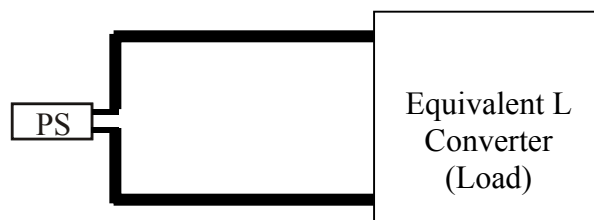
The final stability test that is required is the power supply as the source and the equivalent L converter (AgZplusPCM4_L) as the load.   The technique is the same as the one described in section 2.7 for a single source, single load system.   If the final test and all subtests prove stable, then the system is guaranteed to be stable.   If any test fails, then the system cannot be shown to be stable.   The final stability test is shown in Figure 2-35.   There are no intersections in any of the graphs and the system is therefore stable.

Figure 2-35. Stability of Port PCM4 with Equivalent Load
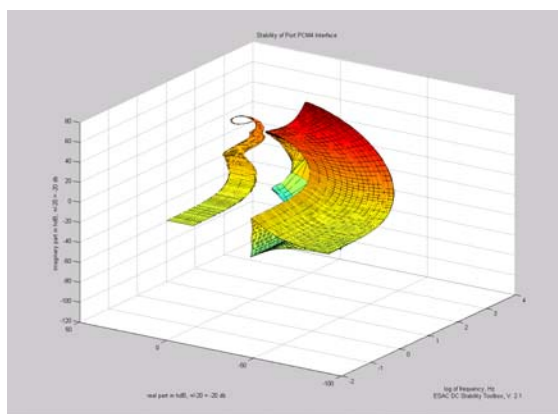
3 Data

Three system configurations were tested: the full configuration, the system with one bus and power supply removed, and the system with one bus removed. The second configuration simulates a casualty condition where one bus and power supply have been lost. The third configuration simulates a casualty condition where one bus has been lost, but both power supplies are still in operation. A gain margin of 3 dB and phase margin of 20 degrees was considered sufficient to guarantee stability. With each configuration, capacitance values and stabilizing control gain, K_{sf}, were varied to determine the influence of each parameter on system stability. Results are summarized in Appendix I.

3.1 Full Configuration

This is the system that was described in section 2.10.

1. Power Supply (PS) Capacitance Decreased 95%

Figure 3-1. Zone 1 – Stability of Q-PCM1 to Q-PCM1 Interface
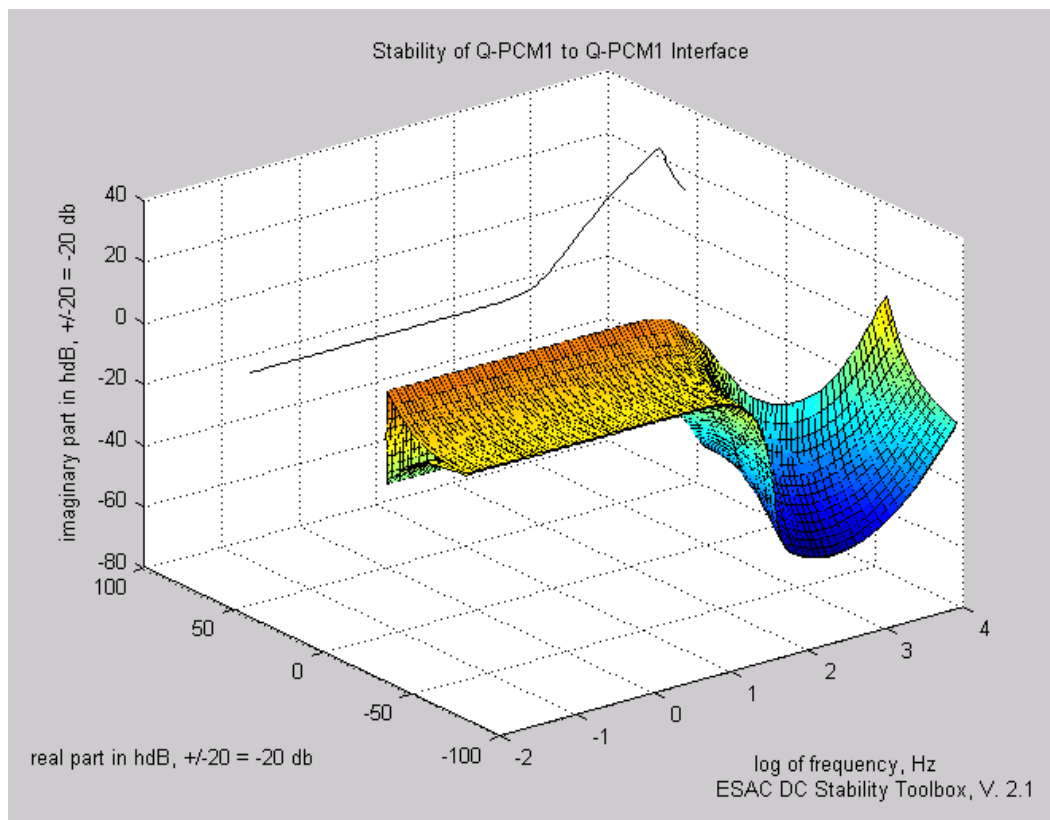
Note: All figures have the same axes.

Figure 3-2.   Zone 1 – Stability of Dual Q-PCM1 to Q-PCM2 Interface
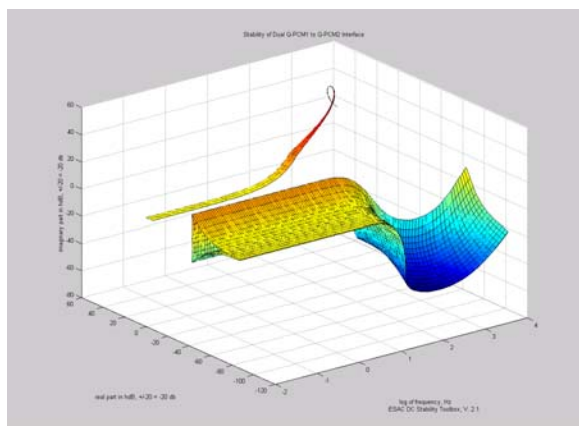

Figure 3-3.   Zone 2 – Stability of Dual Q-PCM1 to MC Interface
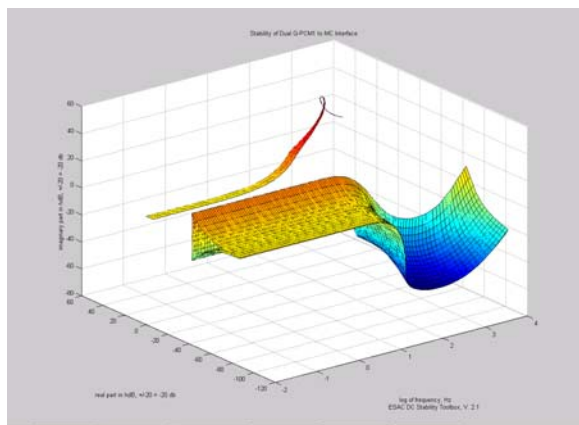
Figure 3-4.   Zone 3 – Stability of Dual Q-PCM1 to CPL Interface

Figure 3-5.   Stability of Three Zonal Load and Starboard Power Supply Interface
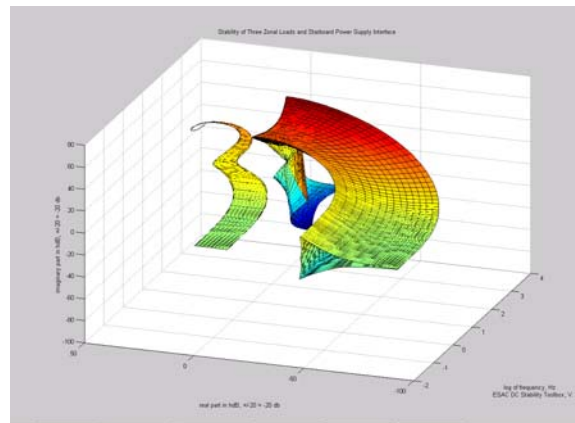
Figure 3-6.   Stability of Port PCM4 with Equivalent Load
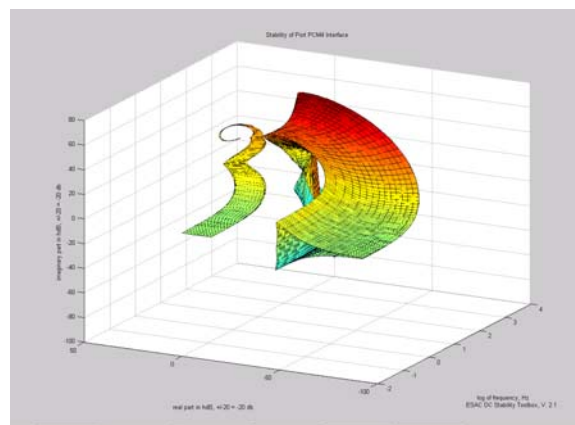
The two PCM stability tests from Zone 2 and Zone 3 are not shown because these results are identical to the Zone 1 Q-PCM1 to Q-PCM1 interface stability test. Upon inspection, no admittance space intersects with its constraint. Therefore, all subtests pass thereby guaranteeing system stability for all operating conditions. The system is stable.

It turns out that the zonal stability tests do not vary significantly among any of the tested cases. They are hereby omitted from subsequent study results.

2. Ship Service Converter Module (SSCM) Output Capacitance Decreased 90%

Figure 3-7. Stability of Three Zonal Loads and Starboard Power Supply Interface
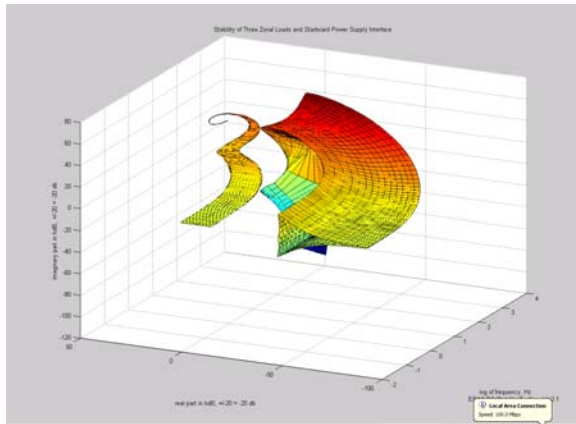
Figure 3-8. Stability of Port PCM4 with Equivalent Load
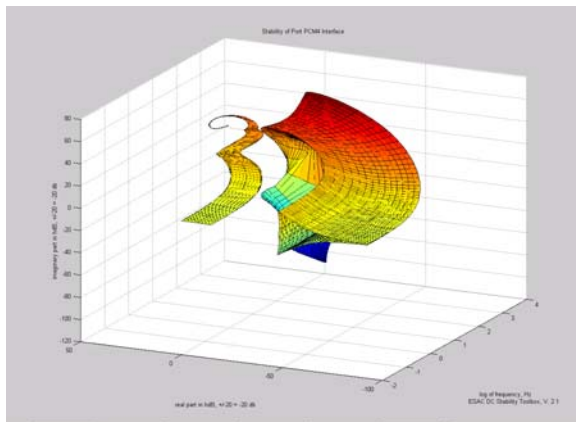
Upon inspection, no curves intersect and the system is therefore stable.

3. Stabilizing Control Gain, K_{sf} is Halved

Figure 3-9. Stability of Three Zonal Loads and Starboard Power Supply Interface
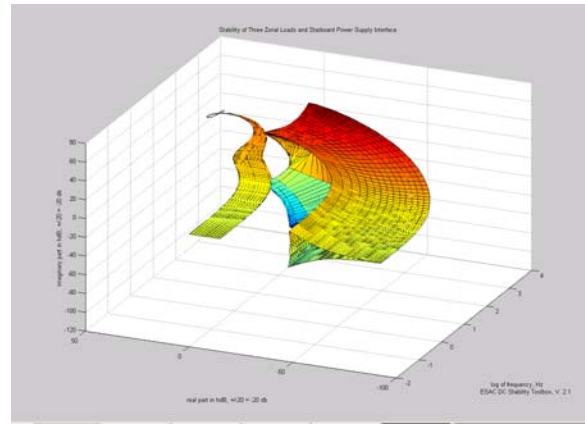
Figure 3-10. Stability of Port PCM4 with Equivalent Load
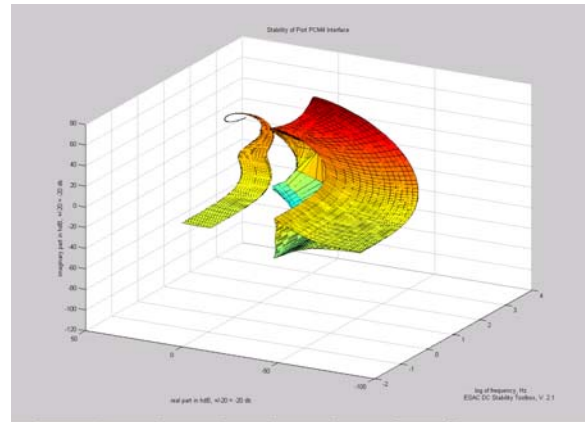
Upon inspection, both curves contain intersections and therefore stability cannot be guaranteed for all operating conditions.

4. *K*$_{sf}$ is Halved, PS Capacitance is Doubled

5. *K*$_{sf}$ is Halved, SSCM Output Capacitance is Doubled

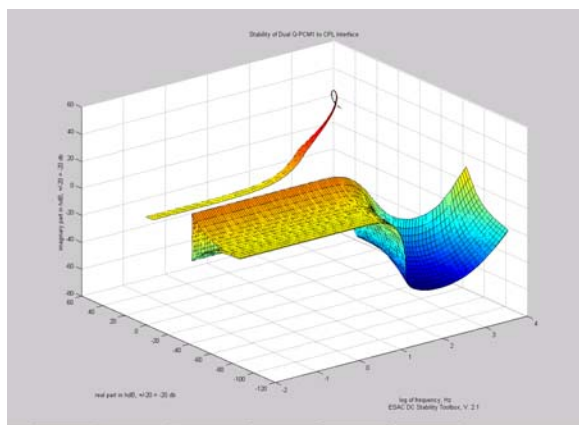Figure 3-11. Stability of Three Zonal Loads and Starboard Power Supply Interface

Figure 3-13. Stability of Three Zonal Loads and Starboard Power Supply Interface
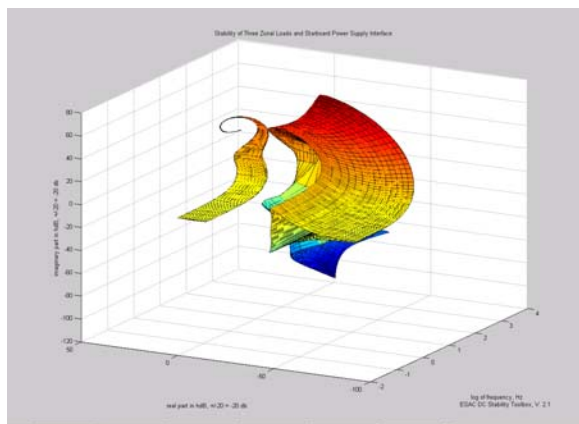
Figure 3-12. Stability of Port PCM4 with Equivalent Load
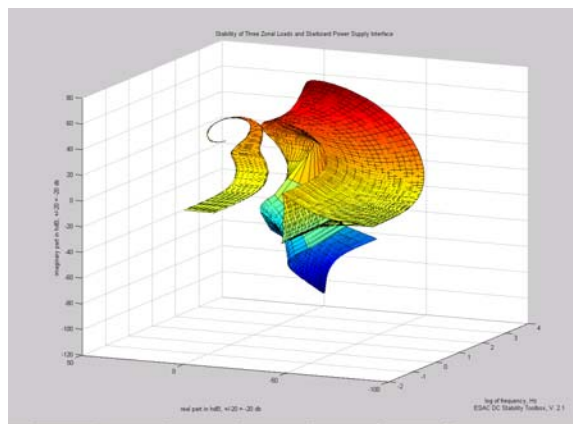
Figure 3-14. Stability of Port PCM4 with Equivalent Load

Neither curve intersects – the system is stable.

System is stable.

6. K_{sf} is Halved, SSCM Input Capacitance is Doubled

Figure 3-15. Stability of Three Zonal Loads and Starboard Power Supply Interface
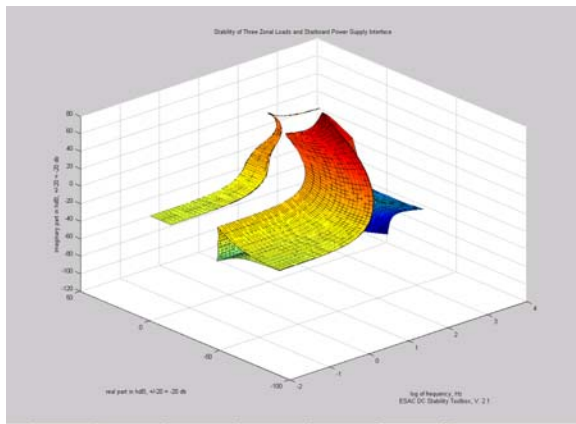
Figure 3-16. Stability of Port PCM4 with Equivalent Load
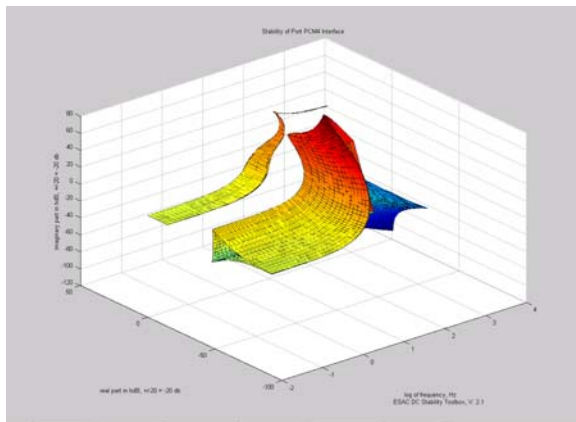
System is stable.

7. K_{sf} is Set to Zero (No Disturbance Propagation)

Figure 3-17. Stability of Three Zonal Loads and Starboard Power Supply Interface

Figure 3-18. Stability of Port PCM4 with Equivalent Load

System is unstable.

8. K_{sf} is Zero, PS Output Capacitance is Increased Tenfold

9. K_{sf} is Zero, SSCM Output Capacitance is Increased Tenfold

Figure 3-19. Stability of Three Zonal Loads and Starboard Power Supply Interface

Figure 3-21. Stability of Three Zonal Loads and Starboard Power Supply Interface

Figure 3-20. Stability of Port PCM4 with Equivalent Load

Figure 3-22. Stability of Port PCM4 with Equivalent Load

System is stable.

System is unstable.

10. K_{sf} is Zero, SSCM Input Capacitance is Increased Tenfold

Figure 3-23.   Stability of Three Zonal Loads and Starboard Power Supply Interface
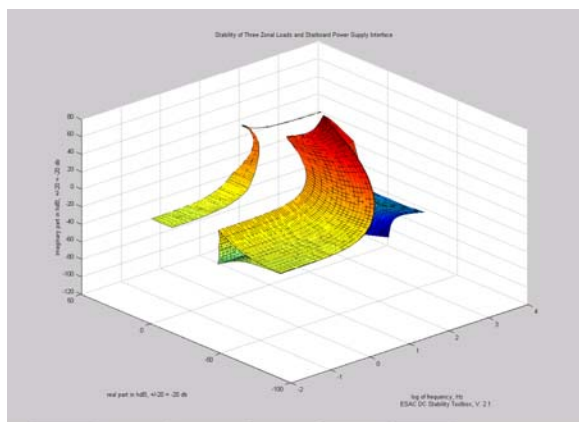
Figure 3-24.   Stability of Port PCM4 with Equivalent Load
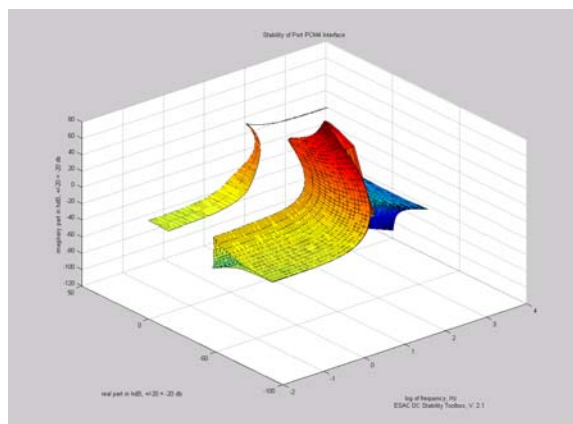
System is stable.

3.2 Alternate Configuration One – Bus and Power Supply Removed

In this scenario, one bus and one power supply has been removed. The system becomes one power supply feeding three zones that consist of an H-converter (SSCM) and an L-converter (individual loads) in series. The H and L converters are combined into 3 different equivalent L-converters (one for each zone with a stability test required for each). The three equivalent L-converters are in parallel and are then combined into an equivalent L-converter with no stability subtest required. Refer to Appendix H for a diagram of the system.

1. No Parameter Change

Figure 3-25. Zone 1 – Stability of Q-PCM1 to Q-PCM2 Interface
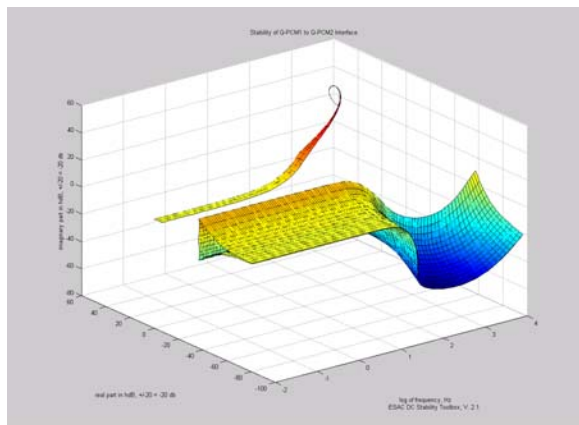
Figure 3-26. Zone 2 – Stability of Q-PCM1 to MC Interface
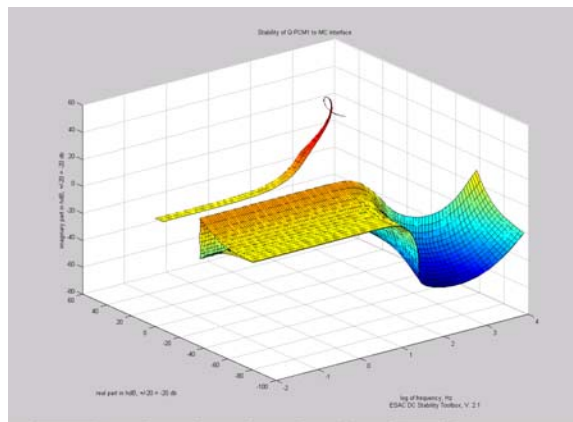
Figure 3-27. Zone 3 – Stability of Q-PCM1 to CPL Interface
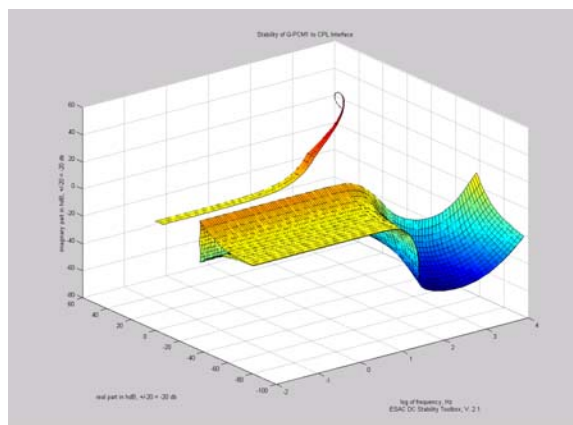
Figure 3-28.   Stability of Port PCM4 with Equivalent Load
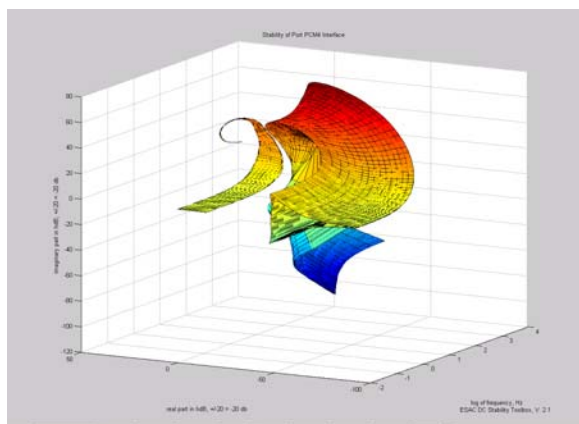
Upon inspection, no impedance space intersects with its constraint. Therefore, all subtests guarantee system stability for all operating conditions. The system is stable.

It turns out that the zonal stability tests do not vary significantly among any of the single bus cases. They are hereby omitted from subsequent study results.

2. PS Capacitance Decreased 50%

Figure 3-29.   Stability of Port PCM4 with Equivalent Load
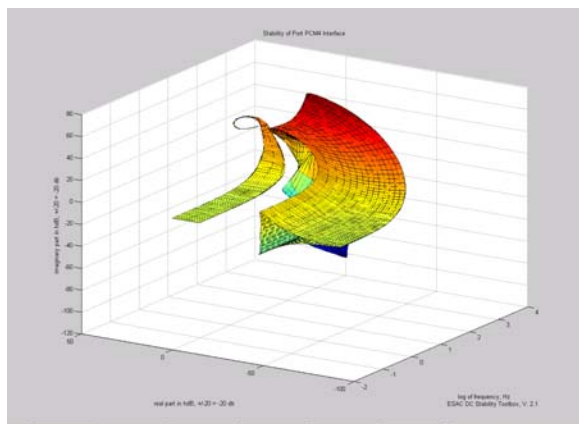
System is nearly stable[*].

3. SSCM Output Capacitance Decreased 25%

Figure 3-30.   Stability of Port PCM4 with Equivalent Load
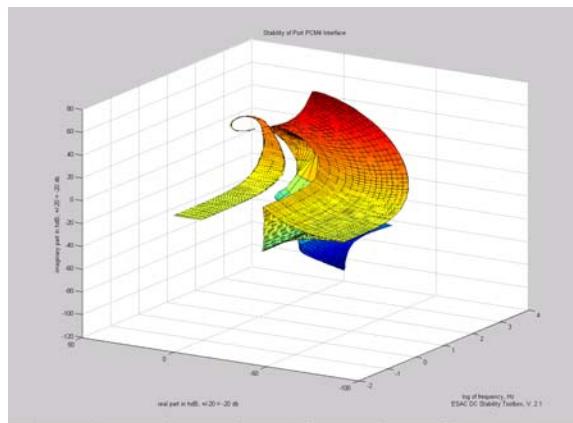
System is nearly stable.

---

[*] Nearly stable as used here indicates that the impedance curve "nicked" the constraint curve, signifying some potential instabilities. The simulation was run again, this time with gain and phase margins of almost zero, and the impedance curve avoided the constraint curve at all frequencies (not shown in the data). The meaning then of "nearly stable" is that the system was stable, but with a gain and/or phase margin of less than 3 dB and 20 degrees, respectively.

4. SSCM Input Capacitance Decreased 90%

Figure 3-31.　Stability of Port PCM4 with Equivalent Load
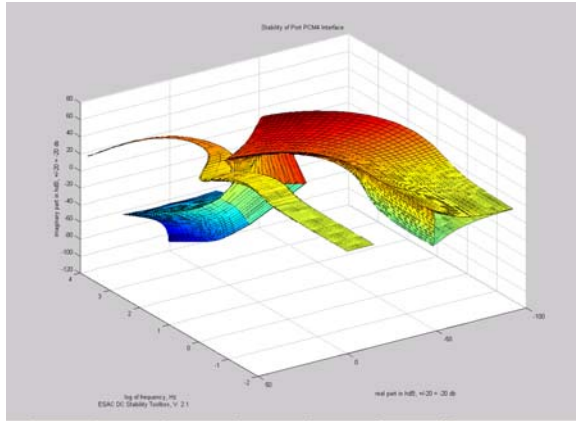
System is stable (the impedance curve misses the constraint curve by a very small amount).

5. K_{sf} is halved

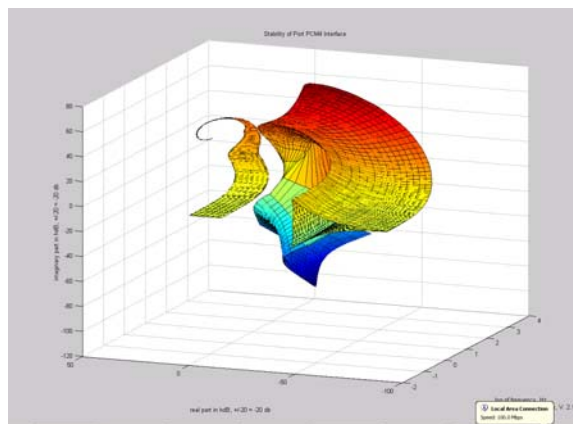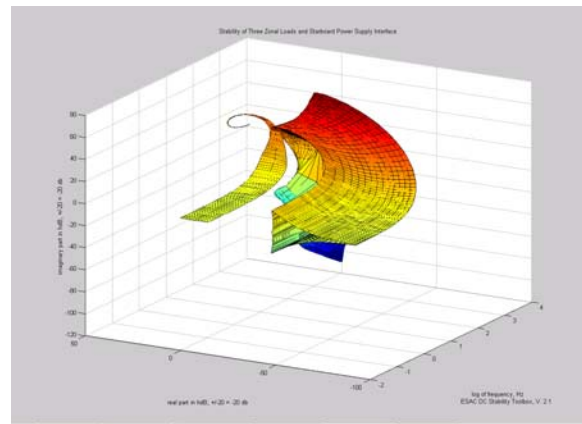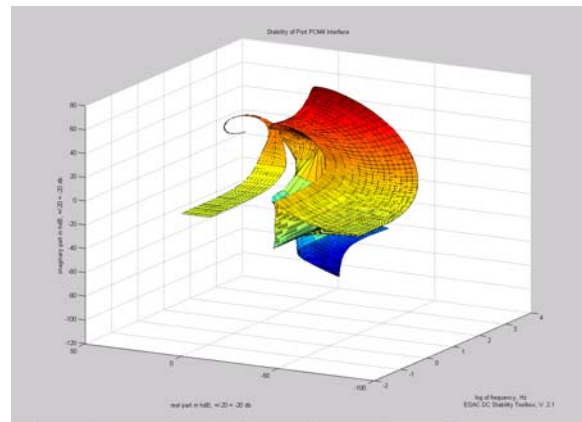Figure 3-32.　Stability of Port PCM4 with Equivalent Load
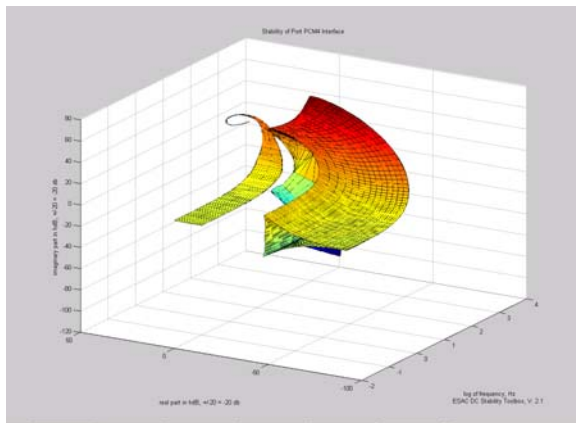
System is unstable.

6.　K_{sf} is Halved, PS Capacitance is Doubled

Figure 3-33.　Stability of Port PCM4 with Equivalent Load
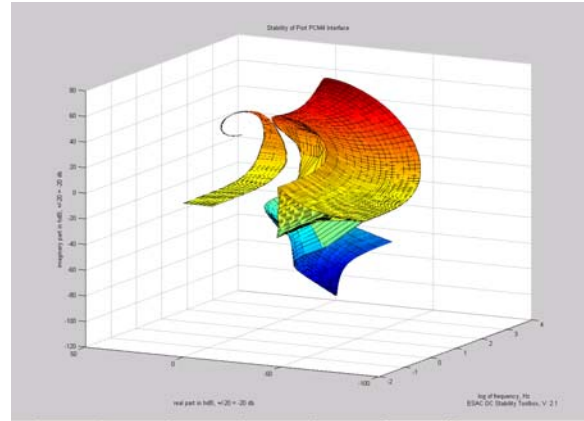
System is stable.

7. K_{sf} is Halved, SSCM Output Capacitance is Doubled

Figure 3-34.　Stability of Port PCM4 with Equivalent Load
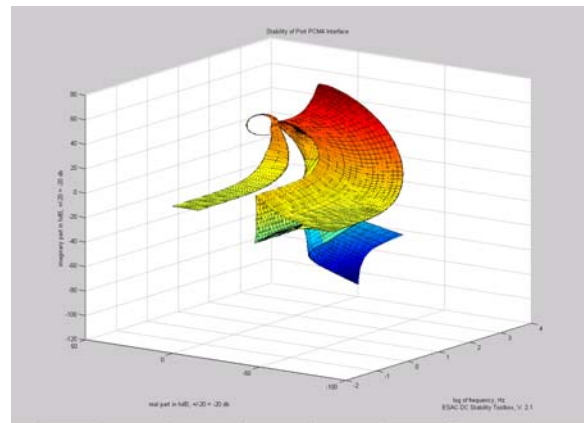
System is nearly stable.

8. K_{sf} is halved, SSCM Input Capacitance is Doubled

Figure 3-35.   Stability of Port PCM4 with Equivalent Load
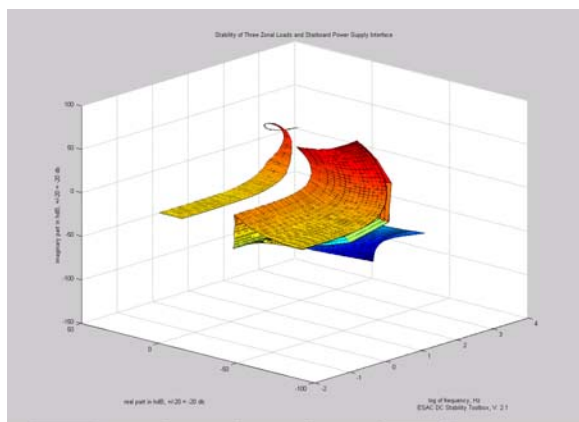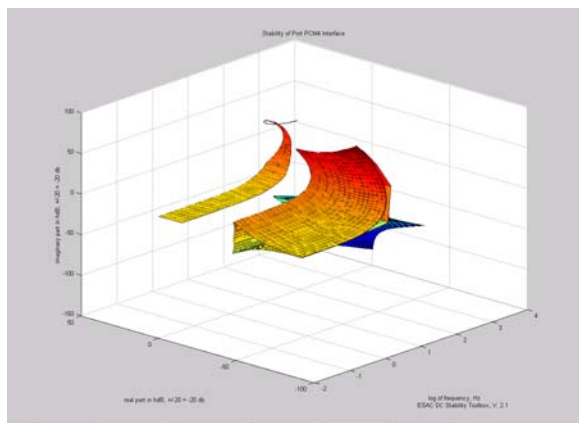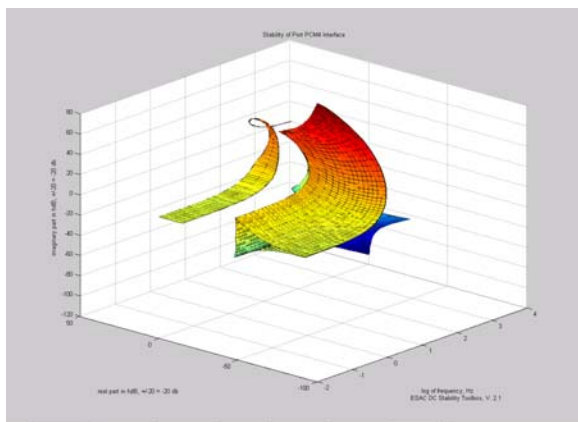

System is stable.

9. K_{sf} is Set to Zero

Figure 3-36.   Stability of Port PCM4 with Equivalent Load
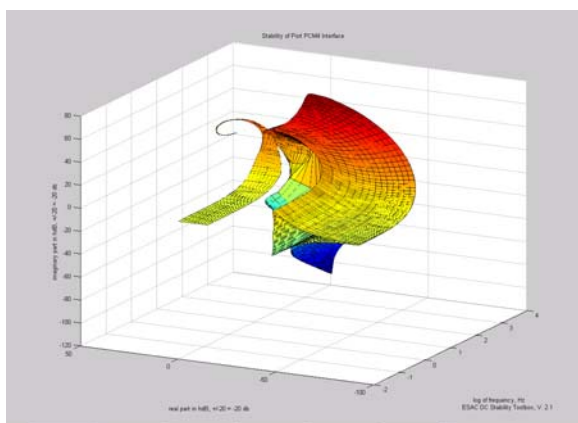
System is unstable.

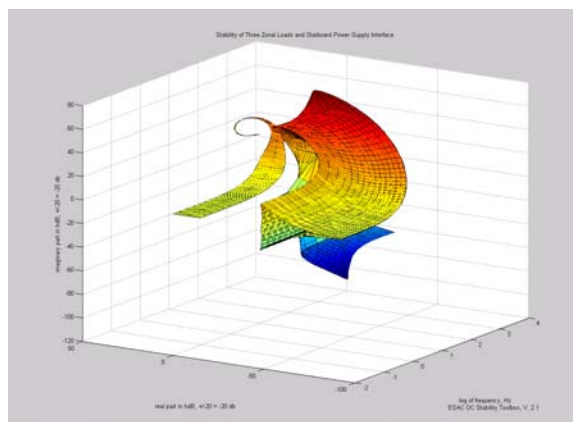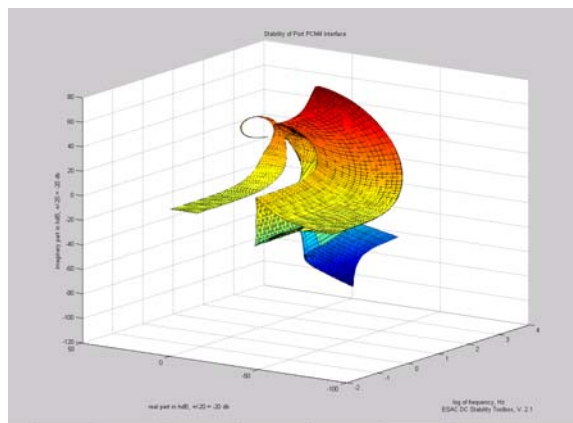10. K_{sf} is Zero, PS Capacitance is Increased Tenfold

Figure 3-37.   Stability of Port PCM4 with Equivalent Load
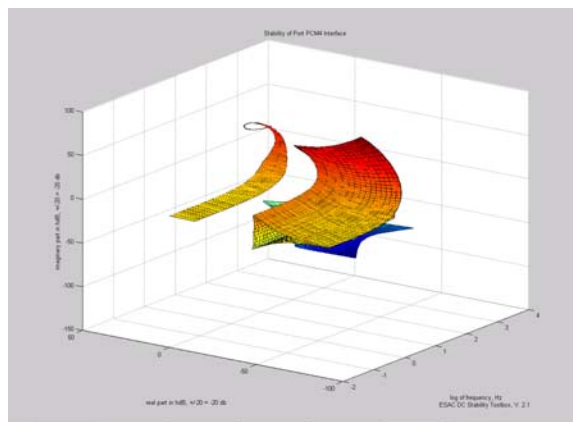
System is stable.

11. K_{sf} is Zero, SSCM Output Capacitance is Increased Tenfold

Figure 3-38.   Stability of Port PCM4 with Equivalent Load
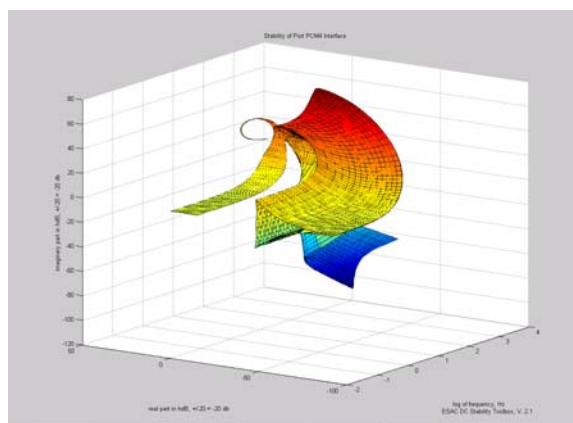
System is unstable.   No amount of output capacitance will stabilize the system.

12. K_{sf} is Zero, SSCM Input Capacitance is Increased Tenfold

Figure 3-39. Stability of Port PCM4 with Equivalent Load
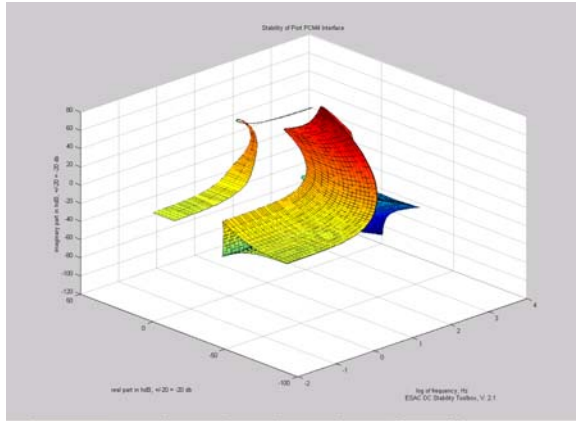
System is stable.

3.3 Alternate Configuration Two – One Bus Removed

In this scenario, a casualty is envisioned where one bus has been lost but both power supplies remain. Both power supplies feed the single operational bus. As in alternate configuration one, the three zones consist of an H-converter (SSCM) and an L-converter (individual loads) in series. The H and L converters are combined into 3 different equivalent L-converters (one for each zone with a stability test required for each). The three equivalent L-converters are in parallel and are then combined into an equivalent L-converter with no stability subtest required. Because the process of reducing the three zones into one equivalent L-converter is identical to that of alternate configuration one, the stability subtests are omitted here. For alternate configuration two, one more reduction is necessary. This step is the combination of the two power supplies in parallel. After these are combined into an equivalent source, the final stability test between the equivalent source and equivalent load is run. Refer to Appendix H for a diagram of the system.

1. No Parameter Change

Figure 3-40. Parallel Sources - Stability of Q-PCM4 to Q-PCM4 Interface
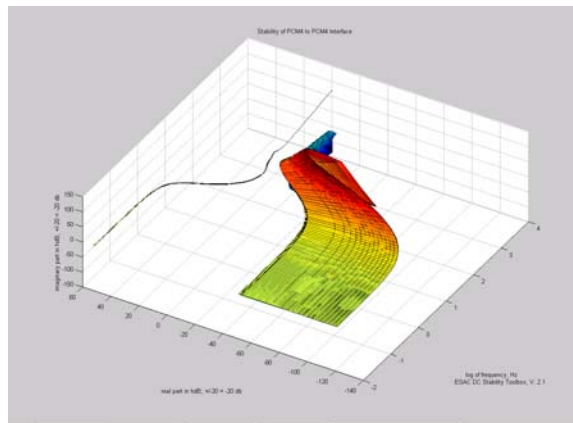
Figure 3-41. Final Test - Stability of Equivalent Source/Equivalent Load
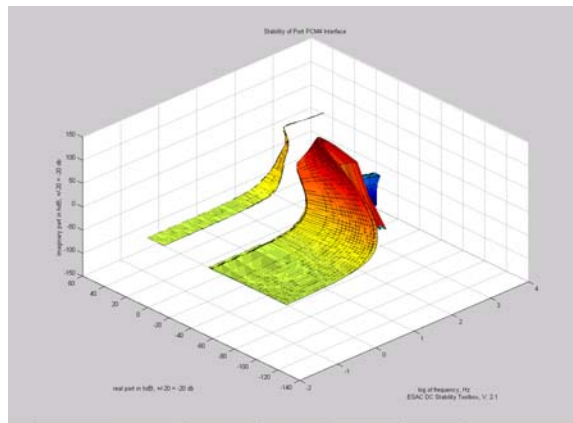
From Figures 3-40 through 3-41, it is clear there are no intersections and the system is stable.

2. PS Capacitance Decreased 90%

3. SSCM Output Capacitance Decreased 90%

Figure 3-42.   Parallel Sources - Stability of Q-PCM4 to Q-PCM4 Interface

Figure 3-44.   Parallel Sources - Stability of Q-PCM4 to Q-PCM4 Interface
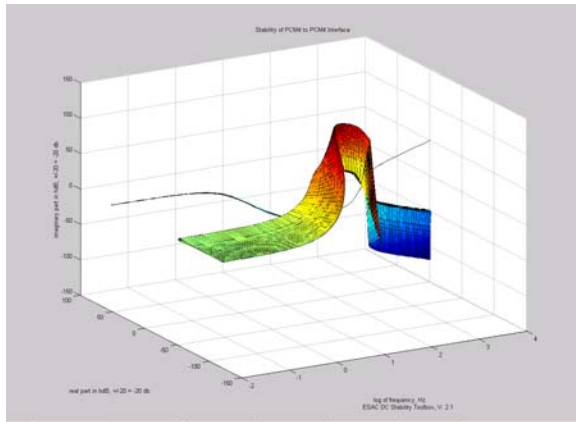
Figure 3-43.   Final Test - Stability of Equivalent Source/Equivalent Load
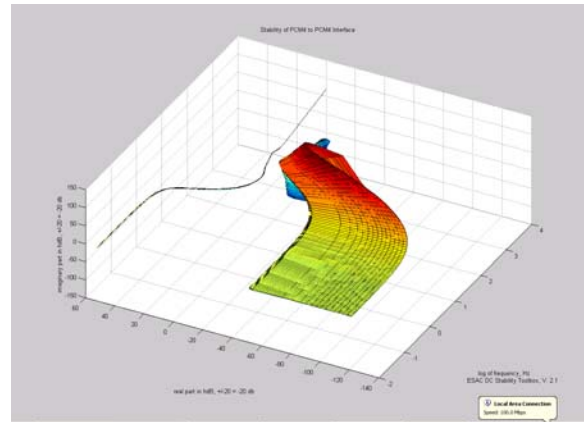
Figure 3-45.   Final Test - Stability of Equivalent Source/Equivalent Load

Upon inspection, no impedance space intersects with its constraint. The apparent intersection in Figure 3-42 is caused by a line-of-sight effect. The system is stable.
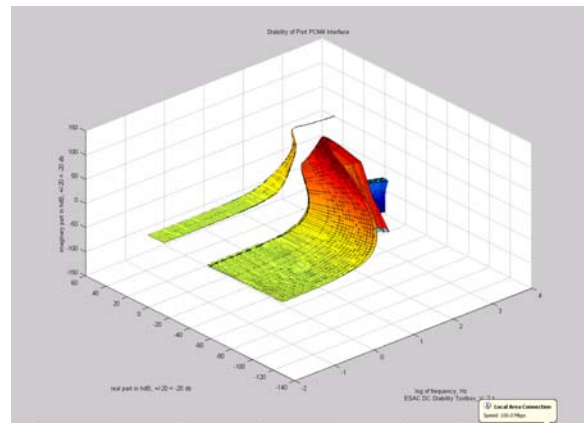
System is stable.

4. SSCM Input Capacitance Decreased 90%

Figure 3-46. Parallel Sources - Stability of Q-PCM4 to Q-PCM4 Interface
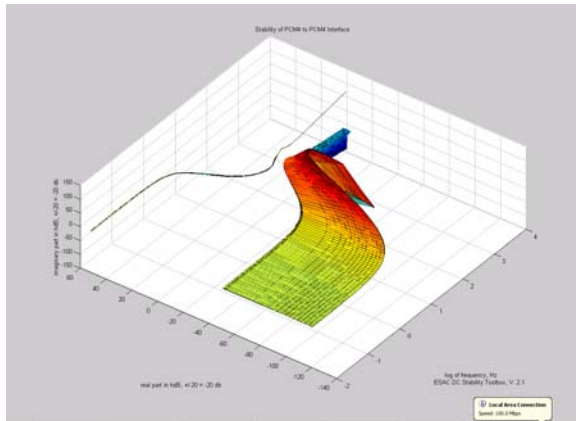
Figure 3-47. Final Test - Stability of Equivalent Source/Equivalent Load
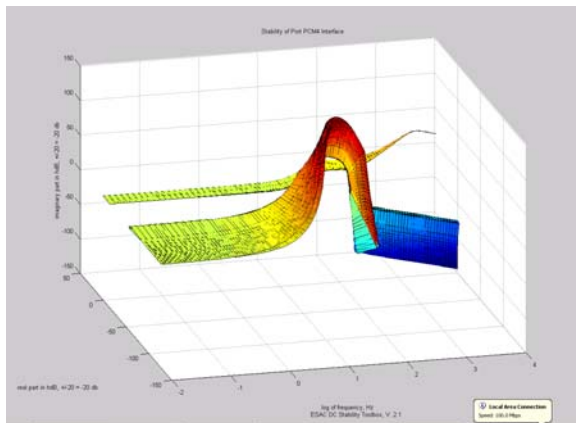
Apparent intersection is a line-of-sight effect. System is stable.

5. K_{sf} is halved

Figure 3-48. Parallel Sources - Stability of Q-PCM4 to Q-PCM4 Interface
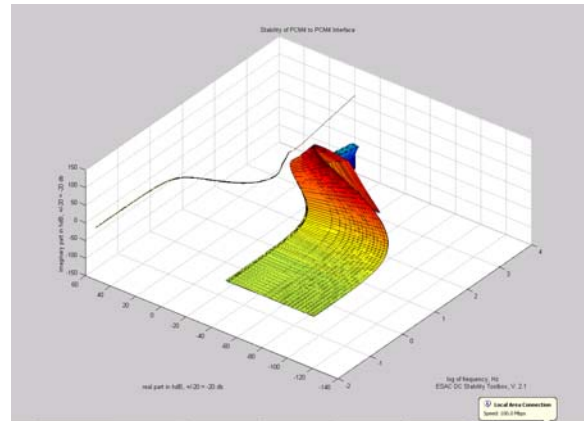
Figure 3-49. Final Test - Stability of Equivalent Source/Equivalent Load
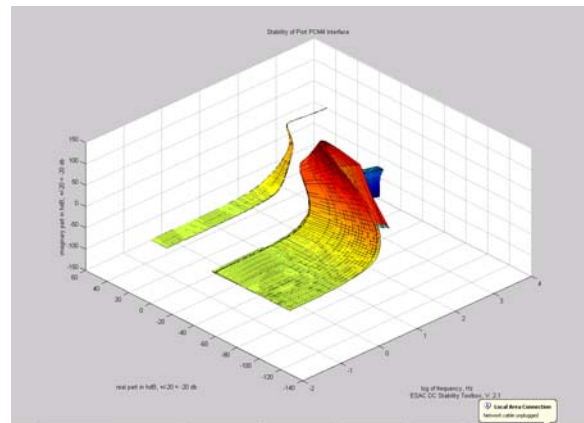
System is stable.

6. K_{sf} is Set to Zero.

7. K_{sf} is Zero, SSCM Output Capacitance is Decreased 90%

Figure 3-50. Parallel Sources - Stability of Q-PCM4 to Q-PCM4 Interface

Figure 3-52. Parallel Sources - Stability of Q-PCM4 to Q-PCM4 Interface
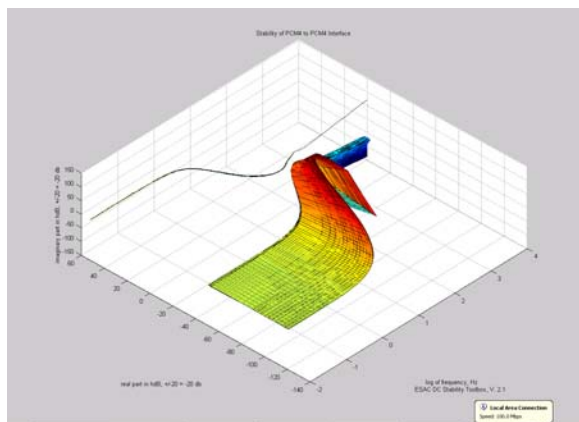
Figure 3-51. Final Test - Stability of Equivalent Source/Equivalent Load
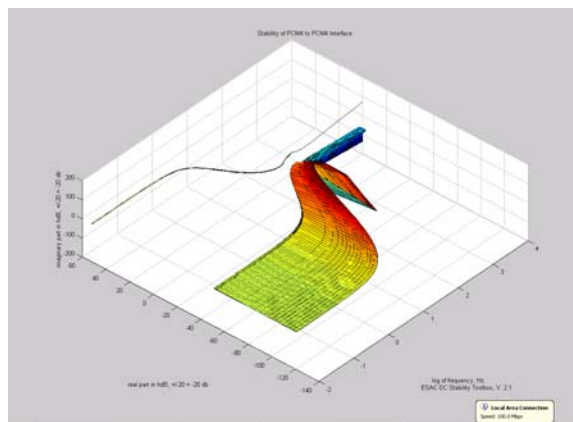
Figure 3-53. Final Test - Stability of Equivalent Source/Equivalent Load
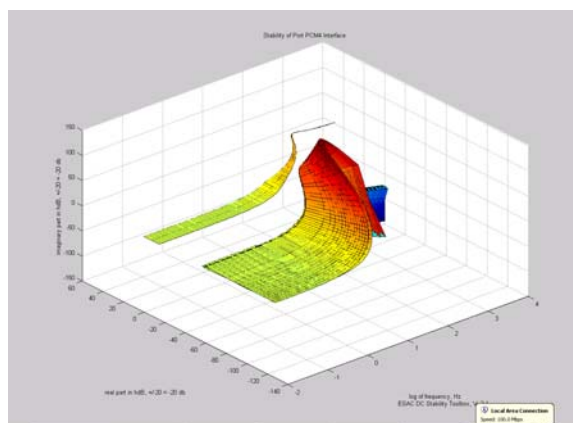
System is stable.

System is stable.

8. K_{sf} is Zero, SSCM Input Capacitance is Decreased 90%

Figure 3-54. Parallel Sources - Stability of Q-PCM4 to Q-PCM4 Interface
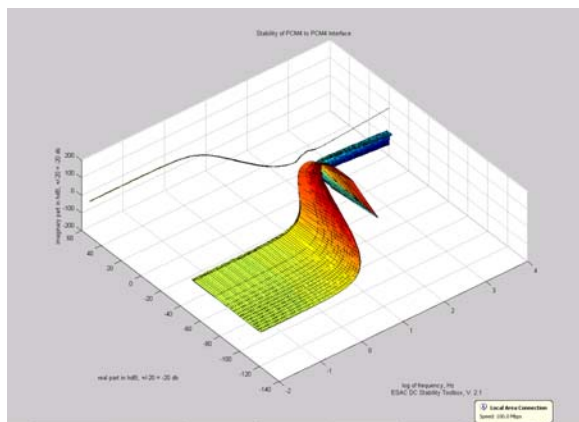
Figure 3-55. Final Test - Stability of Equivalent Source/Equivalent Load
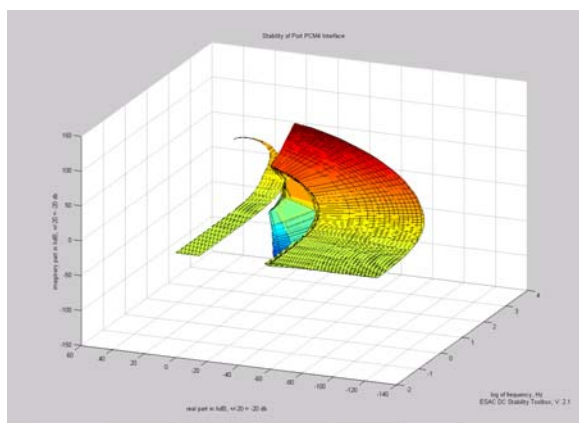
System is unstable.

9. K_{sf} is Zero, PS Capacitance Decreased 90%

Figure 3-56. Parallel Sources - Stability of Q-PCM4 to Q-PCM4 Interface
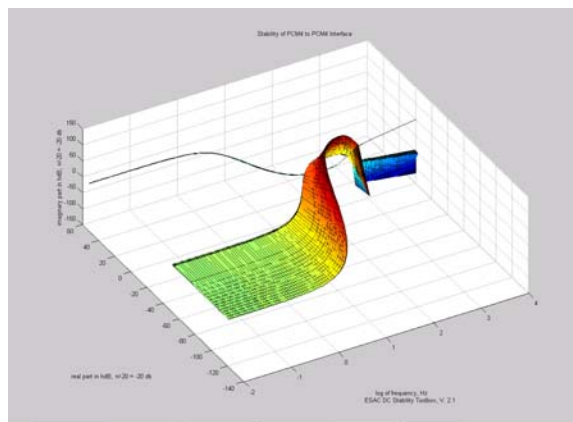
Figure 3-57. Final Test - Stability of Equivalent Source/Equivalent Load
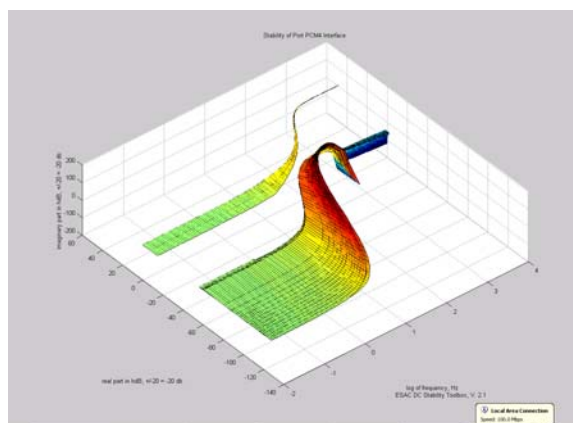
Apparent intersection is a line-of-sight effect. System is stable.

4 Summary

4.1 Results

For the full system configuration, the nonlinear stabilizing control allows capacitive energy storage on the power supply and converter modules to be greatly reduced while still guaranteeing stable stability. When K_{sf} is reduced by half, the testbed system demonstrates some potential instabilities because there is not enough energy storage in the system to maintain stability for all operating conditions. This is supported by the fact that when K_{sf} is reduced by half and power supply or converter module capacitance is doubled, stability is restored. By logical extension, removing stabilizing control (by setting K_{sf} equal to zero) requires a large increase in capacitance to regain stability. This conclusion is validated by tests performed when K_{sf} is set to zero and the results display large admittance space intersections. In this case, stability can be regained by a tenfold increase in capacitance

For alternate configuration one involving the loss of a bus and a power supply, stability results were similar. The testbed system with no parameter changes was shown to remain stable when SSCM input capacitance was reduced by as much as 90%. However, SSCM output capacitance and power supply capacitance could only be reduced by 25% and 50%, respectively, in order to be nearly stable[*]. The system was unstable with K_{sf} halved but could be stabilized by doubling power supply capacitance and SSCM input capacitance. The system was nearly stable with K_{sf} halved and SSCM output capacitance doubled. Setting K_{sf} equal to zero destabilized the system, but again was stabilized by a tenfold increase in power supply and SSCM input capacitance. Unlike the full system, it is interesting to note that no increase in the amount of SSCM output capacitance would stabilize the system.

Alternate configuration two turned out to be very interesting. For all tests run, except one, the system was very stable. The system was stable with and without stabilizing control. The only unstable situation was caused by setting K_{sf} equal to zero and by reducing SSCM input capacitance by 90%. The robustness of this system can be understood when compared to alternate configuration one. Alternate configuration two is identical to alternate configuration one, with the exception that there is a second power supply on the DC bus. This "strengthens" the bus and effectively reduces source impedance by half, which is a stabilizing effect. It is also interesting to observe that, unlike the previous two configurations, reducing SSCM input capacitance had the most destabilizing effect on the system.

4.2 Conclusions

The relationship between the converter module capacitances and stability is complex. For the full and first alternate configurations, system instability was most sensitive to decreasing SSCM

---

[*] Nearly stable as used here indicates that the impedance curve "nicked" the constraint curve, signifying some potential instabilities. The simulation was run again, this time with gain and phase margins of almost zero, and the impedance curve avoided the constraint curve at all frequencies (not shown in the data). The meaning then of "nearly stable" is that the system was stable, but with a gain and/or phase margin of less than 3 dB and 20 degrees, respectively.

output capacitance and least sensitive to decreasing SSCM input capacitance. Conversely, increasing SSCM input capacitance was the most effective way to stabilize the system while increasing SSCM output capacitance had little or no effect on stability. In both the stabilizing and destabilizing cases, the system displayed an intermediate sensitivity to changes in power supply capacitance.

Clearly, Sudhoff's stabilizing control algorithm was very effective at stabilizing the system with reduced energy storage. Without the algorithm present ($K_{sf} = 0$), much larger capacitance values were needed for the system to be stable. By selecting the appropriate K_{sf} value, stability can be achieved. A value must be found that will enable enough disruption to pass through the power converter to assist in maintaining stability without adversely affecting other components or overall system stability.

It may be possible to take advantage of the increased stability of the second alternate configuration. If one DC bus is lost but both power supplies remain operational, the system may be made more survivable by allowing the power supplies to share the remaining bus.

4.3 Recommendations

This was a preliminary investigation into the effectiveness of a stabilizing controller for the University of Missouri at Rolla integrated power system testbed. Further research on this topic could be conducted in several areas to include:

- More casualty scenario based structural changes
- Stability sensitivity to capacitive and non-capacitive parameter changes
- Time domain transient simulation studies using Nonlinear Average Value Models to verify results
- Experimental tests to validate results
- Exploration of the tradeoffs between system performance and stability

5 Endnotes

1. Zivi, E., McCoy, T., "Control of a Shipboard Integrated Power System," *Presentation to Conference on Information Sciences and Systems*, John Hopkins University, May 25, 1999.
2. Glover, S., Sudhoff, S., "An Experimentally Validated Nonlinear Stabilizing Control for Power Electronics Based Power Systems," *Proceedings of the 1998 SAE Aerospace Power Systems Conference*, pp. 71-80.
3. McCoy, T., Lively, K., Thompson, T., Zivi, E., "Advanced Control Concepts for an Integrated Power System (IPS) Warship," *Presentation to Fifth International Naval Engineering Conference and Exhibition*, March 15, 2000.
4. Amin, Massoud. "National Infrastructures as Complex Interactive Networks," in *Automation, Control, and Complexity: An Integrated Approach,* T. Samad and J.R. Weyrauch, Eds., New York: Wiley, 2000, ch.14, pp. 263-286.
5. Zivi, E., McCoy T. "Control of a Shipboard Integrated Power System," *Proceedings of the Thirty-third Annual Conference on Information Sciences and Systems*, March 18, 1999.
6. Zivi, E., McCoy, T., "Control of a Shipboard Integrated Power System," *Presentation to Conference on Information Sciences and Systems*, John Hopkins University, May 25, 1999.
7. Lively, K., McCoy, T., Thompson, T., Zivi, E. "USN Advanced Control Concepts for an Integrated Power System (IPS) Warship," *Proceedings of the INEC 2000 Conference*, Hamburg, Germany, March 14-16, 2000.
8. Cerrito, J. "Neural Network Control of the Integrated Power System," U.S.N.A. Trident Scholar Project Report, Number 273 (2000), p. 13.
9. Cerrito, J. "Neural Network Control of the Integrated Power System," United States Naval Academy Trident Scholar Project Report, Number 273 (2000).
10. Zivi, E., Cerrito, J., Doney, D., "Neural Network Fault Tolerant Estimation of an Integrated Power System," *Proceedings of Applied Simulation and Modeling Conference*, July 24-26, 2000, Banff, Canada.
11. Vanecko, J. "Advanced Shipboard Control Systems," United States Naval Academy Trident Scholar Project Report, Number 286, (2001).
12. "ONR Control Challenge Problem" posted at http://www.usna.edu/EPNES/ONR_Control_Challenge.pdf
13. Sudhoff, S., DC Stability Toolbox, Version 2.1, Lecture 2.
14. Sudhoff, S.D. "Control of Zonal DC Distribution Systems: A Stability Perspective." Naval Combat Survivability: Task 3 Final Report, January 16, 2002.
15. *Ibid.*
16. *Ibid.*
17. *Ibid.*
18. Sudhoff, S., Schmucker, D., Youngs, R., Hegner H. "Stability Analysis of DC Distribution Systems Using Admittance Space Constraints." Proceedings of The Institute of Marine Engineers All Electric Ship 98, London, September 29-30, 1998.
19. S.D. Sudhoff, S.F. Glover, P.T. Lamm, D.H. Schmucker, D.E. Delisle, "Stability Analysis of DC Power Electronics Based Distribution Systems Using Admittance Space Constraints," *IEEE Transactions on Aerospace and Electronics Systems*, Vol. 36. No. 3. July 2000, pp. 965-973.

20. S.D. Sudhoff, "Admittance Space Based Stability Specification," Proceedings of the 1998 ONR -Drexel-NSWC Workshop on Electric Shipboard System Modeling, Simulation and Control, June 22-23, 1998, Philadelphia, PA, USA

21. S.D. Sudhoff, S.F. Glover, P.T. Lamm, D.H. Schmucker, D.E. Delisle, "Stability Analysis of DC Power Electronics Based Distribution Systems Using Admittance Space Constraints," *IEEE Transactions on Aerospace and Electronics Systems*, Vol. 36. No. 3. July 2000, pp. 965-973.

22. Sudhoff, Stability Toolbox, Lecture 2.

23. *Ibid*.

24. *Ibid*.

25. S.D. Sudhoff, S.F. Glover, P.T. Lamm, D.H. Schmucker, D.E. Delisle, "Stability Analysis of DC Power Electronics Based Distribution Systems Using Admittance Space Constraints," *IEEE Transactions on Aerospace and Electronics Systems*, Vol. 36. No. 3. July 2000, pp. 965-973.

26. Sudhoff, Stability Toolbox, Lecture 2.

27. *Ibid*.

28. S.D. Sudhoff, S.F. Glover, P.T. Lamm, D.H. Schmucker, D.E. Delisle, "Stability Analysis of DC Power Electronics Based Distribution Systems Using Admittance Space Constraints," *IEEE Transactions on Aerospace and Electronics Systems*, Vol. 36. No. 3. July 2000, pp. 965-973.

29. Sudhoff, Stability Toolbox, Lecture 2.

30. Sudhoff, S.D. "Control of Zonal DC Distribution Systems: A Stability Perspective." Naval Combat Survivability: Task 3 Final Report, January 16, 2002.

31. Sudhoff, Stability Toolbox, Lecture 2.

32. *Ibid*.

33. Sudhoff, S., DC Stability Toolbox, Version 2.1, Lecture 5.

6 Bibliography

Amin, Massoud. "Toward Self-Healing Energy Infrastructure Systems," in <u>IEEE Computer Applications in Power</u>, January 2001, pp. 20-28.

Amin, Massoud. "National Infrastructures as Complex Interactive Networks," in <u>Automation, Control, and Complexity: An Integrated Approach</u>, T. Samad and J.R. Weyrauch, Eds., New York: Wiley, 2000, ch.14, pp. 263-286.

Cerrito, J. "Neural Network Control of the Integrated Power System," <u>United States Naval Academy Trident Scholar Project Report</u>, Number 273 (2000).

Fitzgerald, M., "DD-21's Fatal Flaw," <u>US Naval Institute Proceedings</u>, February, 1999.

Glover, S., Sudhoff, S., "An Experimentally Validated Nonlinear Stabilizing Control for Power Electronics Based Power Systems," <u>Proceedings of the 1998 SAE Aerospace Power Systems Conference</u>, pp. 71-80.

Klain, R., "How Can We Save Ships with Small Crews?," <u>US Naval Institute Proceedings</u>, September, 1999.

Krekich, A.J., "Smart Ship: The Future is Here," <u>US Naval Institute Proceedings</u>, January, 1998.

Krause, P.C., Wasynczuk, O., Sudhoff, S.D. <u>Analysis of Electric Machinery.</u> IEEE, Inc.: New York, 1995.

Lively, K., McCoy, T., Thompson, T., Zivi, E. "USN Advanced Control Concepts for an Integrated Power System (IPS) Warship," <u>Proceedings of the INEC 2000 Conference</u>, Hamburg, Germany, March 14-16, 2000.

Nise, N.S. <u>Control Systems Engineering, 2nd ed.</u> Addison-Wesley: California, 1995.

Sudhoff, S., ESAC DC Stability Toolbox Version 2.1, January 16, 2002, Release.

Sudhoff, S., Schmucker, D., Youngs, R., Hegner H. "Stability Analysis of DC Distribution Systems Using Admittance Space Constraints." <u>All-Electric Ship Conference</u>, London, September 1998.

Sudhoff S.D., Glover S.F., "Three Dimensional Stability Analysis of DC Power Electronics Based Systems," <u>Proceedings of the Power Electronics Specialist Conference</u>, Galway, Ireland, June 19-22, 2000, pp. 101-106.

Sudhoff S.D., Glover S.D., Lamm P.T., Schmucker D.H., Delisle D.E., "Stability Analysis of DC Power Electronics Based Distribution Systems Using Admittance Space Constraints," IEEE Transactions on Aerospace and Electronics Systems, Vol. 36. No. 3. July 2000, pp. 965-973.

Sudhoff, S.D. "Control of Zonal DC Distribution Systems: A Stability Perspective." Naval Combat Survivability: Task 3 Final Report, January 16, 2002.

Sudhoff S.D., Glover S.F., Żak S.H., Pekerak S.D., Zivi E.J., Delisle D.E, Sauer J., "Control of Zonal DC Distribution Systems: A Stability Perspective," SAE Power Systems Conference, Coral Springs, Florida, October 29-31, 2002.

Vanecko, J. "Advanced Shipboard Control Systems," United States Naval Academy Trident Scholar Project Report, Number 286, (2001).

Vining, P., "Can a Minimum-Manned Ship Survive Combat?," US Naval Institute Proceedings, April, 1999.

Zivi, E., Cerrito, J., Doney, D., "Neural Network Fault Tolerant Estimation of an Integrated Power System," Proceedings of Applied Simulation and Modelling Conference, July 24-26, 2000, Banff, Canada.

Zivi, E., McCoy T. "Control of a Shipboard Integrated Power System," Proceedings of the Thirty-third Annual Conference on Information Sciences and Systems, March 18, 1999.

APPENDIX A

A.1. Power Supply (Q-PCM4, or PS) Parameter List

The parameters of the power supply, when operated in an uncontrolled mode are as follows. Recall the nominal input voltage is 560 V AC at a frequency of 60 Hz.

Name	Description.	Value	Unit	NLAM	Detailed	Stability
L_{tran}	Leakage of transformer (primary and secondary, Referred to primary)	1	mH	X	X	X
n_{ps}	Primary to secondary turns ratio	1.51		X	X	X
L_{dc}	DC link inductance	3	mH	X	X	X
r_{ldc}	DC link inductor resistance	0.1	Ω	X	X	X
C_{dc}	Output capacitance	464	μ F	X	X	X
r_{cdc}	Output capacitance ESR	0.4	Ω	X	X	X

For stability analysis purposes, the power supply can be viewed as a independent voltage of value $3\sqrt{2}v_{llrms}/(\pi n_{ps})$ where v_{llrms} is the line-to-line rms voltage of the transformer primary referred to the secondary (560 V) in series with an ideal diode, a resistance of value $r_{ldc}+3L_{tran}\omega_e/(\pi n_{ps}^2)$ where ω_e is the radian frequency of the source, and an inductance of $2L_{tran}+L_{dc}$, all in parallel with the series combination of the output capacitor and its ESR.

A.2. Ship Service Converter Module (Q-PCM1, or SSCM) Parameter List

Name	Desc.	Value	Unit	NLAM	Detailed	Stability
r_{lin}	Fig. 1	0	Ω			X
L_{lin}	Fig. 1	0	H			X
r_{cin}	Fig. 1	1.127	Ω	X	X	X
C_{in}	Fig. 1	449.7	μ F	X	X	X
v_{sw}	Tran. Drop	1.2	V	X	X	
r_{sw}	Tran. Res.	20	$m\Omega$	X	X	
v_d	Diode. Drop	1	V	X	X	
r_d	Diode. Res.	10	$m\Omega$	X	X	
L_{out}	Fig. 1	0.995	mH	X	X	
r_{lout}	Fig. 1	0.12	Ω	X	X	
C_{out}	Fig. 1	447.6	μ F	X	X	X
r_{Cout}	Fig. 1	0.128	Ω	X	X	X
τ_{invc}	Fig. 2	0.15	ms	X	X	X

τ_{invout}	Fig. 2	0.15	ms	X	X	X
τ_{iniout}	Fig. 2	0.15	ms	X	X	X
v_{out}^*	Fig. 2	420	V	X	X	X
d	Fig. 2	1	Ω	X	X	X
τ_{sf1}	Fig. 2	20	ms	X	X	X
τ_{sf2}	Fig. 2	4	ms	X	X	X
K_{sf}	Fig. 2	0.1		X	X	X
Δv_{outmax}^*	Fig. 2	20	V	X	X	X
K_{pv}	Fig. 2	0.628	A/V	X	X	X
K_{iv}	Fig. 2	197	A/(Vs)	X	X	X
i_{limit}	Fig. 2	20	A	X	X	
K_{ii}	Fig. 2	5	1/s	X	X	
i_{intlim}	Fig. 2	2	A	X	X	
h	Hyst. Level (0 to pk)	1.75	A		X	

Figure A-1. Q-PCM1
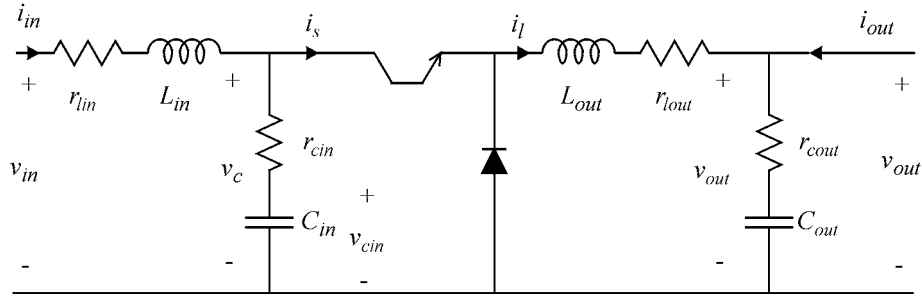
Figure A-2. Q-PCM1 Control Algorithm

$$H_{sf}(s) = K_{sf}\frac{\tau_{sf1}s}{(\tau_{sf1}s+1)(\tau_{sf2}s+1)}$$
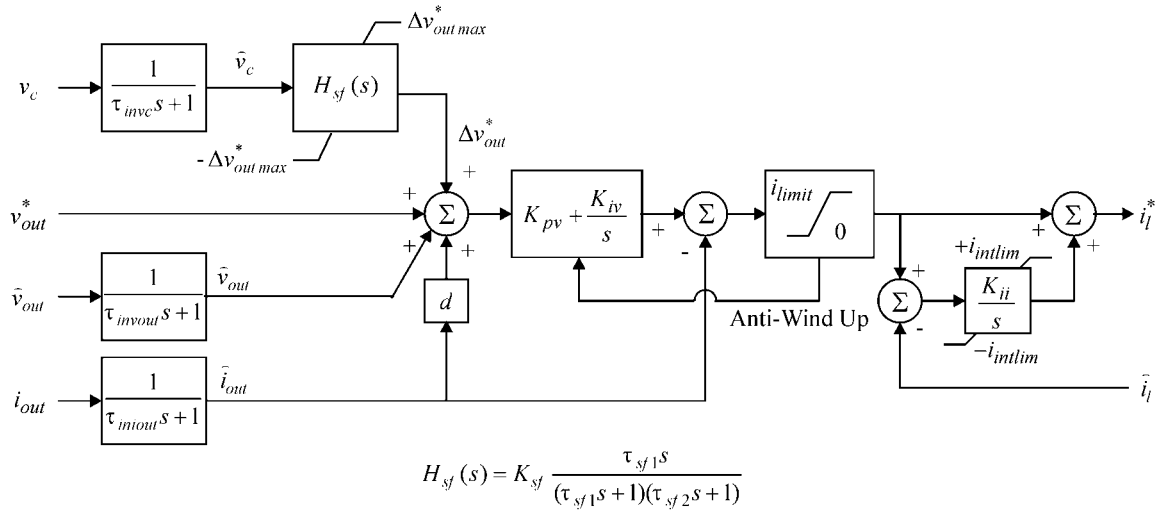
A.3. Load Parameter List

Each of the loads (SSIM, MC, CPL) can be modeled as a constant power load with a shunt capacitance (and the capacitor has ESR). Parameters are as follows:

Ship Service Inverter Module (Q-PCM2, or SSIM)
Capacitance is 590 μF.
ESR of Capacitor is 127 mΩ.
Power is 0 to 5 kW.

Motor Controller (MC)
Capacitance is 580 μF.
ESR of Capacitor is 253 mΩ.
Power is 0 to 5 kW.

Constant Power Load (CPL)
Capacitance is 374 μF.
ESR of Capacitor is 189 mΩ.
Power is 0 to 5 kW.

APPENDIX B

NYQUIST CRITERION

This section follows the derivation as set forth in *Control Systems Engineering*, 2nd ed., by Norman S. Nise. The Nyquist criterion uses information about the open-loop system, *G(s)H(s)*, to determine the stability of the closed-loop system. Consider the closed-loop system shown in Figure B-1.

Figure B-1. Closed-loop system

$$\text{Closed-loop system} = \frac{G(s)}{1+G(s)H(s)}$$
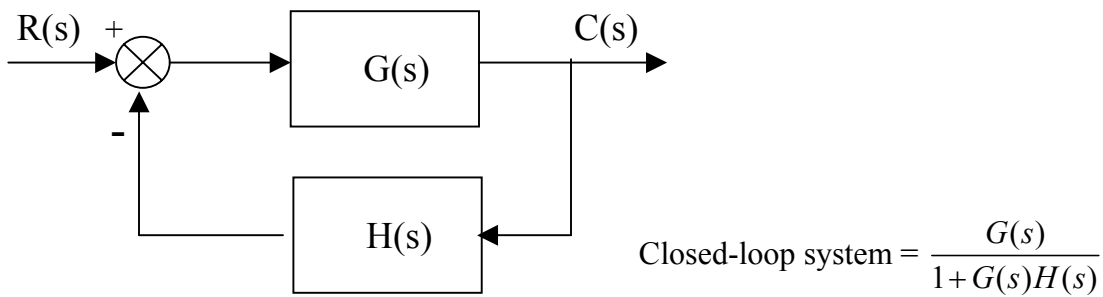
We let

$$G(s) = \frac{N_G}{D_G} \qquad (1.1a)$$

$$H(s) = \frac{N_H}{D_H} \qquad (1.1b)$$

N_G and D_G are polynomials in s with no common factors. N_H and D_H are also polynomials in s with no common factors. We find

$$G(s)H(s) = \frac{N_G N_H}{D_G D_H} \qquad (1.2a)$$

$$1+G(s)H(s) = 1 + \frac{N_G N_H}{D_G D_H} = \frac{D_G D_H + N_G N_H}{D_G D_H} \qquad (1.2b)$$

$$T(s) = \frac{G(s)}{1+G(s)H(s)} = \frac{N_G N_H}{D_G D_H + N_G N_H} \qquad (1.2c)$$

From Eqs. (1.2), we conclude that (1) the poles of 1+G(s)H(s) are the same as the poles of G(s)H(s), the open-loop system, and (2) the zeros of 1+G(s)H(s) are the same as the poles of T(s), the closed-loop system.

Next, let us define the term *mapping*. If we take a complex number on the *s*-plane and substitute it into a function, *F(s)*, another complex number results. This process is called *mapping*. For example, substituting $s = 4 + j3$ into the function $(s^2 + 2s + 1)$ yields $16 + j30$. We say that $4 + j3$ maps into $16 + j30$ through the function $(s^2 + 2s + 1)$.

Finally, we discuss the concept of mapping *contours*. Consider the collection of points, called a *contour*, shown in Figure 2 as a contour *A*. Also, assume that

$$F(s) = \frac{(s - z_1)(s - z_2)\cdots}{(s - p_1)(s - p_2)\cdots}$$

Contour *A* can be mapped through *F(s)* into contour *B* by substituting each point of contour *A* into the function *F(s)* and plotting the resulting complex numbers. For example, point *Q* in Figure B-2 maps into point *Q'* through the function *F(s)*.

Figure B-2. Mapping contours
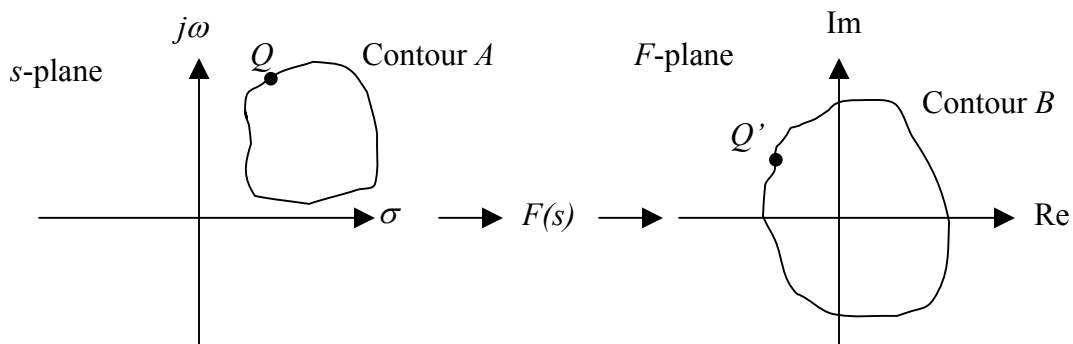
A unique relationship exists between the number of poles of *F(s)* contained inside contour *A*, the number of zeros of *F(s)* contained inside contour *A*, and the number of counterclockwise encirclements of the origin for the mapping of contour *B*. This interrelationship can be used to determine the stability of closed-loop systems. This method of determining stability is called the *Nyquist criterion*. For a derivation of the Nyquist criterion, refer to Nise, pp. 556-560.

By extending the contour to include the entire right half-plane, as shown in Figure B-3, we can count the number of right half-plane, closed-loop poles inside contour *A* and determine a system's stability.

Figure B-3. Half circle with infinite radius and centered at origin
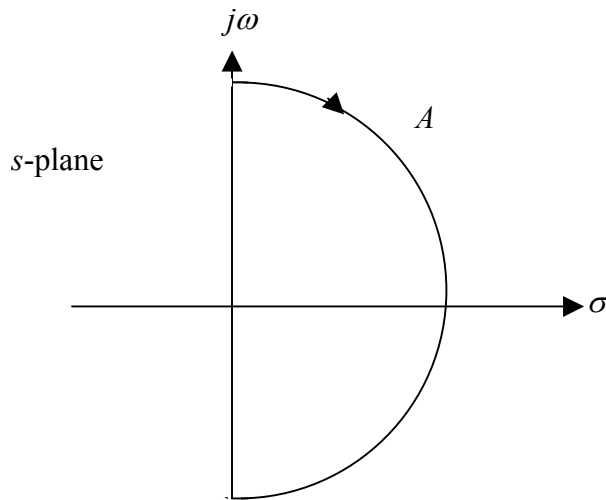
If a contour, *A*, that encircles the entire right half-plane is mapped through *G(s)H(s)*, then *the number of closed-loop zeros, Z, in the right half-plane equals the number of open-loop poles, P, that are in the right half-plane minus the number of counterclockwise revolutions, N, around −1 of the mapping; that is, Z = P − N. The mapping is called the Nyquist diagram, or Nyquist plot, of G(s)H(s).*

APPENDIX C

C.1. MATLAB Code for Stability Analysis of DC-ZEDS, Full Configuration

SYSTEM SETUP – setup.m

```
% Analysis of NCS 01 System
% S.D. Sudhoff
% 2/11/02

% System Set up

% Adjustment Factors for System Capacitances - Inserted by Chiafair on 3/21/02
af4=1.0;                                % adjustment factor for output capacitance of Q-PCM4 (Power Supply)
                                        % af4=1.1 --> output cap. is increased by 10%
                                        % af4=0.9 --> output cap. is decreased by 10%
af1in=1.0;                              % af for input cap for Q-PCM1 (SSCM)
af1out=1.0;              % af for output cap for Q-PCM1 (SSCM)
af2=1.0;                                % af for cap for Q-PCM2 (SSIM)
afmc=1.0;                % af for cap for Motor Controller (MC)
afcpl=1.0;                              % af for cap for Constant Power Load (CPL)
afksf=1.0;        % af for stabilizing filter bandpass gain (Ksf)

% Step 1: Set Up Stability Criteria
gm=3;                                    % gain margin in dB
pm=20.0;                  % phase margin in degrees
tr=40.0;                                 % truncation radious in dB
n1=15.0;                                 % number of points used in horizontel trace
n2=5.0;                                  % number of points used in slanted trace
[sc] = esacsc(gm,pm,tr,n1,n2);

% Step 2: Create the s-vector.
freqmin=0.01;                            % minimum frequency considered in Hz
freqmax=10000.0;          % maximum frequency considered in Hz
nfreq=120;                % number of frequencies considered
s = svec1(freqmin,freqmax,nfreq);   % create the s vector for the Nyquist contour

% Step 3: Decide on number of sides and interpolating points.
NS=8;                                    % number of sides to generalized source impedance
NI=1;                                    % number of intermediate point to generalized source impedance

% Step 4: Characterize Q-PCM4 (Power Supply)
vpllmin=560.0*0.95;                      % minimum source voltage (l-l,rms)
vpllmax=560.0*1.05;        % maximum source voltage (l-l,rms)
nv=3;                                    % number of voltages to consider
wemin=2*pi*60*0.95;        % minimum source frequency (rad/s)
wemax=2*pi*60*1.05;        % maximum source frequency (rad/s)
nwe=3;                                   % number of source frequencies to try
llpmin=1.00e-3;                          % minimum transformer leakage inductance (primary side)
llpmax=1.00e-3;                          % maximum transformer leakage inductance (seconary side)
```

```
nl=1;                                      % number of reactances to try
nps=1.513;                                 % turns ratio
ldc=3.0e-3;                  % dc link inductance
rdc=0.1;                                   % dc link inductor resistance


%edited by Chiafair 3/21/02 <*af4>
cdc=464e-6*af4;              % output capacitance


kp=0.0;                                    % controller proportional gain
ki=0.0;                                    % controller integral gain
[PCM4_S] = rectsrce(vpllmin,vpllmax,nv,wemin,wemax,nwe,llpmin,llpmax,nl,nps,ldc,rdc,cdc,kp,ki,s,NS,NI);


% Step 5: Characterize Q-PCM1 (SSCM)
pmn=0.0;                                   % minimum output power (W)
pmx=5.0e3;                                 % maximum output power (W)
np=10;                                     % number of output powers considered
vinmn=450;                   % minimum input voltage considered (V)
vinmx=525;                   % maximum input voltage considered (V)
nvin=5;                                    % number of input voltages considered
voutstar=420.0;                            % commanded output voltage (V)
d=1.0;                                     % droop (V/A)
lin=1.0e-10;                               % input inductor inductance (H)
rlin=1.0e-10;                              % input inductor resistance (Ohms)


%edited by Chiafair 3/21/02 <*af1in and *af1out>
cin=450.0e-6*af1in;          % input capacitance (F)
cout=448.0e-6*af1out;        % output capacitance (F)


rcin=1.13;                                 % input capacitance series resistance (Ohms)
rcout=0.128;                               % output capacitor resistance (Ohms)
rlout=0.12;                                % output inductor resistance (Ohms)


kpv=0.628;                                 % proportional gain (A/V)
kiv=197.0;                                 % integral gain (A/(Vs))


tauinvc=1.5e-4;                            % input filter filter time constants
tauinvout=1.5e-4;
tauiniout=1.5e-4;


%edited by Chiafair 3/28/02 <*afksf>
ksf=0.1*afksf;                             % stabilizing filter bandpass gain


tausf1=20.0e-3;                            % stabilizing filter low frequency cutoff
tausf2=4.0e-3;                             % stabilizing filter high freqeuncy cutoff


[PCM1_H11,PCM1_H12,PCM1_H21,PCM1_H22] = convmodlsc(pmn,pmx,np,vinmn,vinmx,nvin, ...
                        voutstar,d,lin,rlin,cin,rcin,cout,rcout,rlout, ...
                        tauinvc,tauinvout,tauiniout,kpv,kiv, ...
                        ksf,tausf1,tausf2,s,NS,NI);


% Step 6: Characterize: Q-PCM2 (SSIM)


%edited by Chiafair 3/21/02 <*af2>
c=590e-6*af2;                              % input capacitance
```

```
r=0.127;                              % input capacitance series resistance
vmax=420.0;                           % maximum input voltage
vmin=400.0;                           % minimum input voltage
nv=5;                                 % number of voltages to use
pmin=0.0;        % minimum power
pmax=5000;         % maximum power
np=10;              % number of powers to use
[PCM2_L] = cpld(c,r,vmin,vmax,nv,pmin,pmax,np,s,NS,NI);


% Step 7: Characterize: Motor Controller (MC)

%edited by Chiafair 3/21/02 <*afmc>
c=580e-6*afmc;     % input capacitance

r=0.253;                              % input capacitance series resistance
vmax=420.0;              % maximum input voltage
vmin=400.0;              % minimum input voltage
nv=5;                                 % number of voltages to use
pmin=0.0;              % minimum power
pmax=5000;            % maximum power
np=10;                                % number of powers to use
[MC_L] = cpld(c,r,vmin,vmax,nv,pmin,pmax,np,s,NS,NI);

% Step 8: Characterize: Constant Power Load (CPL)

%edited by Chiafair 3/21/02 <*afcpl>
c=374e-6*afcpl;     % input capacitance

r=0.189;                              % input capacitance series resistance
vmax=420.0;        % maximum input voltage
vmin=400.0;        % minimum input voltage
nv=5;                                 % number of voltages to use
pmin=0.0;                % minimum power
pmax=5000;              % maximum power
np=10;                                % number of powers to use
[CPL_L] = cpld(c,r,vmin,vmax,nv,pmin,pmax,np,s,NS,NI);

save setupdata gm pm tr n1 n2 sc ...
        s NS NI ...
        PCM4_S ...
        PCM1_H11 PCM1_H12 PCM1_H21 PCM1_H22 ...
        PCM2_L MC_L CPL_L
```

REDUCTION AND STABILITY ANALYSIS OF ZONE ONE – zone1.m

```
% Analysis of NCS 01 System
% S.D. Sudhoff
% 2/11/02

% Analysis of Zone 1

clear all
```

```
load setupdata

[ok,Zone1_Y11,Zone1_Y12,Zone1_Y21,Zone1_Y22,PCM1_H12inv,PCM1_H12_par_PCM1_H12] = ...
HLHp_to_Y(s,sc,PCM1_H11,PCM1_H12,PCM1_H21,PCM1_H22, ...
      PCM1_H11,PCM1_H12,PCM1_H21,PCM1_H22,PCM2_L,NS,NI);
if ok
  disp('Dual Q-PCM1 to Q-PCM2 interface is stable');
else
  disp('Dual Q-PCM1 to Q-PCM2 interface is unstable');
end

[PCM1_H12inv_const] = esacdspec(gm,pm,tr,n1,n2,PCM1_H12,s);
spaceplt(1,6,s,PCM1_H12inv_const,-20.0);
hold on;
spaceplt(1,6,s,PCM1_H12inv,-20.0);
hold off;
title('Stability of Q-PCM1 to Q-PCM1 Interface');

[PCM2_L_const]=esacdspec(gm,pm,tr,n1,n2,PCM1_H12_par_PCM1_H12,s);
spaceplt(2,6,s,PCM2_L_const,-20.0);
hold on;
spaceplt(2,6,s,PCM2_L,-20.0);
hold off;
title('Stability of Dual Q-PCM1 to Q-PCM2 Interface');

save zone1data Zone1_Y11 Zone1_Y12 Zone1_Y21 Zone1_Y22
```

REDUCTION AND STABILITY ANALYSIS OF ZONE TWO – zone2.m

```
% Analysis of NCS 01 System
% S.D. Sudhoff
% 2/11/02

% Analysis of Zone 2

clear all
load setupdata

[ok,Zone2_Y11,Zone2_Y12,Zone2_Y21,Zone2_Y22,PCM1_H12inv,PCM1_H12_par_PCM1_H12] = ...
HLHp_to_Y(s,sc,PCM1_H11,PCM1_H12,PCM1_H21,PCM1_H22, ...
      PCM1_H11,PCM1_H12,PCM1_H21,PCM1_H22,MC_L,NS,NI);
if ok
  disp('Dual Q-PCM1 to Q-PCM2 interface is stable');
else
  disp('Dual Q-PCM1 to Q-PCM2 interface is unstable');
end

%unnecessary if all H and H' converters are identical among the 3 zones
%[PCM1_H12inv_const] = esacdspec(gm,pm,tr,n1,n2,PCM1_H12,s);
%spaceplt(1,6,s,PCM1_H12inv_const,-20.0);
%hold on;
%spaceplt(1,6,s,PCM1_H12inv,-20.0);
```

```
%hold off;
%title('Stability of Q-PCM1 to Q-PCM1 Interface');

[MC_L_const]=esacdspec(gm,pm,tr,n1,n2,PCM1_H12_par_PCM1_H12,s);
spaceplt(3,6,s,MC_L_const,-20.0);
hold on;
spaceplt(3,6,s,MC_L,-20.0);
hold off;
title('Stability of Dual Q-PCM1 to MC Interface');

save zone2data Zone2_Y11 Zone2_Y12 Zone2_Y21 Zone2_Y22
```

REDUCTION AND STABILITY ANALYSIS OF ZONE THREE – zone3.m

```
% Analysis of NCS 01 System
% S.D. Sudhoff
% 2/11/02

% Analysis of Zone 3

clear all
load setupdata

[ok,Zone3_Y11,Zone3_Y12,Zone3_Y21,Zone3_Y22,PCM1_H12inv,PCM1_H12_par_PCM1_H12] = ...
HLHp_to_Y(s,sc,PCM1_H11,PCM1_H12,PCM1_H21,PCM1_H22, ...
      PCM1_H11,PCM1_H12,PCM1_H21,PCM1_H22,CPL_L,NS,NI);
if ok
   disp('Dual Q-PCM1 to Q-PCM2 interface is stable');
else
   disp('Dual Q-PCM1 to Q-PCM2 interface is unstable');
end

%unnecessary if all H and H' converters are identical among the 3 zones
%[PCM1_H12inv_const] = esacdspec(gm,pm,tr,n1,n2,PCM1_H12,s);
%spaceplt(1,6,s,PCM1_H12inv_const,-20.0);
%hold on;
%spaceplt(1,6,s,PCM1_H12inv,-20.0);
%hold off;
%title('Stability of Q-PCM1 to Q-PCM1 Interface');

[CPL_L_const]=esacdspec(gm,pm,tr,n1,n2,PCM1_H12_par_PCM1_H12,s);
spaceplt(4,6,s,CPL_L_const,-20.0);
hold on;
spaceplt(4,6,s,CPL_L,-20.0);
hold off;
title('Stability of Dual Q-PCM1 to CPL Interface');

save zone3data Zone3_Y11 Zone3_Y12 Zone3_Y21 Zone3_Y22
```

REDUCTION TO SINGLE SOURCE-LOAD SYSTEM AND STABILITY ANALYSIS – systemanalysis.m

```
% Analysis of NCS 01 System
% S.D. Sudhoff
% 2/11/02

% Analysis of Full System

load setupdata
load zone1data
load zone2data
load zone3data

% Step 1 Parallel the Three Zonal Loads
[AgZ_Y11,AgZ_Y12,AgZ_Y21,AgZ_Y22] = ...
parY_to_Y(NS,NI, ...
        Zone1_Y11,Zone1_Y12,Zone1_Y21,Zone1_Y22, ...
        Zone2_Y11,Zone2_Y12,Zone2_Y21,Zone2_Y22, ...
        Zone3_Y11,Zone3_Y12,Zone3_Y21,Zone3_Y22);

% Step 2 Combine loads with starboard source
[stable,AgZplusPCM4_L] = YS_to_L(s,sc,AgZ_Y11,AgZ_Y12,AgZ_Y21,AgZ_Y22,PCM4_S,NS,NI);
if stable
   disp('Zonal Load / Starboard Power Supply Interface is stable');
else
   disp('Zonal Load / Starboard Power Supply Interface does not satisfy stability criteria');
end
% Step 2b: Manual check to see if zonal loads and 2nd source form a stable subsystem
[L_const_of_PCM4] = esacdspec(gm,pm,tr,n1,n2,PCM4_S,s);
spaceplt(5,6,s,L_const_of_PCM4,-20.0);
hold on;
spaceplt(5,6,s,AgZ_Y22,-20.0);
hold off;
title('Stability of Three Zonal Loads and Starboard Power Supply Interface');

% Step 3 Check System Stability at the Port Power Supply Interface
% Stet 3a: Check it Automatically
[sok ok] = sinspect(s,sc,PCM4_S,AgZplusPCM4_L,NS,NI);
if ok
   disp('Port PCM4 Rest of System Interface is Stable');
else
   disp('Port PCM4 Rest of System Interface does not Satisfy Stability Criteria');
end
% Step 3b: Check it Manually
spaceplt(6,6,s,L_const_of_PCM4,-20.0);
hold on;
spaceplt(6,6,s,AgZplusPCM4_L,-20.0);
title('Stability of Port PCM4 Interface');
holdoff;
```

C.2. MATLAB Code for Stability Analysis of DC-ZEDS, Alternate Configuration One

SYSTEM SETUP – setup.m

same as full configuration

REDUCTION AND STABILITY ANALYSIS OF ZONE ONE – zone1.m

```
clear all
load setupdata


[ok,Zone1_L] = HL_to_L(s,sc,PCM1_H11,PCM1_H12,PCM1_H21,PCM1_H22, ...
        PCM2_L,NS,NI);
if ok
  disp('Q-PCM1 to Q-PCM2 interface is stable');
else
  disp('Q-PCM1 to Q-PCM2 interface is unstable');
end

[PCM2_L_const] = esacdspec(gm,pm,tr,n1,n2,PCM1_H12,s);
spaceplt(1,6,s,PCM2_L_const,-20.0);
hold on;
spaceplt(1,6,s,PCM2_L,-20.0);
hold off;
title('Stability of Q-PCM1 to Q-PCM2 Interface');


save zone1data Zone1_L
```

REDUCTION AND STABILITY ANALYSIS OF ZONE TWO – zone2.m

```
clear all
load setupdata

[ok,Zone2_L] = HL_to_L(s,sc,PCM1_H11,PCM1_H12,PCM1_H21,PCM1_H22, ...
            MC_L,NS,NI);
if ok
  disp('Q-PCM1 to MC interface is stable');
else
  disp('Q-PCM1 to MC interface is unstable');
end

[MC_L_const] = esacdspec(gm,pm,tr,n1,n2,PCM1_H12,s);
spaceplt(2,6,s,MC_L_const,-20.0);
hold on;
spaceplt(2,6,s,MC_L,-20.0);
hold off;
title('Stability of Q-PCM1 to MC Interface');
```

save zone2data Zone2_L

REDUCTION AND STABILITY ANALYSIS OF ZONE THREE – zone3.m

```
clear all
load setupdata

[ok,Zone3_L] = HL_to_L(s,sc,PCM1_H11,PCM1_H12,PCM1_H21,PCM1_H22, ...
              CPL_L,NS,NI);
if ok
  disp('Q-PCM1 to CPL interface is stable');
else
  disp('Q-PCM1 to CPL interface is unstable');
end

[CPL_L_const] = esacdspec(gm,pm,tr,n1,n2,PCM1_H12,s);
spaceplt(3,6,s,CPL_L_const,-20.0);
hold on;
spaceplt(3,6,s,CPL_L,-20.0);
hold off;
title('Stability of Q-PCM1 to CPL Interface');


save zone3data Zone3_L
```

REDUCTION TO SINGLE SOURCE-LOAD SYSTEM AND STABILITY ANALYSIS – systemanalysis.m

```
load setupdata
load zone1data
load zone2data
load zone3data

% Step 1 Parallel the Three Zonal Loads
[AgL] = parL_to_L(NS,NI,Zone1_L,Zone2_L,Zone3_L);

% Step 2 Check System Stability at the Port Power Supply Interface
% Stet 2a: Check it Automatically
[sok ok] = sinspect(s,sc,PCM4_S,AgL,NS,NI);
if ok
  disp('Port PCM4 Rest of System Interface is Stable');
else
  disp('Port PCM4 Rest of System Interface does not Satisfy Stability Criteria');
end

% Step 2b: Check it Manually
[L_const_of_PCM4] = esacdspec(gm,pm,tr,n1,n2,PCM4_S,s);
spaceplt(4,6,s,L_const_of_PCM4,-20.0);
hold on;
spaceplt(4,6,s,AgL,-20.0);
```

```
hold off;
title('Stability of Port PCM4 Interface');
```

C.3. MATLAB Code for Stability Analysis of DC-ZEDS, Alternate Configuration Two

SYSTEM SETUP – setup.m

same as full configuration

REDUCTION AND STABILITY ANALYSIS OF ZONE ONE – zone1.m

same as alternate configuration one

REDUCTION AND STABILITY ANALYSIS OF ZONE TWO – zone2.m

same as alternate configuration one

REDUCTION AND STABILITY ANALYSIS OF ZONE THREE – zone3.m

same as alternate configuration one

REDUCTION TO SINGLE SOURCE-LOAD SYSTEM AND STABILITY ANALYSIS – systemanalysis.m

```
load setupdata
load zone1data
load zone2data
load zone3data

% Step 1 Parallel the Three Zonal Loads
[AgL] = parL_to_L(NS,NI,Zone1_L,Zone2_L,Zone3_L);

% Step 2 Parallel the Two Sources
[stable,ES,S2_L] = parS_to_S(s,sc,PCM4_S,PCM4_S,NS,NI);

[L_const_of_PCM4] = esacdspec(gm,pm,tr,n1,n2,PCM4_S,s);
spaceplt(4,6,s,L_const_of_PCM4,-20.0);
hold on;
spaceplt(4,6,s,S2_L,-20.0);
hold off;
title('Stability of PCM4 to PCM4 Interface');
```

```
% Step 3 Check System Stability at the Effective Power Supply Interface
% Stet 3a: Check it Automatically
[sok ok] = sinspect(s,sc,ES,AgL,NS,NI);
if ok
   disp('Dual PCM4 Rest of System Interface is Stable');
else
   disp('Dual PCM4 Rest of System Interface does not Satisfy Stability Criteria');
end

% Step 3b: Check it Manually
[L_const_of_ES] = esacdspec(gm,pm,tr,n1,n2,ES,s);
spaceplt(5,6,s,L_const_of_ES,-20.0);
hold on;
spaceplt(5,6,s,AgL,-20.0);
hold off;
title('Stability of Port PCM4 Interface');
```

APPENDIX D

D.1. Buck Converter

Because DC converter modules (SSCMs) are a type of buck converter, a simple buck converter was modeled to investigate its behavior. The circuit diagram is shown in Figure D-1. By controlling the frequency and duty cycle of the solid state switch, the voltage across the load is regulated at a lower average output than the input voltage. An RLC filter is connected between the switch and the load. A diode allows current to continue to flow through the inductor when the switch is open. The two system state variables are the current through the inductor and voltage across the load/capacitor.

Figure D-1. Buck Converter
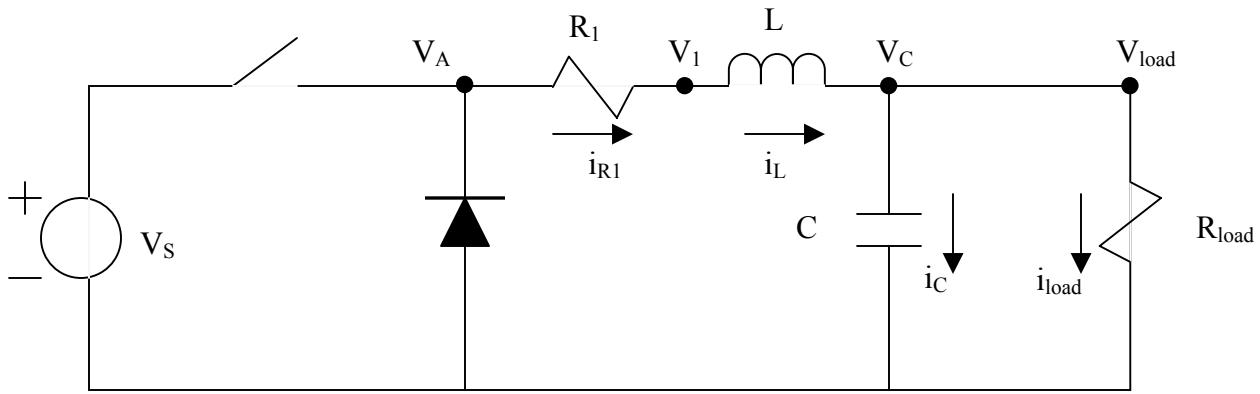
The buck converter was simulated in Advanced Continuous Simulation Language after deriving the state equations for the system. When the switch is closed, $V_A = V_S$ and current flows through all components except the diode. The component equations are

Resistive load: $V_{load} = i_{load} * R_{load}$ Circuit Resistance: $V_A - V_1 = i_{R_1} * R_1$ (1)

The node equation is

$$i_L = i_C + i_{load}$$ (2)

The two state equations are

$$\text{Inductor: } L * \frac{di_L}{dt} = V_L$$ (3)

$$\text{Capacitor: } V_C = \frac{1}{C} \int i_C dt \qquad (4)$$

It is evident that

$$V_C = V_{Load} \quad \text{and} \quad i_{R_1} = i_L \qquad (5)$$

Rearranging the state equations,

$$\frac{dV_C}{dt} = \frac{1}{C} i_C$$

$$\frac{di_L}{dt} = \frac{1}{L} V_L \qquad (6)$$

Substitution using the component and node equations results in

$$\frac{dV_C}{dt} = \frac{1}{C} i_C = \frac{1}{C}(i_L - i_{Load}) = \frac{1}{C}(i_L - \frac{V_C}{R_L})$$

$$\frac{di_L}{dt} = \frac{1}{L}(V_1 - V_C) = \frac{1}{L}(i_L R_S - V_C) + \frac{V_A}{L} \qquad (7)$$

which are the state equations formulated in terms of the states and input.

When the switch is opened, current flows through the diode and $V_A = 0$. The stored energy in the inductor and capacitor then dissipates through the load.

Refer to Appendix F for the ACSL code of a buck converter.

R_1 is the circuit resistance, L is the inductance, V_s is the source voltage, C is the capacitance, T is the period of the switch (and corresponds to a frequency of 20 kHz), d is the duty cycle of the switch, and R_{load} is the load resistance. The initial run used the following parameters:

R_1 = 1 Ω   T   = 50 µs
L   = 1 mH   d   = 0.3 (or 30%)
V_s = 10 V R_{load} = 20 Ω
C   = 10 µF

Results can be found in Appendix E. The results of the first run show a second-order underdamped system and are seen in Figure E-1. The capacitor voltage stabilizes at a near constant value and the inductor current reaches a limit-cycle about a constant current. The current oscillation is due to the switch, which changes V_A. The amplitude of the oscillation will be large for small duty cycles and small for large duty cycles.

The load resistance was then changed to 2, 10, and 100 Ohms and the results are shown in Figures E-2 through E-4. Figure E-2 shows an overdamped system and Figure E-3 shows an underdamped system similar to the initial run. Figure E-4 also shows an underdamped system, but was terminated when the current through the inductor reaches zero. The amplitude of the current does not change significantly.

The load resistance was then kept constant at 100 Ω and the duty cycle was changed to 50%, 70%, 90%, and 100%. The results are shown in Figures E-5 through E-8. Maximum current and voltage increases when the duty cycle is increased, which is intuitively obvious, because more energy is applied to the system. Oscillation decreases as duty cycle increases and is completely smooth at 100% duty cycle (the switch is always closed and thus the circuit is time-invariant).

D.2. "Inductive spike"

One of the assumptions warranting further discussion is the ideal switch. It is assumed that when the switch is closed, $V_A = 10$ V and when the switch is open, $V_A = 0$ V. This is not the case in reality. The presence of the inductor causes large voltage variations if the derivative of the current is large. When the switch opens or closes, V_A changes rapidly and therefore the magnitude of di_L/dt becomes very large. This causes the voltage across the inductor to become very large as well and results in a voltage "spike." However, this is not modeled in the example and is not seen in the simulation results.

APPENDIX E

ACSL Plots of Buck Converter Simulations
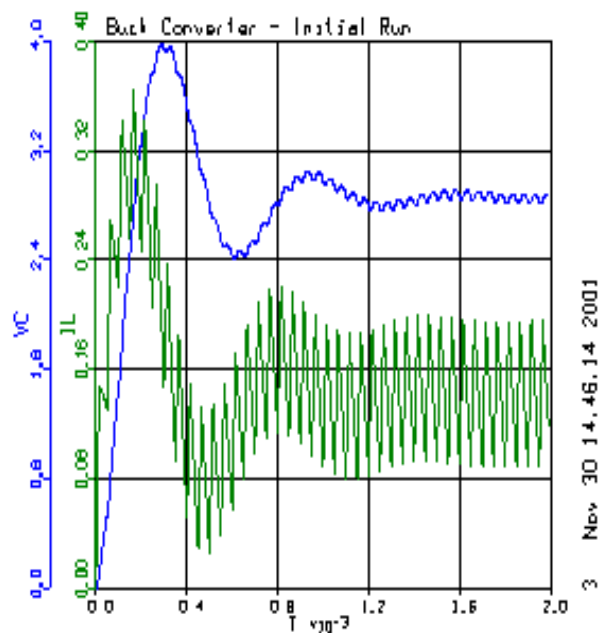
Figure E-1. Run 1
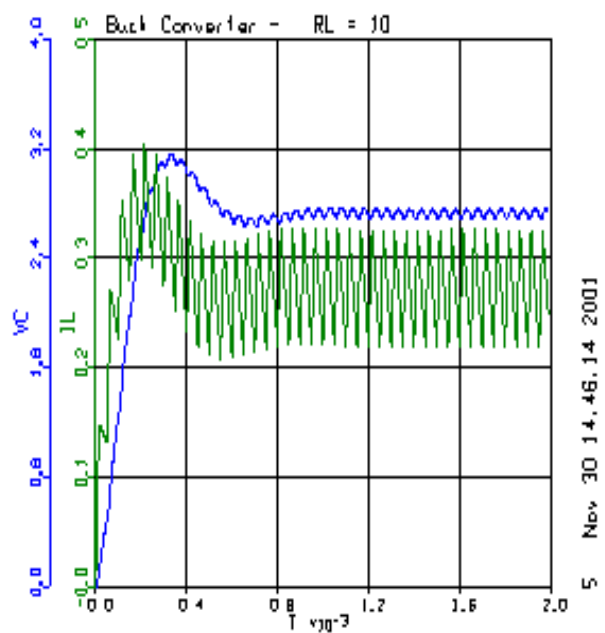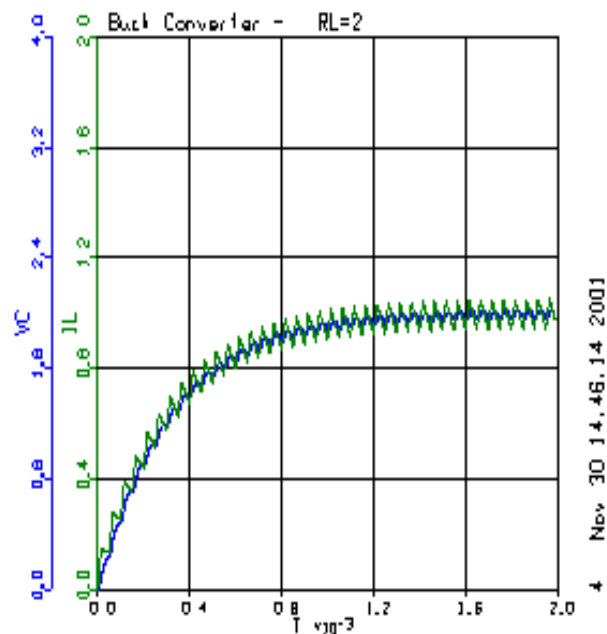

Figure E-3. Run 3

Figure E-2. Run 2

Figure E-4. Run 4
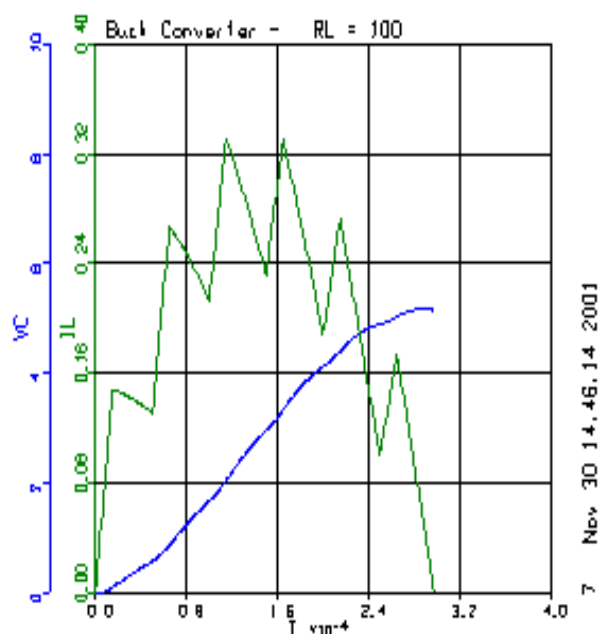
Figure E-5. Run 5
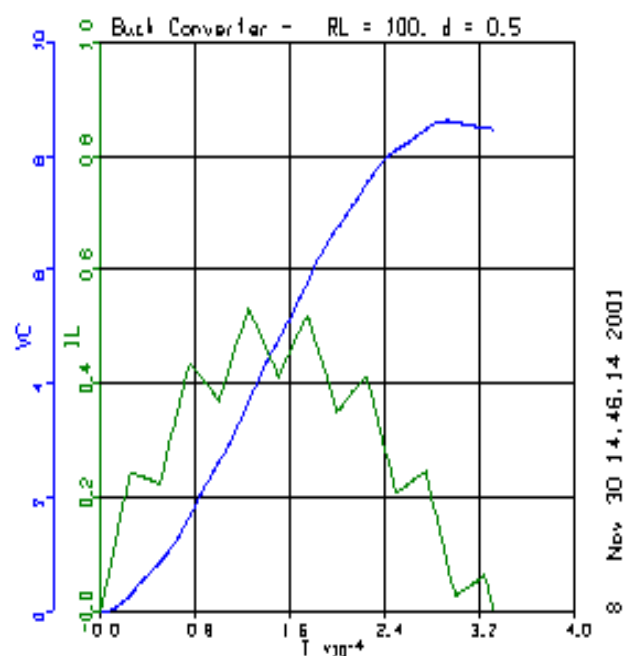
Figure E-7. Run 7
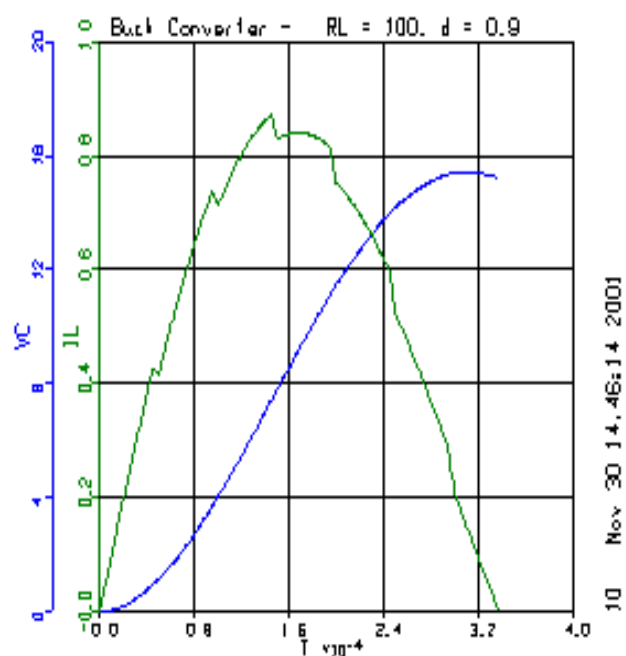
Figure E-6. Run 6
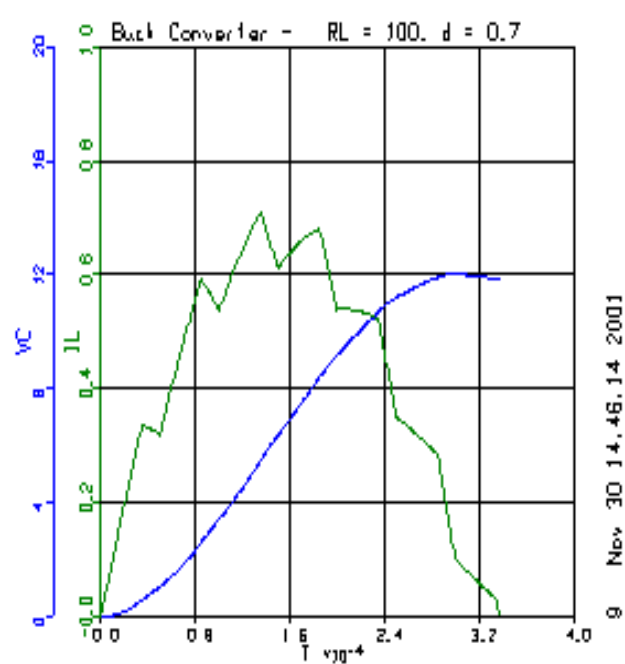
Figure E-8. Run 8
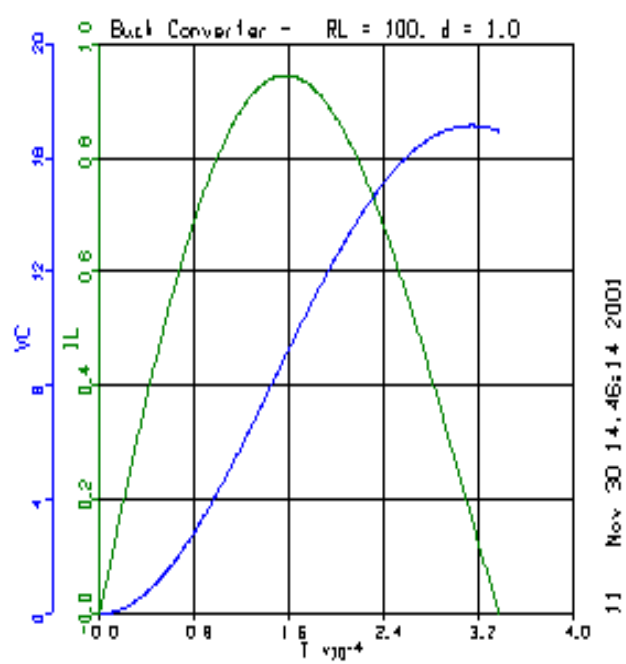
APPENDIX F

```
! buckconv.csl
!09NOV2001, Dan Chiafair
!modified 05DEC2001

PROGRAM Buck Converter

INITIAL
  !Sample parameters
  CONSTANT tstop = 0.00099
  CONSTANT R1= 1.0, L = 1.0e-3, vs = 10.0, C = 1.0e-5, RL= 20
  CONSTANT d = 1.00 ! Duty cycle
  CONSTANT vc_i = 0.0, il_i = 0.0    ! initial conditions
  va = vs
  iR1 = iL
END ! of initial

DYNAMIC

DERIVATIVE

MAXTERVAL MAXT = 0.00001              ! maximum integration interval

!State Equations
!p_iL and p_vc are the time derivatives of iL and vc
!p_iL = (va - vc - R1*iL)/L
!p_vc = (iL - vc/RL)/C

!Integrate derivatives of states
vc = INTEG(p_vc, vc_i)
iL = INTEG(p_iL, il_i)

! Alternate ACSL code for buck converter - corrected 12/05/01
p_iL = (v1 - vc)/L
p_vc = ic/C
ic    = iL - iRL
v1    = va - iR1*R1
iRL   = vc/RL

SCHEDULE disc .XN. iL              ! when current equals zero, execute "disc"

END ! of Derivative
```

```
DISCRETE S1on                          ! switch is closed
  INTERVAL tperiod = 0.00005           ! 50 microseconds = 20-kHz
  va=vs
  SCHEDULE S1off .AT. t+d*tperiod      ! implementation of duty cycle
END ! of S1on

DISCRETE S1off                         ! switch is open
  va = 0.0
END

DISCRETE disc                          ! occurs when current equals zero
 !va = vc                              ! because no current flows,
                                       ! VR1 and VL are zero
 TERMT(.TRUE., 'Termination on va=vc')
END

CINTERVAL CINT=1.0e-6                   ! Communication interval

TERMT(T .GE. tstop, 'Termination on Time Limit')

END ! of dynamic
END ! of program
```

APPENDIX G

These MATLAB routines combine various power system components, or converters, into a single, equivalent component.

SC_to_S: combines a source converter and cable to an equivalent source converter; no stability test is required

Figure G-1. Mapping an S and C converter into an Equivalent S-converter
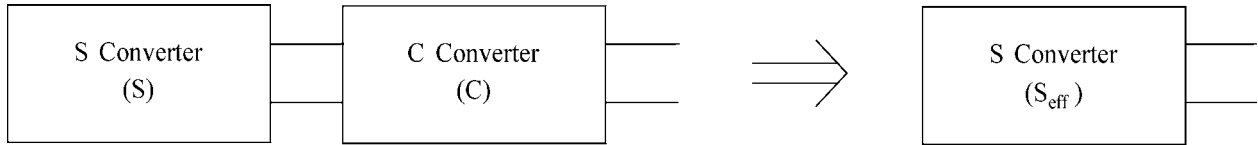
$$S_{eff} = S + C$$

LC_to_L: combines a load converter and cable to an equivalent load converter; a stability test is required with C as the source and L as the load

Figure G-2. Mapping an L and C converter into an Equivalent L-converter

$$L_{eff} = \frac{L}{1 + LC}$$

HL_to_L: combines an H converter and an L converter into an equivalent L converter; a stability test is required with H_{12} as the source and L as the load

Figure G-3. Mapping an L and H converter into an Equivalent L-converter
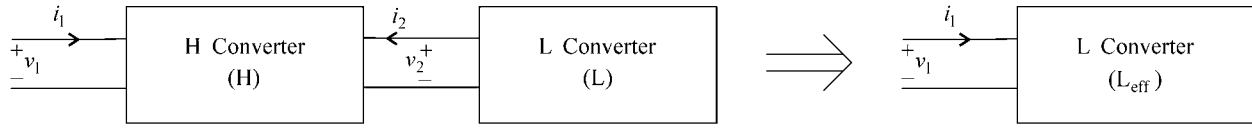
$$L_{eff} = \left[H_{21} - \frac{H_{22}H_{11}L}{1 + H_{12}L} \right]$$

SH _to_S: combines an S converter feeding an H converter into an equivalent S converter; a stability test is required with S as the source and H_{21} as the load

Figure G-4. Mapping an S and H converter into an Equivalent S-converter

$$S_{eff} = \left[H_{12} - \frac{SH_{12}H_{22}}{1 + SH_{21}} \right]$$

parL_to_L: combines L converters in parallel into an equivalent L converter; stability test is not required

Figure G-5. Mapping Parallel L-converters into an Equivalent L-converter
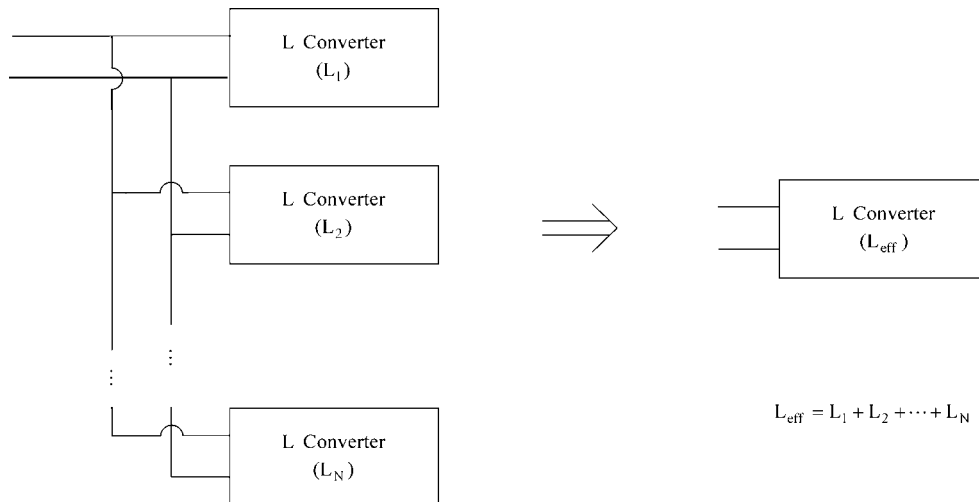
$$L_{eff} = L_1 + L_2 + \cdots + L_N$$

parY_to_Y: combines Y converters in parallel into an equivalent Y converter
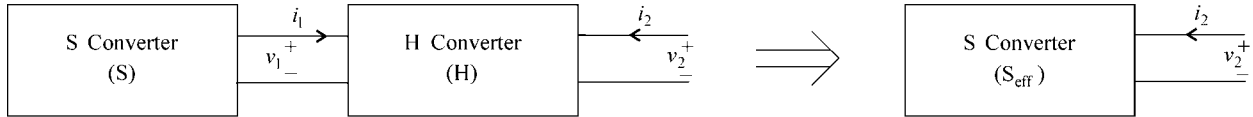
Figure G-6. Mapping Parallel Y-converters into an Equivalent Y-converter

$$Y_{eff} = Y_1 + Y_2 + \cdots + Y_N$$
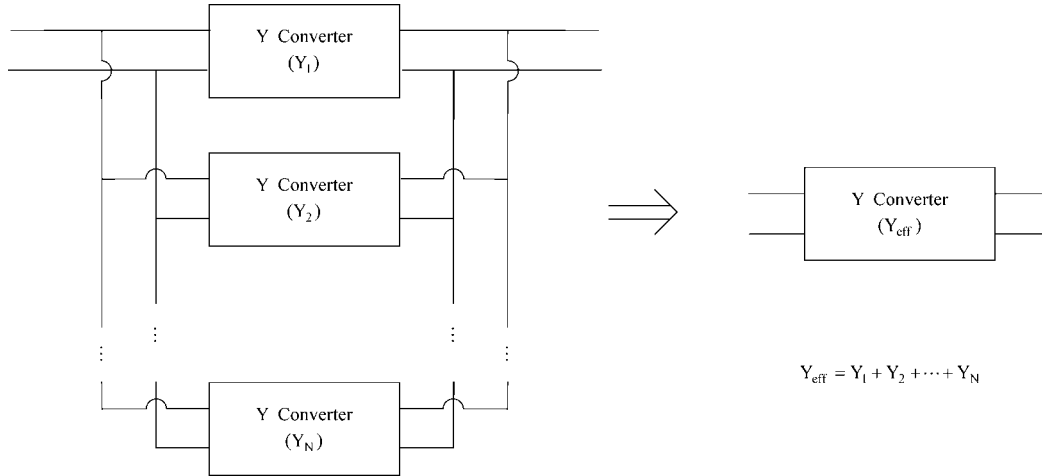
HLHp_to_Y: refer to diagram below; two stability tests are required: 1) $H_{\alpha 12}$ as source and $H_{\beta 12}^{-1}$ as the load, 2) parallel combination of $H_{\alpha 12}$ and $H_{\beta 12}$ as source and L as the load

Figure G-7. Mapping H-L-H' converters into an Equivalent Y-converter

$$\begin{bmatrix} i_{\alpha 1} \\ i_{\beta 1} \end{bmatrix} = \begin{bmatrix} Y_{11} & Y_{12} \\ Y_{21} & Y_{22} \end{bmatrix} \begin{bmatrix} v_{\alpha 1} \\ v_{\beta 1} \end{bmatrix}$$

$$Y_{11} = H_{\alpha 21} - \frac{H_{\alpha 22} H_{\alpha 11} \left[1 + LH_{\beta 12} \right]}{H_{\beta 22} + H_{\alpha 12} + LH_{\alpha 12} H_{\beta 12}} \qquad Y_{12} = \frac{H_{\alpha 22} H_{\beta 11}}{H_{\beta 22} + H_{\alpha 12} + LH_{\alpha 12} H_{\beta 12}}$$

$$Y_{21} = \frac{H_{\alpha 11} H_{\beta 22}}{H_{\beta 22} + H_{\alpha 12} + LH_{\alpha 12} H_{\beta 12}}$$

$$Y_{22} = H_{\beta 21} - \frac{H_{\beta 22} H_{\beta 11} \left[1 + LH_{\alpha 12} \right]}{H_{\beta 22} + H_{\alpha 12} + LH_{\alpha 12} H_{\beta 12}}$$
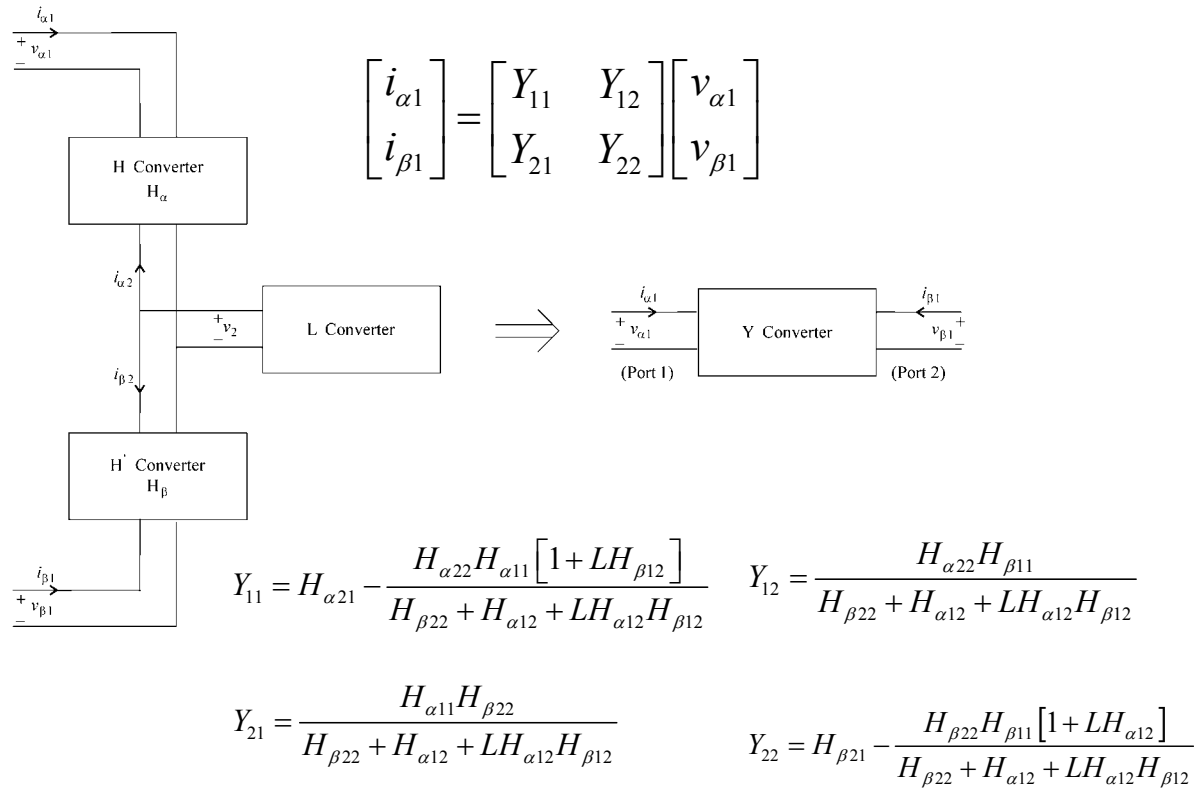
YS_to_L: represents a Y converter with a source converter at Port 2 as an equivalent L converter viewed from Port 1; a stability test is required with S as the source and Y_{22} as the load

Figure G-8. Mapping Y and S converters into an Equivalent L-converter
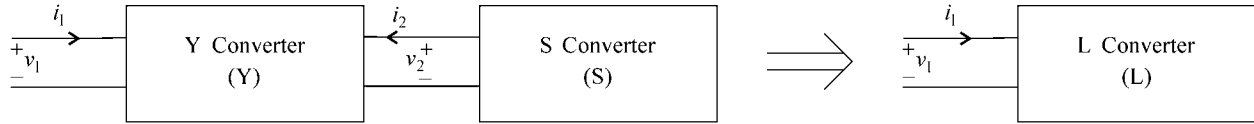
$$L = Y_{11} - \frac{S Y_{21} Y_{12}}{1 + Y_{22} S}$$

Y_to_L: represents a Y converter whose ports have been connected together in parallel as an equivalent L converter; a stability test is not required

Figure G-9. Mapping a Y-converter into an Equivalent L-converter
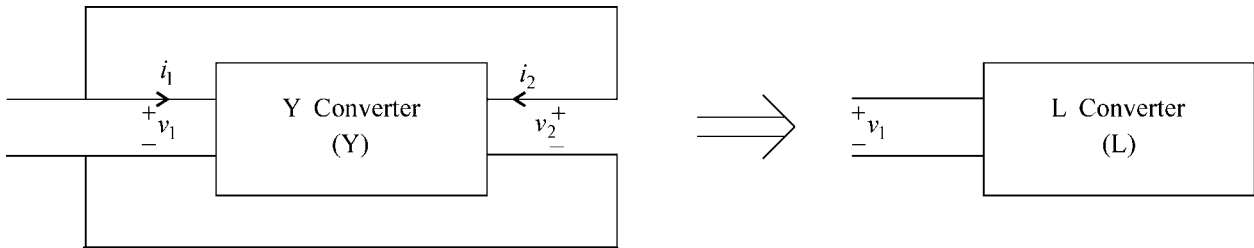
$$L = Y_{11} + Y_{12} + Y_{21} + Y_{22}$$

parS_to_S: During this study, it was discovered that a routine that combines two sources in parallel would be useful to the analysis of the second alternate system configuration. After contacting Professor Sudhoff, he graciously added this routine to the toolbox.

APPENDIX H

This shows the two alternate system structures of an integrated power system that were analyzed in order to simulate casualty conditions.

Alternate Configuration One

One bus and power supply have been lost.
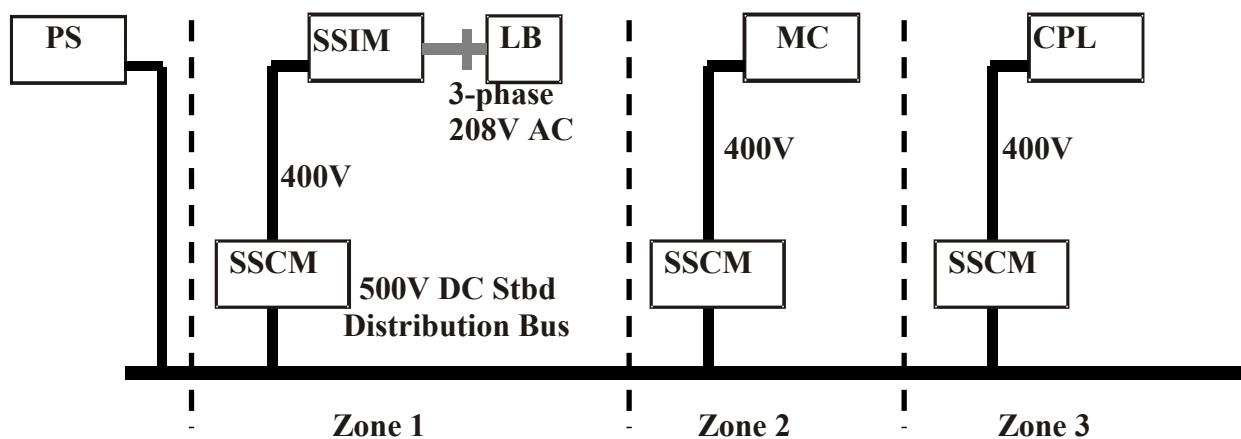
Alternate Configuration Two

One bus has been lost, but both power supplies remain operational.

APPENDIX I

I.1. Tabulated Results for Full Configuration

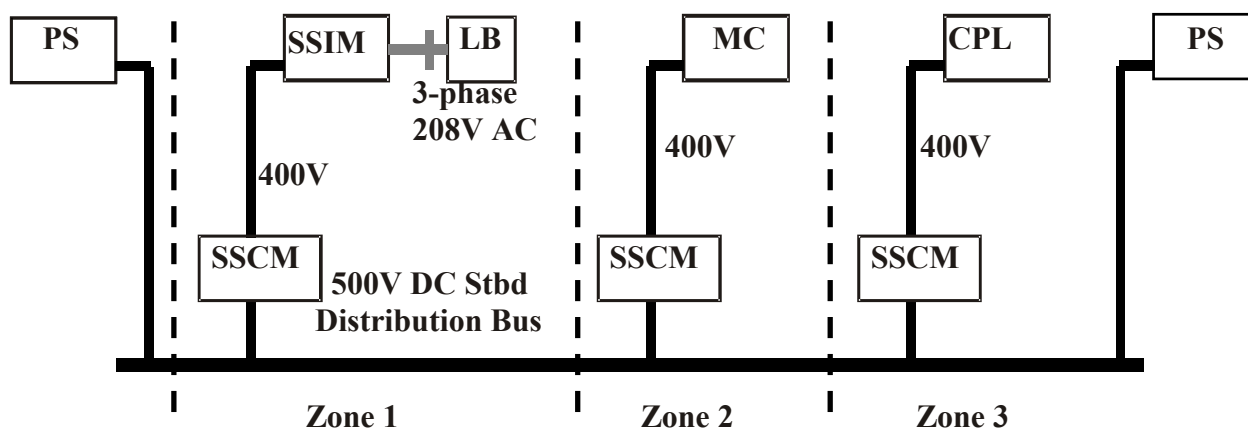| GROUP	PARAMETER	Scale factor	Stable	Nearly Stable*	Unstable
No changes			X		
Capacitance Changes	Constant Power Load Capacitance	0.1	X		
	Motor Controller Capacitance	0.1	X		
	SSIM Capacitance	0.1	X		
	Power Supply Capacitance	1.1	X		
		1.8	X		
		0.9	X		
		0.8	X		
		0.05	X		
	SSCM Output Capacitance	1.1	X		
		1.2	X		
		1.4	X		
		1.8	X		
		0.9	X		
		0.8	X		
		0.01	X		
Ksf Changes	Ksf	2	X		
		4	X		
		0.5		X	
		0.25			X
		0			X
Ksf is halved	SSCM Output Capacitance	2	X		
		8	X		
	SSCM Input Capacitance	2	X		
		8	X		
	Power Supply Capacitance	2	X		
		4	X		
		8	X		
Ksf is quartered	SSCM Output Capacitance	4			X
Ksf = 0	SSCM Output Capacitance	10			X
	SSCM Input Capacitance	10	X		
	Power Supply Capacitance	10	X		

---

* Nearly stable as used here indicates that the impedance curve "nicked" the constraint curve, signifying some potential instabilities. The simulation was run again, this time with gain and phase margins of almost zero, and the impedance curve avoided the constraint curve at all frequencies (not shown in the data). The meaning then of "nearly stable" is that the system was stable, but with a gain and/or phase margin of less than 3 dB and 20 degrees, respectively.

I.2. Tabulated Results for Alternate Configuration One

GROUP	PARAMETER	Scale factor	Stable	Nearly Stable	Unstable
No changes			X		
Capacitance Changes	Power Supply Capacitance	0.5		X	
		0.1			X
	SSCM Output Capacitance	0.75		X	
		0.1			X
	SSCM Input Capacitance	0.1	X		
Ksf Changes	Ksf	0.8		X	
		0.5			X
		0.2			X
		0			X
Ksf is halved	SSCM Output Capacitance	2		X	
		8		X	
	SSCM Input Capacitance	2	X		
		8	X		
	Power Supply Capacitance	2	X		
		8	X		
Ksf = 0	SSCM Output Capacitance	10			X
		20			X
	SSCM Input Capacitance	10	X		
	Power Supply Capacitance	10	X		

I.3. Tabulated Results for Alternate Configuration Two

GROUP	PARAMETER	Scale factor	Stable	Nearly Stable	Unstable
No changes			X		
Capacitance Changes	Power Supply Capacitance	0.1	X		
	SSCM Output Capacitance	0.25	X		
		0.1	X		
	SSCM Input Capacitance	0.1	X		
Ksf Changes	Ksf	0.5	X		
		0.2	X		
		0	X		
Ksf = 0	SSCM Output Capacitance	0.1	X		
	SSCM Input Capacitance	0.1			X
	Power Supply Capacitance	0.1	X		

[1] Zivi, E., McCoy, T., "Control of a Shipboard Integrated Power System," *Presentation to Conference on Information Sciences and Systems*, John Hopkins University, May 25, 1999.

[2] Glover, S., Sudhoff, S., "An Experimentally Validated Nonlinear Stabilizing Control for Power Electronics Based Power Systems," *Proceedings of the 1998 SAE Aerospace Power Systems Conference*, pp. 71-80.

[3] McCoy, T., Lively, K., Thompson, T., Zivi, E., "Advanced Control Concepts for an Integrated Power System (IPS) Warship," *Presentation to Fifth International Naval Engineering Conference and Exhibition*, March 15, 2000.

[4] Amin, Massoud. "National Infrastructures as Complex Interactive Networks," in Automation, Control, and Complexity: An Integrated Approach, T. Samad and J.R. Weyrauch, Eds., New York: Wiley, 2000, ch.14, pp. 263-286.

[5] Zivi, E., McCoy T. "Control of a Shipboard Integrated Power System," Proceedings of the Thirty-third Annual Conference on Information Sciences and Systems, March 18, 1999.

[6] Zivi, E., McCoy, T., "Control of a Shipboard Integrated Power System," *Presentation to Conference on Information Sciences and Systems*, John Hopkins University, May 25, 1999.

[7] Lively, K., McCoy, T., Thompson, T., Zivi, E. "USN Advanced Control Concepts for an Integrated Power System (IPS) Warship," Proceedings of the INEC 2000 Conference, Hamburg, Germany, March 14-16, 2000.

[8] Cerrito, J. "Neural Network Control of the Integrated Power System," U.S.N.A. Trident Scholar Project Report, Number 273 (2000), p. 13.

[9] Cerrito, J. "Neural Network Control of the Integrated Power System," United States Naval Academy Trident Scholar Project Report, Number 273 (2000).

[10] Zivi, E., Cerrito, J., Doney, D., "Neural Network Fault Tolerant Estimation of an Integrated Power System," Proceedings of Applied Simulation and Modelling Conference, July 24-26, 2000, Banff, Canada.

[11] Vanecko, J. "Advanced Shipboard Control Systems," United States Naval Academy Trident Scholar Project Report, Number 286, (2001).

[12] "ONR Control Challenge Problem" posted at http://www.usna.edu/EPNES/ONR_Control_Challenge.pdf

[13] Sudhoff, S., DC Stability Toolbox, Version 2.1, Lecture 2.

[14] Sudhoff, S.D. "Control of Zonal DC Distribution Systems: A Stability Perspective." Naval Combat Survivability: Task 3 Final Report, January 16, 2002.

[15] *Ibid.*

[16] *Ibid.*

[17] *Ibid.*

[18] Sudhoff, S., Schmucker, D., Youngs, R., Hegner H. "Stability Analysis of DC Distribution Systems Using Admittance Space Constraints." Proceedings of The Institute of Marine Engineers All Electric Ship 98, London, September 29-30, 1998.

[19] S.D. Sudhoff, S.F. Glover, P.T. Lamm, D.H. Schmucker, D.E. Delisle, "Stability Analysis of DC Power Electronics Based Distribution Systems Using Admittance Space Constraints," *IEEE Transactions on Aerospace and Electronics Systems*, Vol. 36. No. 3. July 2000, pp. 965-973.

[20] S.D. Sudhoff, "Admittance Space Based Stability Specification," Proceedings of the 1998 ONR -Drexel-NSWC Workshop on Electric Shipboard System Modeling, Simulation and Control, June 22-23, 1998, Philadelphia, PA, USA

[21] S.D. Sudhoff, S.F. Glover, P.T. Lamm, D.H. Schmucker, D.E. Delisle, "Stability Analysis of DC Power Electronics Based Distribution Systems Using Admittance Space Constraints," *IEEE Transactions on Aerospace and Electronics Systems*, Vol. 36. No. 3. July 2000, pp. 965-973.

[22] Sudhoff, Stability Toolbox, Lecture 2.

[23] *Ibid*.

[24] *Ibid*.

[25] S.D. Sudhoff, S.F. Glover, P.T. Lamm, D.H. Schmucker, D.E. Delisle, "Stability Analysis of DC Power Electronics Based Distribution Systems Using Admittance Space Constraints," *IEEE Transactions on Aerospace and Electronics Systems*, Vol. 36. No. 3. July 2000, pp. 965-973.

[26] Sudhoff, Stability Toolbox, Lecture 2.

[27] *Ibid*.

[28] S.D. Sudhoff, S.F. Glover, P.T. Lamm, D.H. Schmucker, D.E. Delisle, "Stability Analysis of DC Power Electronics Based Distribution Systems Using Admittance Space Constraints," *IEEE Transactions on Aerospace and Electronics Systems*, Vol. 36. No. 3. July 2000, pp. 965-973.

[29] Sudhoff, Stability Toolbox, Lecture 2.

[30] Sudhoff, S.D. "Control of Zonal DC Distribution Systems: A Stability Perspective." Naval Combat Survivability: Task 3 Final Report, January 16, 2002.

[31] Sudhoff, Stability Toolbox, Lecture 2.

[32] *Ibid*.

[33] Sudhoff, S., DC Stability Toolbox, Version 2.1, Lecture 5.